Netherlands Enterprise Agency

Scour and Scour Mitigation for Nederwiek Wind Farm Zone

>> *Sustainable. Agricultural. Innovative. International.*



Netherlands Enterprise Agency

RVO Approval for Publication

Please Note that this Report is a Final Draft, Certification is in progress, a final version will be published as soon as possible.

Document Characteristics

Version	Title	Date of Approval for Publication	Reference Contractor	Reference RVO
	Scour and Scour Migigation for Nederwiek Wind Farm Zone	November 2024	Svasek Hydraulics	WOZ2240142

Approval

Approval for public disclosure	Position
Jacob Dekker	Project Manager RVO Offshore Wind Energy
Peter-Paul Lebbink	Programme Manager RVO Offshore Wind Energy

Intern gebruik

Scour and scour mitigation Nederwiek Wind Farm Zone

NW-I, NW-II and NW-III

Final draft

2183/002/D/YSte

November 12, 2024

Kratonkade 23
3024 ES Rotterdam
The Netherlands
T +31 - 10 - 467 13 61
E office@svasek.com
I www.svasek.com

Document title	Scour and scour mitigation Nederwiek Wind Farm Zone NW-I, NW-II and NW-III
Short document title	Scour and scour mitigation NWWFZ
Status	Final draft
Date	November 12, 2024
Project name	Nederwiek Morphology and scour assessment
Project number	2183
Client	Rijksdienst voor Ondernemen Nederland
Contact	Marjolyn Witteveen
Reference	2183/002/D/YSte

Author	Yannick Steenman, Anna Kroon
Checked by (internal)	Bas van Leeuwen
Checked by (external)	Gijs Hoffmans

SUMMARY

As part of its climate goals, the Dutch Government aims to have 55 TWh/a of offshore wind energy installed by 2032. Offshore wind farms will be built within designated Wind Farm Zones. RVO and Dutch transmission system operator TenneT have, therefore, started preparations for the further development of the Nederwiek Wind Farm Zone (NWWFZ) under the 21 GW roadmap. The Nederwiek Wind Farm Sites (NWWFS) I-III (up to 6,000 MW) are currently being developed for tendering.

The NWWFS scour and morphology study aims to improve the understanding of the seabed morphology, morphodynamics, and infrastructure-related scour potential at the Nederwiek Wind Farm Zone (NWWFZ). These objectives are separated into two reports. The first report focuses on the seabed morphology and morphodynamics at Nederwiek (Svašek Hydraulics, 2024). This report focuses on the infrastructure-related scour and potential scour protections at the NWWFZ.

This study delivers a general order of magnitude on a feasibility level of the to-be-expected scour at the NWWFZ. The scour analysis is performed quantitatively for monopiles with a pile diameter of D = 12 m using a time-dependent scour development model. This model calculates the equilibrium scour hole depth and characteristic timescale of scour for many timesteps to calculate the development of the scour hole through time. The maximum scour hole depths for these three non-exceedance values are summarized in Table A for the individual Nederwiek sites and for the entire NWWFZ.

Table A: Predicted scour depths across the NWWFZ. The percentage values indicate the non-exceedance values. Indicated scour depths are the maximum scour depth during the entire simulation. The simulations are based on monopiles with a pile diameter of D = 12 m. $S_{n\%}$ stands for the n% non-exceedance scour depth

Location	$S_{5\%}$ [m]	$S_{5\%}/D$ [-]	$S_{50\%}$ [m]	$S_{50\%}/D$ [-]	$S_{95\%}$ [m]	$S_{95\%}/D$ [-]
Total	5.0 – 8.4	0.4 – 0.7	10.7 – 14.9	0.9 – 1.2	18.2 – 21.8	1.5 – 1.8
NW-I	7.0 – 8.4	0.6 – 0.7	13.1 – 14.9	1.1 – 1.2	20.1 – 21.8	1.7 – 1.8
NW-II/III	5.0 – 8.1	0.4 – 0.7	10.7 – 14.4	0.9 – 1.2	18.2 – 21.4	1.5 – 1.8

Figure A shows the spatial distribution of $S_{max,50\%}$ in the entire NWWFZ. The scour depths in Nederwiek 1 (NW-I) are generally higher compared to Nederwiek 2 & 3 (NW-II/III). This can be attributed to the higher flow velocities and lower wave dominance due to lower waves at NW-I compared to NW-II/III. As the flow and waves within NW-I are relatively uniform, the highest scour depths are found at the deepest waters between the sandbanks. The lowest scour depths are found on the crests of the sandbanks.

The flow and the waves within NW-II/III are less uniform. Slightly higher waves are found in the area's north compared to the south, and lower flow velocities are found in the area's north compared to the south. The bed levels generally decrease from the southeast towards the northwest. As a result, the lowest scour depths occur in the northeast corner of the area, where the waves are the most dominant, the water depth is average, and the flow velocities are low. More towards the south of NW-II/III, the effect of the sandbanks becomes prevalent. The highest scour depths are located at the deeper points between the sandbanks, whereas the scour depth is lower on the crests of the sandbanks.

Note that in the determination of the fixation point of monopiles, it is a conservative estimate to take the sum of bed level lowering due to sand waves in conjunction with the scour depths as predicted without sand wave migration. It is expected that scour will be reduced when the seabed lowers. The scour hole is expected to be able to follow the development of the bedform migration due to the different timescales.

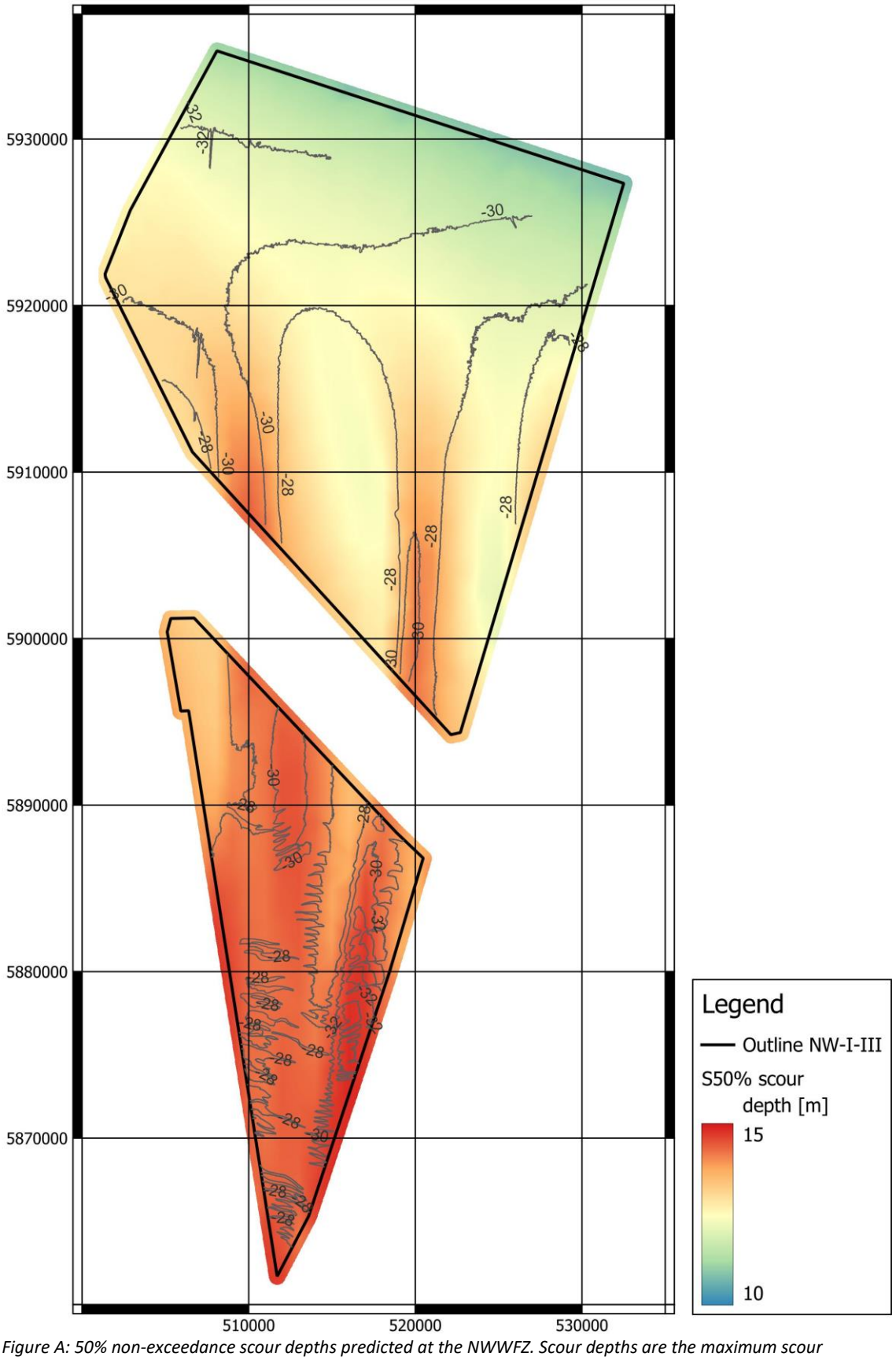

Figure A: 50% non-exceedance scour depths predicted at the NWWFZ. Scour depths are the maximum scour depths during the simulations. Simulations are performed for monopiles with D = 12 m.

The scour holes will develop quicker in NW-I due to the more frequent high flow velocities. Equilibrium scour hole depths are predicted to be reached 5 to 10 years after construction. The scour hole development in NW-II/III varies spatially, with slower scour development towards the north and faster scour development towards the south. The equilibrium scour hole depths are generally reached between 5 to 25 years in NW-II/III. Using the typical slopes of 1:2 and 1:3 and the expected scour hole depths ($S_{50\%}$) from Figure A, the lateral scour hole extent at the NWWFZ varies between 20 – 45 m.

The scour depths as calculated for the monopile foundation are extended qualitatively to he piled jacket, suction bucket, and gravity-based structures. Multi-legged structures, such as the piled jacked and multi-bucket structures, are subject to global and local scour. The global scour is estimated to be in the order of a few meters. Suction bucket and gravity-based structures are especially vulnerable to destabilization due to scour. As the scour depths for monopiles are predicted to be significant for the entire NWWFZ, it is expected that both structure types should be protected with scour protections. For the other foundation types, it can be considered to adapt the design to the predicted scour depths, to protect the foundation immediately, or to monitor the scour development and react accordingly.

This study demonstrates the design approach of a dynamically stable, loose rock scour protection at the NWWFZ. This design aims to provide the reader with a general estimate of the required rock gradings for the armour layer that can be used for a feasibility analysis. This is not to say that scour protections other than loose rock are not feasible for the NWWFZ. Mattress-like scour protections can be a reasonable alternative to scour protections if sufficient sand-tightness can be guaranteed.

The deformation model from JIP HaSPro (2023) is used with the 90% non-exceedance values to calculate the required gradings of the armour layer of a dynamically stable loose rock scour protection. The deformation limit is set at 0.5 meters. A simplified extreme value analysis is performed to derive preliminary design conditions for the design of the scour protection, which are based on the 50-year return period wave conditions.

Figure B shows the required gradings for a dynamically stable scour protection with a maximum deformation of 0.5 m. The figure shows that the most shallow locations often require heavier protection than deeper areas. This is most evidently visible on the crest of the sandbanks, where the largest stones are required for the armour layer. These sandbanks are located in the southeast of NW-II/III and towards the northwest of NW-I.

A 2-8” or 3-9” grading of high-density rock can effectively protect most of NW-I and the north-western sections of NW-II/III. These gradings are commonly employed as single-layer scour protections. If the grading width meets the internal stability criteria, these gradings can serve as a single-layer scour protection at Nederwiek. Only the shallower areas strictly require a double-layered scour protection based on external stability. Furthermore, a few locations in NW-I can be protected with normal density rock with a grading of 3-9”.

It can generally be said that the wave load increases from southwest to northeast in NW-II/III. The maximum design wave height and maximum design peak velocity are located at the northeast corner of NW-II/III. As a result, the northeast section of NW-II/III requires heavier protection than is expected for other locations at the same water depth.

The scour protection in NW-I should be designed with the predicted sea bed level changes due to bedform migration. The migrating sand waves in NW-I can cause bed level variances of several meters. Scour protection will prevent the bed from lowering close to the foundation but will not stop the seabed from lowering at some distance. This can result in an increased load on the scour protection due to sill-like behaviour and problems with the cable touch-down point.

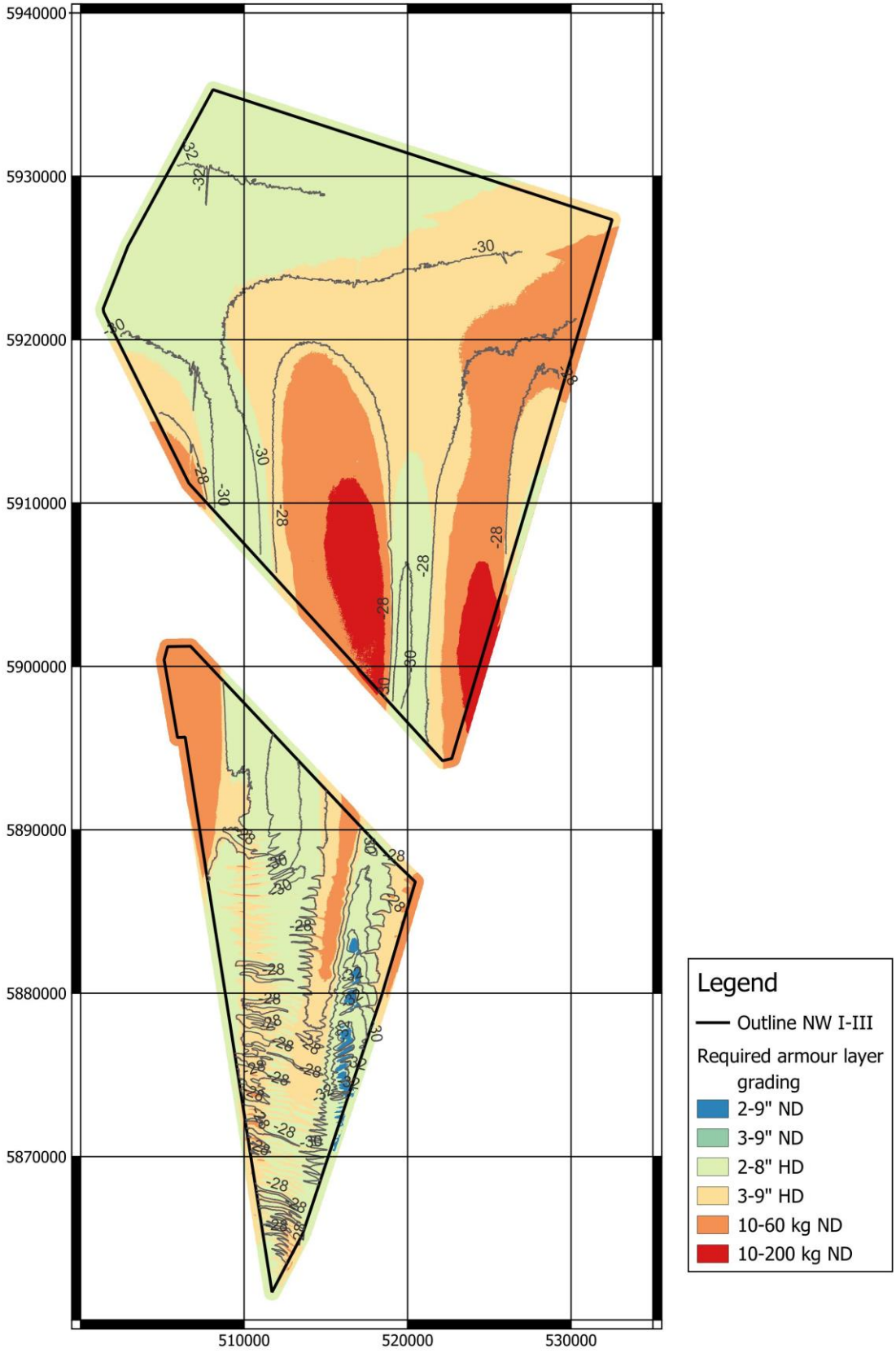

Figure B: Required armour layer grading to achieve a maximum deformation of 0.5 m in the NWWFZ with 90% confidence. ND = Normal Density rock; HD = High density rock.

SAMENVATTING

Als onderdeel van zijn klimaatdoelstellingen streeft de Nederlandse overheid ernaar om tegen 2032 55 TWh/jaar aan offshore windenergie te hebben geïnstalleerd. Offshore windparken zullen worden gebouwd binnen aangewezen Windenergiegebieden. RVO en de Nederlandse netbeheerder TenneT zijn daarom begonnen met de voorbereidingen voor de verdere ontwikkeling van de Nederwiek Wind Farm Zone (NWWFZ) onder de 21 GW routekaart. De Nederwiek Wind Farm Sites (NWWFS) I-III (tot 6.000 MW) worden momenteel ontwikkeld voor aanbesteding.

De NWWFS studie naar erosie en morfologie heeft als doel het begrip van de zeebodemmorfologie, morfodynamica en infrastructuur gerelateerde erosiepotentie in de NWWFZ te verbeteren. Deze doelstellingen zijn verdeeld over twee rapporten. Het eerste rapport richt zich op de zeebodemmorfologie en morfodynamica bij Nederwiek (Svašek Hydraulics, 2024). Dit rapport richt zich op de infrastructuur gerelateerde ontgronding en mogelijke erosiebescherming in de NWWFZ.

Deze studie levert een algemene orde van grootte van de te verwachten erosie in de NWWFZ. De erosieanalyse is kwantitatief uitgevoerd voor monopiles met een paaldiameter van D = 12 m, waarbij gebruik is gemaakt van een tijdsafhankelijk model voor het bepalen van de erosieontwikkeling. Dit model berekent de evenwichtsdiepte van de erosiekuil en de karakteristieke tijdschaal van erosie over meerdere tijdstappen om de ontwikkeling van de erosiekuil door de tijd heen te berekenen. De maximale erosiekuildieptes voor drie zekerheidswaardes zijn samengevat in Tabel A voor de individuele Nederwiek-locaties en voor het gehele NWWFZ.

Tabel A: Voorspelde erosiekuildieptes in de NWWFZ. De procentuele waarden geven het percentiel van de erosiekuildieptes aan. De aangegeven erosieputdieptes zijn de maximale erosieputdieptes gedurende de gehele simulatie. De simulaties zijn gebaseerd op monopiles met een paaldiameter van D = 12 m. $S_{n\%}$ staat voor het n^e percentiel van de erosiekuildieptes.

Location	$S_{5\%}$ [m]	$S_{5\%}/D$ [-]	$S_{50\%}$ [m]	$S_{50\%}/D$ [-]	$S_{95\%}$ [m]	$S_{95\%}/D$ [-]
Total	5.0 – 8.4	0.4 – 0.7	10.7 – 14.9	0.9 – 1.2	18.2 – 21.8	1.5 – 1.8
NW-I	7.0 – 8.4	0.6 – 0.7	13.1 – 14.9	1.1 – 1.2	20.1 – 21.8	1.7 – 1.8
NW-II/III	5.0 – 8.1	0.4 – 0.7	10.7 – 14.4	0.9 – 1.2	18.2 – 21.4	1.5 – 1.8

Figuur A toont de ruimtelijke verdeling van $S_{max,50\%}$ in de gehele NWWFZ. De erosiekuildieptes in Nederwiek 1 (NW-I) zijn over het algemeen dieper in vergelijking met Nederwiek 2 & 3 (NW-II/III). Dit kan worden toegeschreven aan de hogere stroomsnelheden en de lagere mate van golfdominantie door lagere golven bij NW-I in vergelijking met NW-II/III.

Omdat de stroming en de golven binnen NW-I relatief uniform zijn, worden de diepste erosiekuilen gevonden in de diepste wateren tussen de zandbanken. De meest ondiepe erosiekuilen worden aangetroffen op de toppen van de zandbanken.

De stroming en golven in NW-II/III zijn minder uniform. In het noorden van het gebied worden lagere stroomsnelheden en iets hogere golven waargenomen vergeleken met het zuiden. De waterdieptes nemen toe vanaf het zuidoosten naar het noordwesten in het gebied. Hierdoor treden de meest ondiepe erosiekuilen op in de noordoostelijke hoek van het gebied. Hier zijn de golven het meest dominant, de waterdieptes gemiddeld, en is de stroomsnelheid laag. Maar richting het zuiden van NW-II/III wordt het effect van de zandbanken duidelijk. De diepste erosiekuilen bevinden zich op de diepere gedeeltes tussen de zandbanken, terwijl de erosiekuilen minder diep zijn op de toppen van de zandbanken.

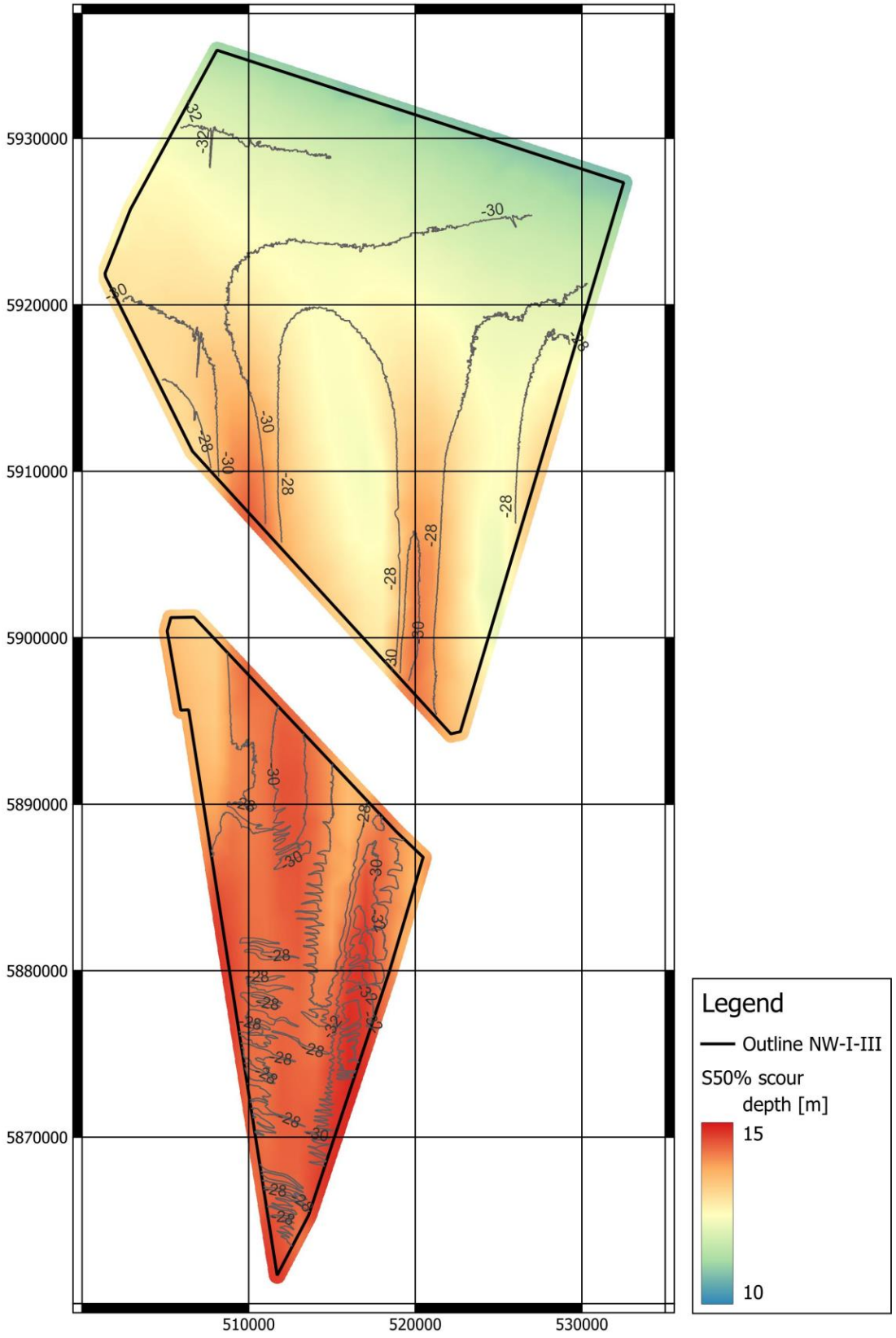

Figuur A: Erosiekuildieptes in de NWWFZ die in 50% van de simulaties niet wordt overschreden. De erosieputdieptes zijn de maximale dieptes tijdens de simulaties. De simulaties zijn uitgevoerd voor monopiles met een diameter van D = 12 m.

Wanneer de ontwikkelaar ervoor kiest om géén bodembescherming aan te brengen, moet de ontwikkelaar in NW-I rekening houden met de migratie van zandgolven bovenop de voorspelde erosiekuildieptes. Het is een conservatieve aanname om een bodemverlaging als gevolg van migrerende zandgolven op te sommen bij de voorspelde erosiekuildieptes. Er wordt verwacht dat de erosie zal verminderen wanneer de zeebodem verlaagt. De erosiekuil wordt in staat geacht om de ontwikkeling van de bodemvormmigratie te volgen vanwege de langere tijdsschaal.

De erosiekuilen zullen zich sneller ontwikkelen in NW-I vanwege de frequentere hoge stroomsnelheden. Het wordt verwacht dat de evenwichtsdieptes van de erosiekuilen 5 tot 10 jaar na de plaatsing van de fundering wordt bereikt. De ontwikkeling van de erosiekuilen in NW-II/III varieert ruimtelijk. Deze ontwikkeling zal langzamer plaatsvinden in het noorden en sneller in het zuiden. De evenwichtsdieptes worden geschat bereikt te zijn tussen de 5 en 25 jaar na de plaatsing van de fundering. Uitgaande van typische taluds van de erosiekuil van 1:2 en 1:3 en de 50% voorspelling van de kuildieptes uit Figuur A is berekend dat de erosiekuilen tussen de 20 en 45 m breed zullen worden.

Op basis van de voorspelde erosiedieptes voor monopile funderingen zijn kwalitatieve inschattingen gemaakt van de erosiediepte voor piled jacket, suction bucket, en gravity-based constructies. Meerpotige constructies zoals de piled jacket en multi-bucket constructies zijn onderhevig aan zowel globale als lokale erosie. De globale erosie wordt geschat enkele meters te zijn. Suction bucket en gravity-based constructies zijn bijzonder kwetsbaar voor destabilisatie door erosie. Gegeven de diepe erosiekuilen die zijn voorspeld in de hele NWWFZ, wordt verwacht dat voor beide constructies een bodembescherming moet worden aangelegd. Voor andere funderingstypen kan worden overwogen om het ontwerp aan te passen aan de voorspelde erosiekuildieptes, om de fundering direct te beschermen, of om te monitoren en te reageren wanneer nodig.

Deze studie demonstreert de ontwerpmethodiek van een dynamische bodembescherming bestaande uit losse stenen in de NWWFZ. Dit ontwerp is bedoeld om de ontwerper een algemene schatting te geven van de vereiste steengroottes voor de toplaag van de bodembescherming. Dit betekent niet dat andere vormen van erosiebescherming niet haalbaar zijn in de NWWFZ. Matrasbeschermingen kunnen een alternatief zijn mits voldoende zanddichtheid in de aansluitingen kan worden gegarandeerd. De getoonde analyse kan alleen als haalbaarheidsanalyse worden beschouwd en kan op geen punt worden gebruikt voor ontwerpdoeleinden.

Het deformation model uit JIP HaSPro (2023) is gebruikt om de benodigde steengroottes voor een dynamisch stabiele bodembescherming met een maximaal toelaatbare deformatie van 0.5 meter te berekenen. Dit is gedaan met de 90% zekerheidswaarden. Er is een vereenvoudigde extreme-waardenanalyse uitgevoerd om voorlopige ontwerpcondities af te leiden. Deze condities zijn gebaseerd op de golfcondities met een terugkeerperiode van 50 jaar.

Figuur B toont de vereiste steengroottes voor een dynamische bodembescherming met een maximaal toelaatbare deformatie van 0.5 meter. De figuur laat zien dat de meest ondiepe locaties het zwaarst moeten worden beschermt. Dit gaat voornamelijk over de toppen van de zandbanken, waar de grootste stenen nodig zijn. Deze zandbanken bevinden zich in het zuidoosten van NW-II/III en in het noordwesten van NW-I.Een 2-8" of 3-9" sortering kan het grootste deel van NW-I en de noord-westelijke secties van NW-II/III beschermen als steen met een hoge dichtheid wordt gebruikt. Deze sorteringen worden vaak gebruikt als enkel-laagse erosiebescherming. Als de sorteringsbreedte voldoet aan de interne stabiliteitscriteria, kunnen deze sorteringen dienen als een enkel-laagse erosiebescherming bij Nederwiek. Alleen de ondiepere gebieden vereisen strikt een dubbele laag erosiebescherming op basis van externe stabiliteit. Verder kunnen enkele locaties in NW-I worden beschermd met normale dichtheid rots met een sortering van 3-9".

De golflast neemt in NW-II/III over het algemeen toe van het zuidwesten naar het noordoosten. De maximale ontwerpgolfhoogte en ontwerpstroomsnelheid bevinden zich in de noordoostelijke hoek van NW-II/III. Hierdoor vereist het noordoostelijke deel van NW-II/III een zwaardere bescherming dan wordt verwacht voor andere locaties met dezelfde waterdiepte. De erosiebescherming in NW-I

moet worden berekend op de voorspelde bodemveranderingen door bodemvormmigratie. De migrerende zandgolven in NW-I kunnen bodemveranderingen van enkele meters veroorzaken. De bodembescherming zal voorkomen dat de bodem nabij de fundering zal worden verlaagd, maar op enige afstand zal de bodem zakken. Dit resulteert in een verhoogde belasting op de erosiebescherming doordat de bodembescherming uitsteekt. Verder kunnen er problemen ontstaan met de kabels.

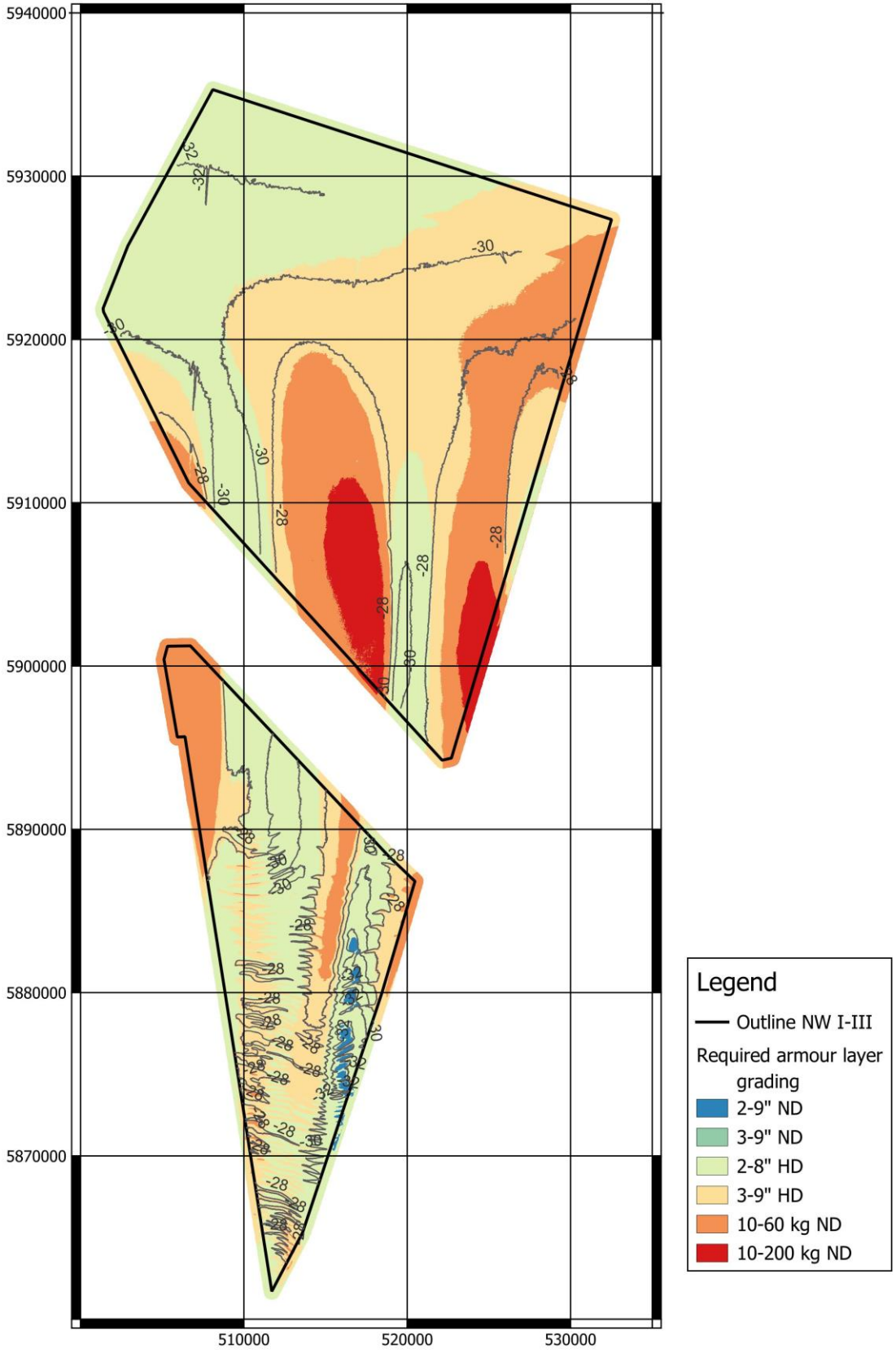

Figuur B: Vereiste gradatie van de beschermlaag om een maximale vervorming van 0,5 m te bereiken in het NWWFZ met 90% betrouwbaarheid. ND = normale dichtheid steen; HD = hoge dichtheid steen

TABLE OF CONTENTS

			Pag.
ABOUT SVAŠEK HYDRAULICS			13
GLOSSARY			14
1	INTRODUCTION		17
	1.1	Background	17
	1.2	Objectives and deliverables	18
	1.3	Important literature	18
	1.4	Structure of report	18
2	NEDERWIEK AREA DESCRIPTION		20
	2.1	Introduction	20
	2.2	Overview of available data	20
	2.2.1	Bathymetry data	20
	2.2.2	Geotechnical and geophysical data	21
	2.2.3	Hydrodynamic data	21
	2.2.4	Summary and gap analysis	22
	2.3	Hydrodynamic properties	22
	2.4	Geotechnical and sedimentological properties	24
	2.5	Seabed morphodynamics	25
	2.6	Sediment mobility	29
3	SCOUR AND SCOUR MITIGATION STRATEGIES		31
	3.1	Introduction	31
	3.2	General description of scour	31
	3.2.1	Scour characteristics and classification	31
	3.2.2	Scour around offshore structures	32
	3.3	Scour mitigation without bedform migration	34
	3.3.1	Strategy A: Free scour development	34
	3.3.2	Strategy B: Immediate scour protection	35
	3.3.3	Strategy C: Monitor & react	36
	3.4	Scour mitigation with bedform migration	37
	3.4.1	Strategy A: Free scour development	37
	3.4.2	Strategy B: Immediate scour protection	37
	3.4.3	Strategy C: Monitor & react	38
	3.5	Recommendations for strategies in Nederwiek	39
4	SCOUR PREDICTIONS		41
	4.1	Introduction	41
	4.2	Scour modelling approach	41
	4.2.1	Scour prediction model	41
	4.2.2	Data availability	43
	4.2.3	Stochastic parameters	45
	4.2.4	Non-stochastic parameters	45
	4.2.5	Simulation period	46
	4.2.6	Grid resolution	46
	4.3	Scour at similar sites	47

	4.4	Scour at different types of construction	49
	4.4.1	Introduction	49
	4.4.2	Monopiles	49
	4.4.3	Piled jacket structures	56
	4.4.4	Suction bucket jackets	56
	4.4.5	Gravity based structures	57
	4.5	Summary of site-specific conclusions	58
	4.5.1	NW-I	58
	4.5.2	NW-II/III	60
5	SCOUR PROTECTION METHODS		63
	5.1	Introduction	63
	5.2	Design requirements for a scour protection	63
	5.2.1	External stability requirement	63
	5.2.2	Interface stability requirement	64
	5.2.3	Flexibility stability requirement	64
	5.3	Scour protections consisting of loose rock	65
	5.3.1	Introduction	65
	5.3.2	Double-layered scour protections	65
	5.3.3	Single-layered scour protections	65
	5.3.4	Statically stable scour protections	65
	5.3.5	Dynamically stable scour protections	66
	5.4	Scour protections consisting of mattresses	66
	5.5	Alternative scour protection methods	67
	5.6	Site specific conclusions	67
	5.6.1	NW-I	67
	5.6.2	NW-II and NW-III	68
6	FEASIBILITY LEVEL SCOUR PROTECTION		69
	6.1	Introduction	69
	6.2	Model approach	69
	6.3	Input parameters	70
	6.3.1	Input parameters and boundary conditions	70
	6.3.2	Rock gradings	72
	6.4	Feasibility level armour layer gradings	72
	6.5	Site specific conclusions	75
	6.5.1	NW-I	75
	6.5.2	NW-II/III	77
7	CONCLUSIONS AND RECOMMENDATIONS		79
	7.1	General Conclusions	79
	7.2	Conclusions NW-I	80
	7.3	Conclusions NW-II/III	84
8	REFERENCES		87

ABOUT SVAŠEK HYDRAULICS

Svašek Hydraulics is a specialised consulting firm in coastal engineering, harbour design, and river engineering. Our activities primarily revolve around studying flow and waves, sediment transport and morphological changes in the seabed caused by these hydrodynamic processes. We work in various water environments, including coastlines, seas, estuaries, and rivers. The concept of “Building with Nature” is deeply embedded in our approach.

Our clients include government agencies, water boards, harbour authorities, contractors, industrial companies, and consulting firms. From our office in Rotterdam, we are actively engaged in projects spanning the globe.

Knowledge and expertise are central at Svašek Hydraulics. This includes process knowledge of waves, currents, and sediment transport, as well as hands-on experience with surveys and their analysis. This fundamental knowledge is supported by years of expertise in (in-house) advanced numerical models.



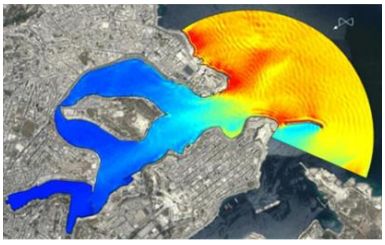

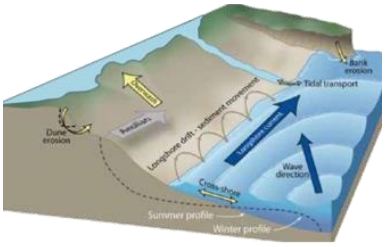

GLOSSARY

Armour layer	The top layer of a scour protection
Backfilling	The re-filling of the scour hole with sediment due to a change in hydrodynamic or morphological conditions
BEB	Best-estimate bathymetry, on average the best estimate of future seabed levels. Locally this level can differ from the actual measured seabed level for a specific year
Bedform migration	The movement of sedimentary structures (sand waves, megaripples) across the seabed due to waves or currents
BSF	Below seafloor
Crest	The highest point of a sandbank, sand wave or megaripple
D_{50}	The representative or average diameter of sediment particles, often used to describe the grain size distribution in a material
Deformation	The displacement of the material used in the scour protection
Design flow velocity	The flow velocity which the scour protection is designed to be able to withstand
Design wave height	The wave height which the scour protection is designed to be able to withstand
Dynamically stable scour protection	A scour protection where some deformation of stones is allowed under the design conditions
Edge scour	Scour on the interface between the scour protection and the unprotected seabed
Equilibrium scour hole depth	The long-term averaged depth of the scour hole after it has formed completely
EVA	Extreme Value Analysis
EVD	Extreme Value Distribution
Filter layer	The intermediary layer between the armour layer and the seabed.
Fines content	The percentage of finer material found in a sediment sample
Global scour	The scour around multiple, closely placed structures where scour from the individual structures interact with one another and combine
Grain size	Size of the sediment particles (diameter) with specific metrics used (e.g. D_{50} corresponds to the median grain size)
HD	High density stone (3050 kg/m^3)
H_s	Significant wave height
IJV	Ijmuiden Ver
KC	Keulegan-Carpenter number
K_s	Hydraulic roughness as a function of particle size
LAT	Lowest Astronomical Tide
Local scour	The scour around one individual structure or around one component of the structure
LSBL	Lowest SeaBed Level, the lowest level to be expected over the considered future period
MBES	MultiBeam Echo Sounder. Measurement equipment for measuring bathymetries
Megaripples	Megaripples Small scale bed features with lengths of several metres and heights up to a few decimetres. Timescales of dynamics are in the order of days
MLW	Mean Low Water

MOB	Undisturbed relative mobility of particles (sediment or rock)
MOB_{th}	Threshold of movement (i.e. when this MOB value is exceeded erosion occurs)
Morphodynamics	Interaction and adjustment of the seabed and hydrodynamic processes as a result of the motion of sediment. In this assessment morphodynamics are considered over period of months (spring-neap cycles) to decades
ND	Normal density stone (2650 kg/m^3)
Non-exceedance	The probability or condition that a given value (such as a flow velocity or scour depth) will not exceed a specified threshold during a certain period or event
NW-I	Description of the southern part of the Nederwiek sites, also known as Nederwiek I
NW-II/III	Description of the northern part of the Nederwiek sites, also known as Nederwiek II/III
NWWFS	Nederwiek Wind Farm Sites
NWWFZ	Nederwiek Wind Farm Zone
Peak over threshold	A statistical method used in extreme value analysis where only data points that exceed a specified threshold are considered, focusing on the most extreme events in a dataset
Relative velocity	The ratio between fully current dominated conditions (U_{rel} = 1) and fully wave dominated conditions (U_{rel} = 0)
Rock grading	The classification of rocks based on their size range and weight for use in construction or protection works, such as in scour protection, to ensure the appropriate size and strength of materials are used for stability
RP	Return period. The period over which it is expected that one of the described conditions occurs. E.g. the RP50 wave height is expected to occur once per 50 years
S	Scour depth
Sand waves	Bed features with lengths of hundreds of metres and heights up to a few metres. Timescales of dynamics are in the order of years to decades
Sandbanks	Largest bed features present which are formed by deflecting tidal current over long timescales. Slow migration with an estimated timescale of centuries
Scour	Erosion of sediments around an obstacle. Obstacles can be foundations, pipelines and cables but also wrecks
Scour hole extent	The distance between the foundation and the deepest point of the scour hole
Scour protection	A protective structure placed to prevent the seabed material from eroding
Sediment mobility	The movement of sediment particles caused by forces such as water currents or waves
S_{max}	The maximum scour hole depth that is predicted to occur in the lifetime of the structure
Spring-neap cycle	Period over which one spring (highest difference between lowest and highest water level) and one neap (smallest difference between lowest and highest water level) tide occur
Statically stable scour protection	A scour protection where no movement of stones is allowed under the design conditions

$T_{backfill}$	Backfilling time scale factor used in the time-dependent scour model. Characteristic time scales of backfilling as calculated by the formulations in Raaijmakers and Rudolph (2008) are multiplied with this factor for erosion events. Factor is included as a sensitivity range to the predictions
Timescale of scour	The time it takes for the scour hole to develop to it's equilibrium depth under certain environmental conditions
TNW	Ten noorden van de Waddeneilanden
T_p	Peak wave period
Trough	The lowest point of a sandbank, sand wave or megaripple
T_{scour}	Scour time scale factor used in the time-dependent scour model. Characteristic time scales of scour as calculated by the formulations in Raaijmakers and Rudolph (2008) are multiplied with this factor for erosion events. Factor is included as a sensitivity range to the predictions
U_c	Depth averaged flow velocity
U_{rel}	Relative current velocity, provides the ratio between ambient current velocity (Uc) and wave-induced orbital velocity (Uw): Urel = Uc / (Uc + Uw)
U_w	Wave-induced orbital velocity
WFS	Wind Farm Sites
WFZ	Wind Farm Zone
Winnowing	The suction removal of seabed material through the scour protection
ρ_s	Density of soil or rock
ρ_w	Density of water

1 INTRODUCTION

1.1 Background

As part of its climate goals, the Dutch Government aims to install 55 TWh/a of offshore wind energy by the end of 2032. Offshore wind farms will be built within designated Wind Farm Zones. Within the designated Wind Farm Zones, the government defines the specific Wind Farm Sites (WFS) where wind farms can be constructed, using a so-called Wind Farm Site Decision ('Kavelbesluit'). This Wind Farm Site Decision contains all conditions for building and operating a wind farm on that specific site.

Wind farm developers can apply for tenders for the permits to build and operate a wind farm according to a Wind Farm Site Decision. The Dutch Government will grant the winners a permit and a grid connection to the mainland. In this context, the Dutch Government has requested RVO to prepare, collect, and publish comprehensive site data for several Wind Farm Zones, which wind farm developers can use to prepare a competitive bid.

RVO and Dutch transmission system operator TenneT have started preparations for further development of the Nederwiek Wind Farm Zone (NWWFZ) under the 21 GW roadmap. The Nederwiek Wind Farm Sites (NWWFS) I-III (up to 6,000 MW) are currently being developed for tendering.

The NWWFS is divided into three different zones, Nederwiek-I (NW-I), Nederwiek-II (NW-II), and Nederwiek-III (NW-III). RVO will make all three zones available for separate tendering. The distinction between NW-II and NW-III has not yet been made. These two zones are therefore considered in conjunction as zone 'NW-II/III'. Figure 1-1 provides an overview of the NWWFS.

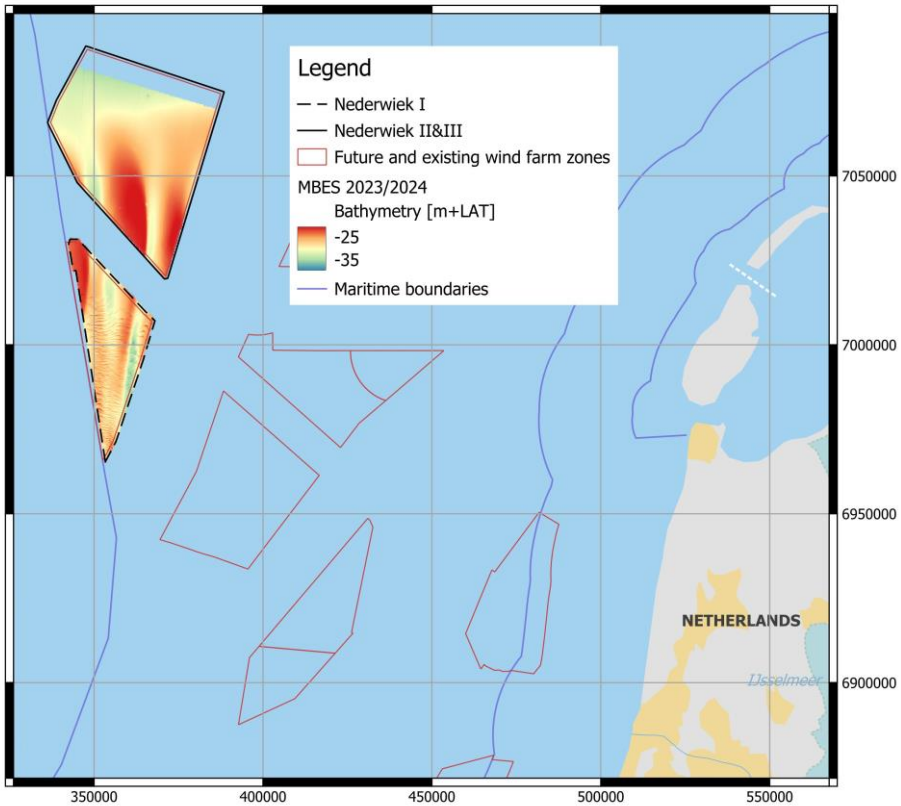

Figure 1-1: Overview of the Nederwiek sites with respect to the Dutch shoreline and future/existing wind farm zones. NW-I is shown with the black dashed line and NW-II/III with the black solid line.

1.2 Objectives and deliverables

The NWWFS study aims to improve the understanding of the seabed morphology, morphodynamics, and infrastructure-related scour potential at the Nederwiek Wind Farm Zone (NWWFZ). These objectives are separated into two reports. The first report focuses on the seabed morphology and morphodynamics at Nederwiek (Svašek Hydraulics, 2024). This report focuses on the infrastructure-related scour and potential scour protections at NWWFZ.

The aim of this scour and scour protection study is to identify and categorize the NW-I and NW-II/III sites concerning the scour depths that may be anticipated as a result of the installation and long-term presence of typical wind farm infrastructure and how such scour may be mitigated. These categorizations are made separately for NW-I and NW-II/III, as the sites will be tendered separately.

The outcome of this study is presented in a descriptive report (this document), a webinar and a GIS archive for the predicted feasibility-level scour depths and indicative scour protection rock gradings at NW-I and NW-II/III.

1.3 Important literature

This report uses the 'Handbook of Scour and Cable Protection Methods' (JIP HaSPro, 2023). This handbook results from a multi-year research programme performed as a Joint Industry Project with the contribution of over 20 industrial partners, including Deltares, DNV, utility-companies, suppliers, engineering firms, and installation contractors. The handbook gives a detailed description of scour, scour mitigation strategies, and scour protection methods. In it, a novel scour protection deformation model is developed based on hundreds of individual test results on different scales. This study uses that model to design a feasibility-level armour layer of loose rock scour protection. Besides JIP HaSPro (2023), reference is made to previous Scour and Scour Mitigation studies from IJmuiden Ver (IJV) Wind Farm Zone and Ten noorden van de Waddeneilanden (TNW) Wind Farm Zone (Deltares, 2022; Deltares, 2023).

1.4 Structure of report

This report starts with an overview of the hydrodynamic and morphological data analysis at the NWWFZ in Chapter 2. This analysis includes the hydrodynamic and sedimentological properties, seabed morphodynamics, and sediment mobility. The study presented in this document summarizes the extensive analysis performed in Svašek Hydraulics (2024).

Chapter 3 follows the area description with a general description of scour and scour mitigation strategies. This chapter explains the scour process, how scour develops around offshore structures, and how to mitigate scour. These mitigation strategies are presented both with and without bedform migration. The chapter ends with the recommended strategies in the NWWFZ.

The feasibility level scour predictions are explained in Chapter 4. Scour predictions are quantified for monopile foundations with a pile diameter of 12 meters and are qualitatively extended for different foundation types. The chapter starts with an extensive description of the methodology used for the scour predictions, followed by an analysis of scour at similar offshore wind farm sites. The methodology is followed by the scour predictions for different construction types, including monopiles, piled jacket structures, suction bucket jackets, and gravity-based structures. The chapter ends with site-specific summaries of the scour predictions separated for NW-I and NW-II/III.

The second half of the study focusses on scour protection, starting with the scour protection methods in Chapter 5. This chapter highlights the requirements of a scour protection, and several

scour protection methods. The loose rock protection method is explained in more detail. The chapter ends with site-specific conclusions for NW-I and NW-II/III.

Chapter 6 explains the design of the armour layer of a feasibility-level scour protection. This chapter starts with the methodology and input parameters and ends with spatial maps of the required amour layer gradings for several non-exceedance values. This chapter ends with site-specific summaries for NW-I and NW-II/III.

This study ends with the conclusions in Chapter 7. These conclusions are separated into general conclusions and site-specific conclusions for NW-I and NW-II/III. The general findings entail the valid conclusions for the entire NWWFZ, whereas the site-specific conclusions focus only on the relevant findings for the considered sites.

2 NEDERWIEK AREA DESCRIPTION

2.1 Introduction

This chapter gives a more fundamental understanding of the environmental conditions at the NWWFZ. This serves as a basis for the analyses later in this study. The area description that is presented in this study is a summary of relevant parts of the Morphodynamics report (Svašek Hydraulics, 2024). The reader is referred to this report for more detail.

The data availability and reliability are discussed in Section 2.2. This includes the bathymetry data, the geotechnical and geophysical data, the hydrodynamic data, and the missing data from the gap analysis. The data availability is followed by more detailed analyses of each section, starting with the hydrodynamic properties at the NWWFZ in Section 2.3. This includes analysis of the tidal flow and the wave conditions. The sedimentological properties are discussed in Section 2.4, which primarily aims to describe the variations in seabed material at the NWWFZ. The seabed morphodynamics follows this in Section 2.5. This section aims to give insight into the prevailing bedforms and expected seabed variability due to bedform migration at the NWWFZ. The chapter ends with the sediment mobility in Section 2.6, which gives insight into the most dominant drivers of sediment transport in the NWWFZ.

2.2 Overview of available data

2.2.1 Bathymetry data

By commission of RVO, additional field survey campaigns have been performed for the NWWFZ. This means that in every location in the NWWFZ, high-resolution (25 m or finer) and low-resolution bathymetries are available. These recent surveys are multi-beam surveys (MBES) with a high resolution in the order of meters (Fugro, 2023,2024a),. The bathymetry of NW-I is shown in Figure 2-1, and the bathymetry of NW-II/III in Figure 2-2.

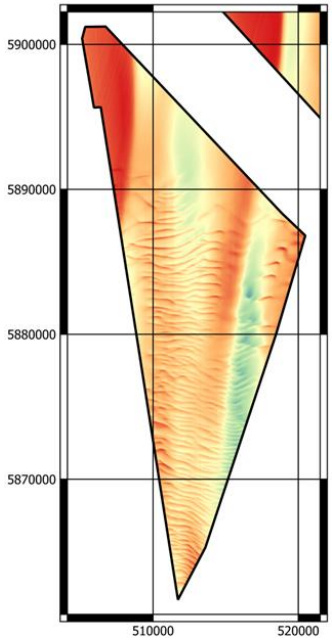

Figure 2-1: 2024 measured bathymetry of NW-I.

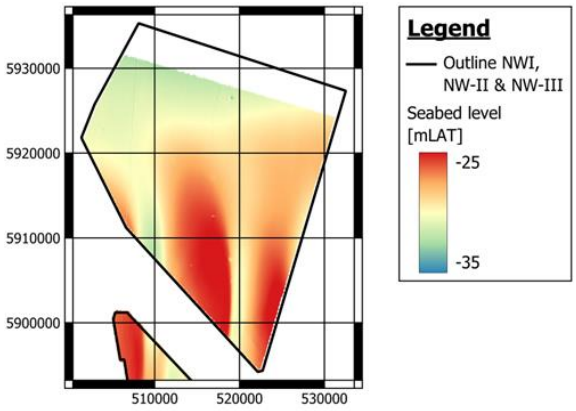

Figure 2-2: 2024 measured bathymetry of NW-II/III.

2.2.2 Geotechnical and geophysical data

Geotechnical data is used to determine the bed composition in terms of grain size, fine content, and erodibility properties. Fugro performed several grab samples, vibrocores and cone penetration tests in the Nederwiek area (Fugro 2024b, 2024c). For several of the Vibrocore samples, additional Laboratory Vane Tests were performed, which indicate the samples' resistance and can be used to estimate the erodibility. The vibrocores reach up to a depth of maximum 5m below the surface. In addition, grain size samples and a surficial seabed composition model are available from the DINOloket (DINOloket, 2024). An overview of the locations of this data and their depth-averaged D50 is presented in Figure 2-3.

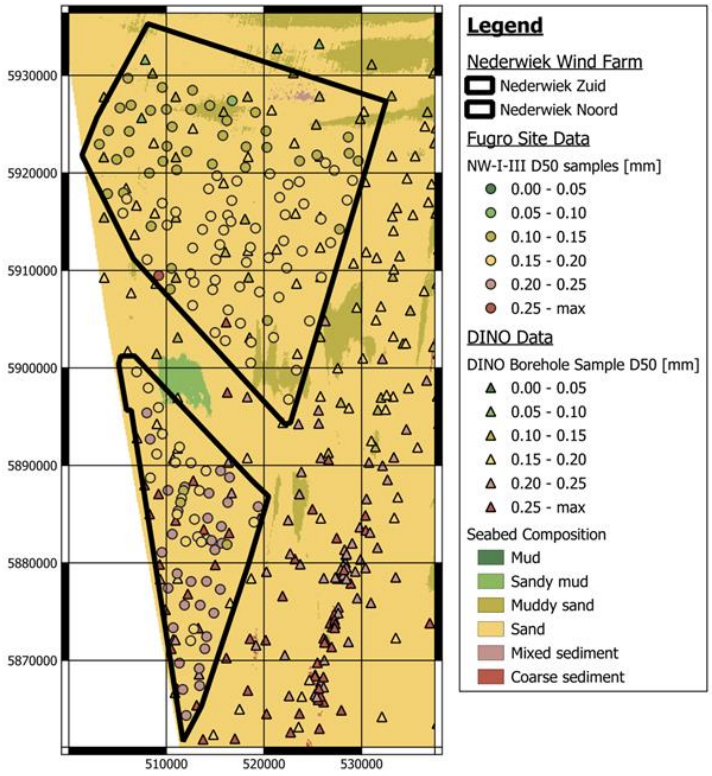

Figure 2-3: Grainsize of Fugro and DINOloket samples together with an overview of seabed composition for the NWWFZ.

2.2.3 Hydrodynamic data

Site specific metocean measurement data collected in the vicinity of the NWWFZ is scarce. Therefore, this study mostly relies on numerical modelling data for the hydrodynamic conditions. The highest resolution metocean modelling study performed near the NWWFZ is by DHI (2023a; 2023b). This dataset is made available via the RVO metocean portal. The spatial resolution of the data in the NWWFZ is approximately 400 m. From the metocean portal, time series of wave parameters, water level parameters and depth-averaged currents are available between January 1st 1979 and September 30th 2023, so almost 45 years. Given the large amount of data, the full dataset has been provided by DHI via data disks.

Quality control has already been performed during the calibration and validation part of this metocean study (DHI 2023a). Nevertheless, data comparisons have been performed, which confirmed that the model data is well capable to represent both operational and extreme conditions at locations K13, NWA and NWB. This gives confidence that the model data can be used as input for design studies for the entire NWWFZ.

2.2.4 Summary and gap analysis

The geotechnical and geophysical data availability is large. However, in-situ measurements are mainly available for surface layers. This makes it more difficult to estimate properties and compositions of deeper layers. As a result not much certainty regarding the extent and homogeneity of deeper low-erodibility clay layers is available. As a consequence no low or non-erodibility layers are accounted for in the scour analysis. Locations where low- to non-erodible material has been found are indicated in the produced scour maps.

The only identified data gap is that extreme value statistics were only available at three distinct locations (at the moment of performing the present study). Therefore, in each grid point an extreme value analysis has been performed. This is documented in Appendix B.

2.3 Hydrodynamic properties

The spatial variation of the average current magnitudes (left panel) and the average wave height (right panel) in the NWWFZ (averaged over the period 1980-2022) are depicted in Figure 2-4. The time series of the wave and current data at one location in NW-II/III are shown in Figure 2-5 as an example of the temporal variation. For more information, see Svašek Hydraulics (2024) Chapter 6.

The flow velocities are the highest and relatively spatially uniform in NW-I. NW-II/III shows more spatial variability of the flow velocities with a general trend of decreasing flow velocities towards the north of the area. The flow velocity is typically mild, exceeding 1 m/s only a few times in 43 years. The flow velocity rarely exceeds 0.7 m/s, with typical peak velocities of 0.6 m/s per tidal cycle.

The dominant current directions show spatial variability. In NW-I, the dominant flood direction is relatively uniform to the north-northeast. The primary tidal flow can be slightly asymmetrical, with the dominant ebb direction varying between the south-southwest and the south-southeast. The peak flood velocities are, on average, around 10-20% higher than the peak ebb velocities.

In NW-II/III, the dominant flood and ebb directions are less spatially uniform. The pattern in the south and northeast of the area is similar to NW-I, with dominant flood directions towards the north-northeast and dominant ebb directions to the south-southeast. Further northwest, the dominant ebb direction moves more towards the southeast to east. The peak ebb and peak flood velocities are nearly equal. Note that the flow velocities northwest of NW-II/III are significantly lower than the rest of the NWWFZ.

The wave heights follow the flow velocities' inverse spatial pattern, though the differences' absolute magnitude is relatively low. The wave heights are relatively low and uniform in NW-I. More variability is observed in NW-II/NW-III, with a general trend of increasing wave heights north of the area. The wave height remains below 4 meters for most of the 43-year period and rarely exceeds 6 meters. The main wave directions are from the north and the south-southwest. This is relatively uniform throughout the entire Nederwiek site.

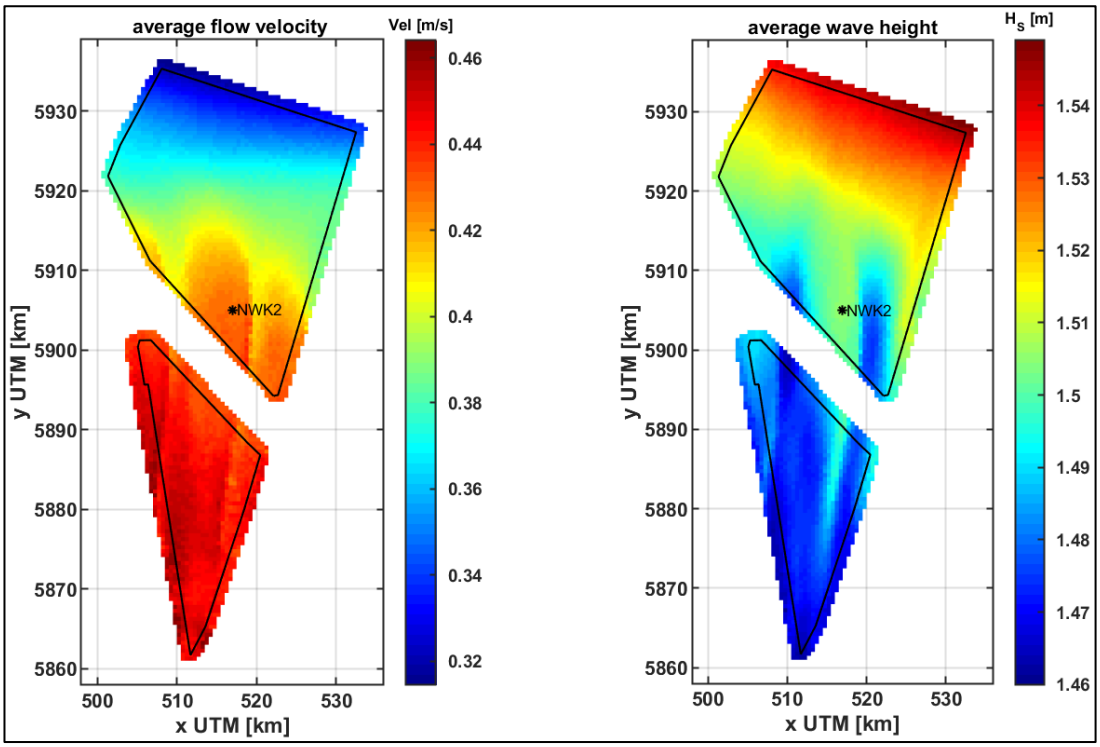

Figure 2-4: Spatial variation of the current magnitudes (left panel) and significant eave height (right panel), averaged over the period 1980-2022. The location of NWK2 (next figure) is shown with the black star.

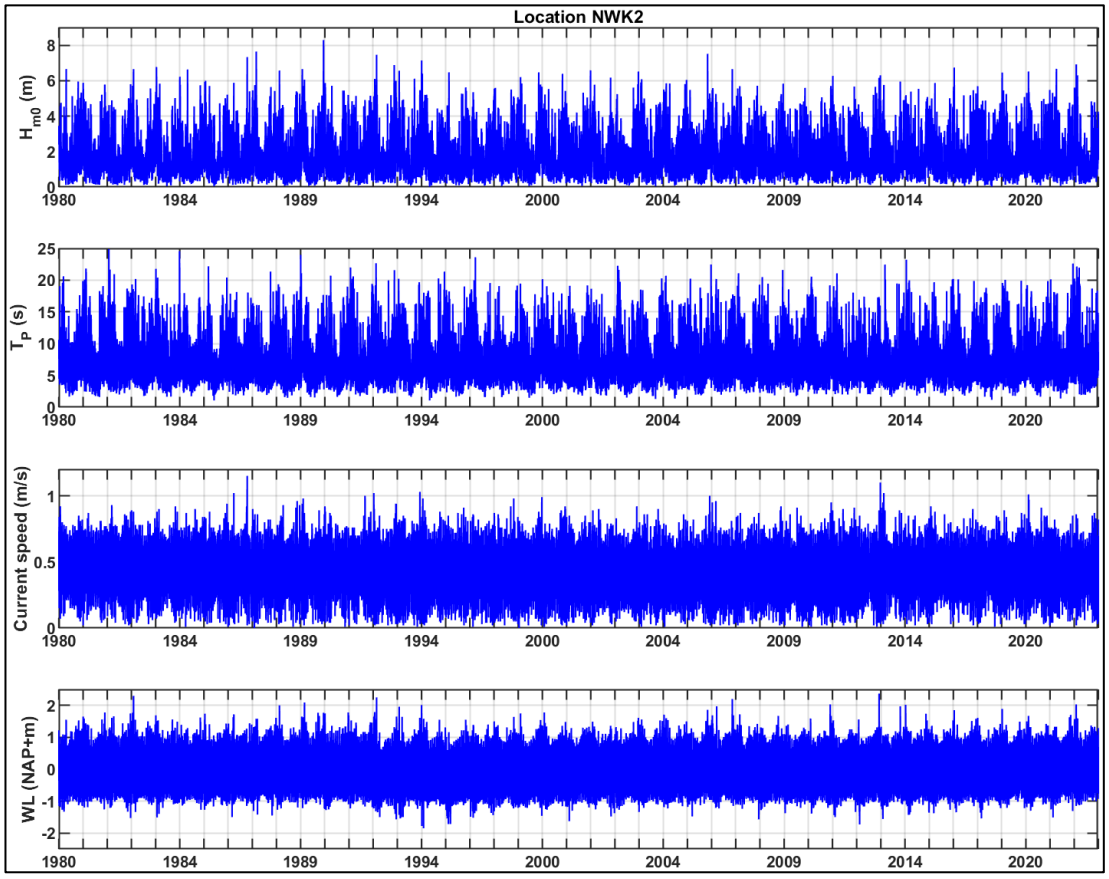

Figure 2-5: Time series of the wave and current data at output location NWK2, period 1980-2022

2.4 Geotechnical and sedimentological properties

The seismostratigraphic analyses indicate that the top layers (1-10 mBSF/-31 to -38 mLAT) at the sites mainly consist of (fine) sand. With loose to very dense slightly silty fine and medium sand, with shells and shell fragments. These are interpreted to be Holocene marine sediments of the Southern Bight Formation. Deeper layers may consist of sand with beds of silt, clay and peat between -34 to -59 mLAT. Clay layers are only found between -37 to -46 mLAT. This is substantiated by the vibrocore analysis that show that the surface layers at the NWWFZ consist almost everywhere of sandy material.

Some patches where low- to non-erodible material are present at a depth between 5 and 19 meter below the seabed. The cohesive material, as found in the Vibrocores, with peak shear strengths of 15-50 kPa, is likely to have low to very low erodibility. However, little is available in the literature on the erosion properties of cohesive material with these shear strengths. Figure 2-6 shows the spatial variation in the depth of this cohesive layer.

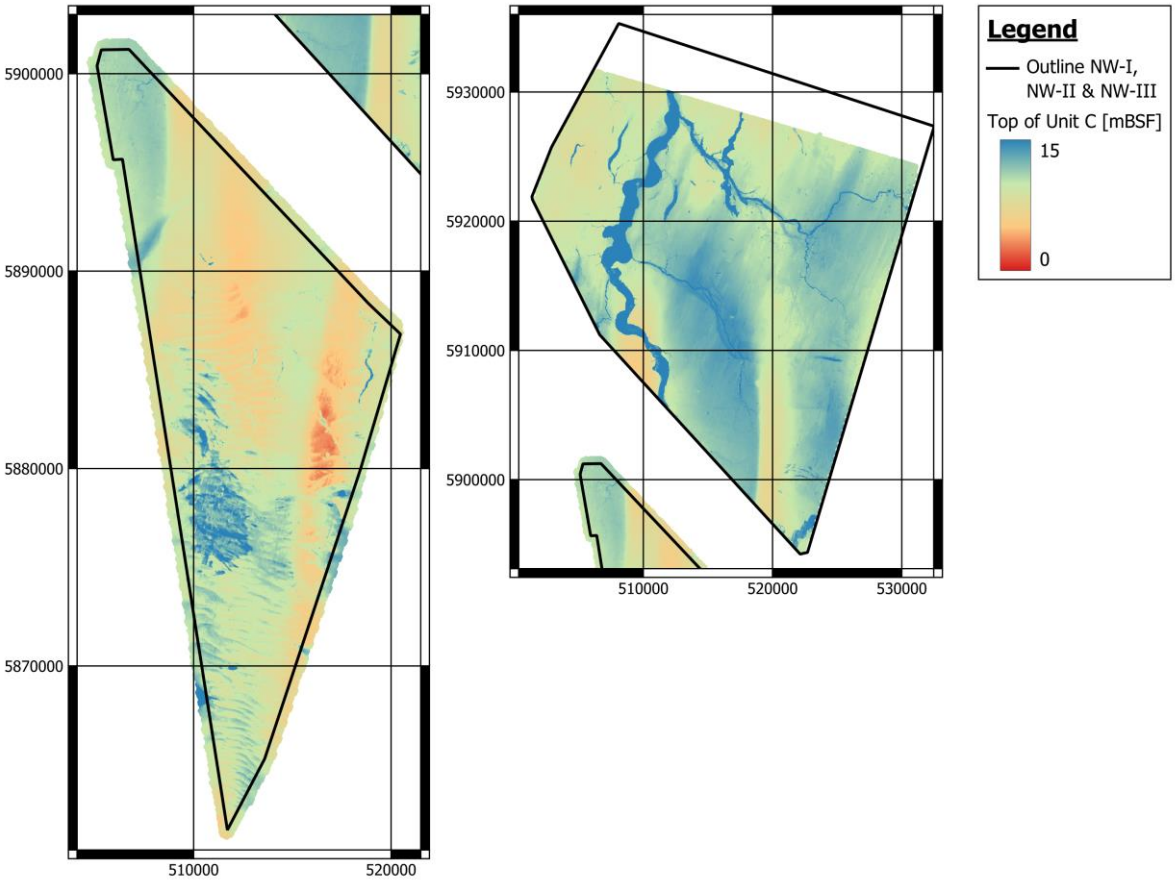

Figure 2-6: Depth of the top of Unit C below the seabed surface for NW-I (left) and NW-II/III (right).

Considering the patchy nature of the presence of the clay unit, it is assumed in the scour analysis of Chapter 4 that no continuous non-erodible layers are present. Patchy non to low-erodible material is present and will be indicated in the scour maps as zones where scour depths may be reduced by the low erodibility of the subsoil.

For the whole area of the NW-I, NW-II and NW-III the D_{50} decreases from the south to the north from about 0.220 mm to 0.120 mm. The site of NW-I shows the largest variation across the field where in the north-western part deeper layers with finer material are present. These also impact the depth-

averaged D_{50} as can be seen in Figure 2-7. The decrease in D_{50} across NW-I is from about 0.220 to 0.160 mm.

NW-II/III shows little variation in overall D50. From south to north the D_{50} decreases from about 0.160 to 0.120 mm. With respect to the spatial D90 distribution, Figure 2-7 shows a stronger gradient from south to north. D_{90} decreases from about 0.320 to 0.164 mm.

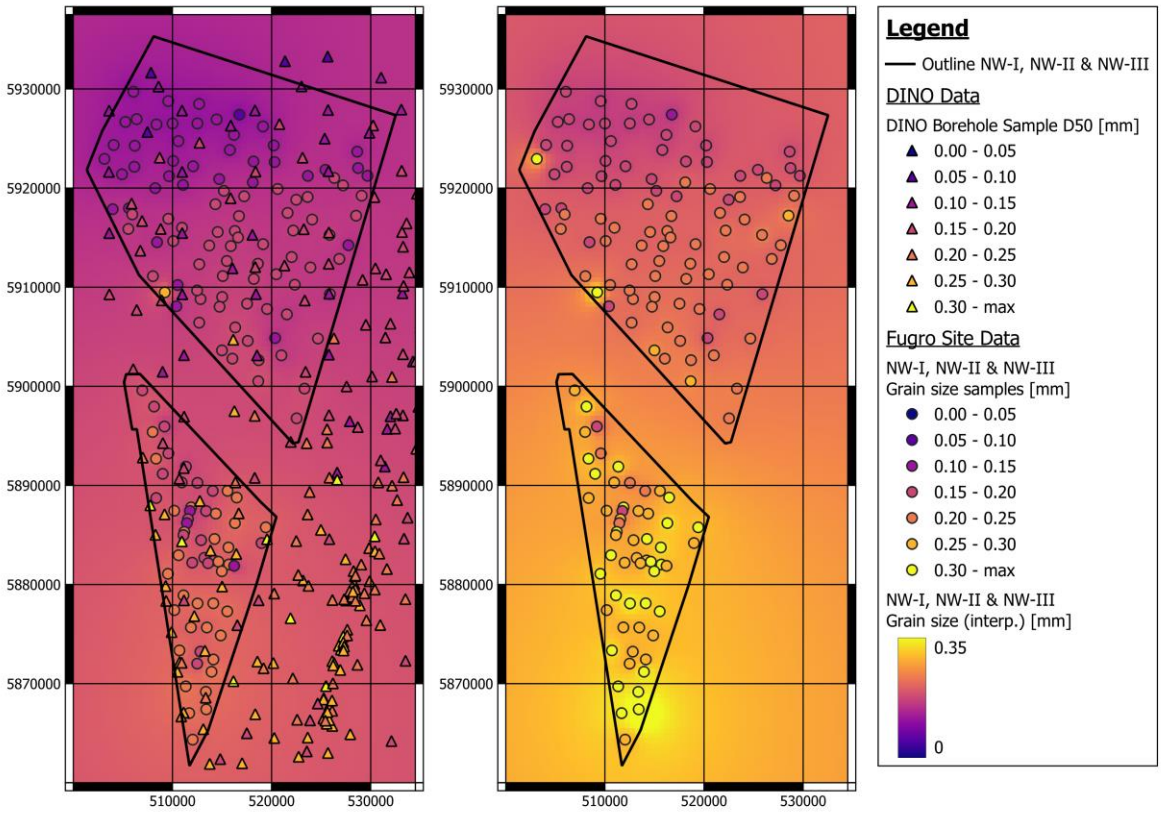

Figure 2-7: Spatial distribution of the median grain size diameter (D_{50}, left) and the 90% passing grain size (D_{90}, right).

2.5 Seabed morphodynamics

Figure 2-1 and Figure 2-2 show that the bed in the NWWFZ is not entirely flat. Different types of wave-like bed shapes occur under the influence of the interaction of hydrodynamic forces (tides, currents, waves) and the sediment forming the seabed. An overview of typical characteristics of the bed features present at the NW-I and NW-II & NW-III sites is presented in Table 2-1. The dimensions and migrating character of sand waves and, to a lesser extent, megaripples can lead to bed level differences up to several meters over the wind farm's lifetime.

Table 2-1: Typical parameters of morphodynamic seabed features at NW-I and NW-II & NW-III sites. The wave lengths and wave heights are indicated with an 'order of magnitude' value by means of the 'O'. Sand waves are the bedforms that result in the largest bed level differences over the wind farm's lifetime.

Bedform	Wave length	Wave heigth	Mobility	Threat to foundations and cables
Sandbanks	*O*(1000) m	*O*(10) m	Stationary	Minimal
Sand wave	*O*(100) m	*O*(1) m	Mobile and persistent	Large
Megaripples	*O*(10) m	*O*(0.1) m	Mobile and transient	Small
Ripples	*O*(0.1) m	*O*(0.01) m	Mobile and transient	Minimal

Sandbanks

There are three main sandbanks present in the area, indicated using arrows in Figure 2-8. These sandbanks are the same in both areas because the NW-II/III sites are located directly north of the NW-I site. The sandbanks are over 5 km wide, around 5 m high, and extend over almost the full length of the NW-I and NW-II/III sites. Only in the northern part of the NW-II/III sites, no sandbanks are present. The sandbanks in the NWWFZ are considered to be stationary with only limited change in the last 20 years.

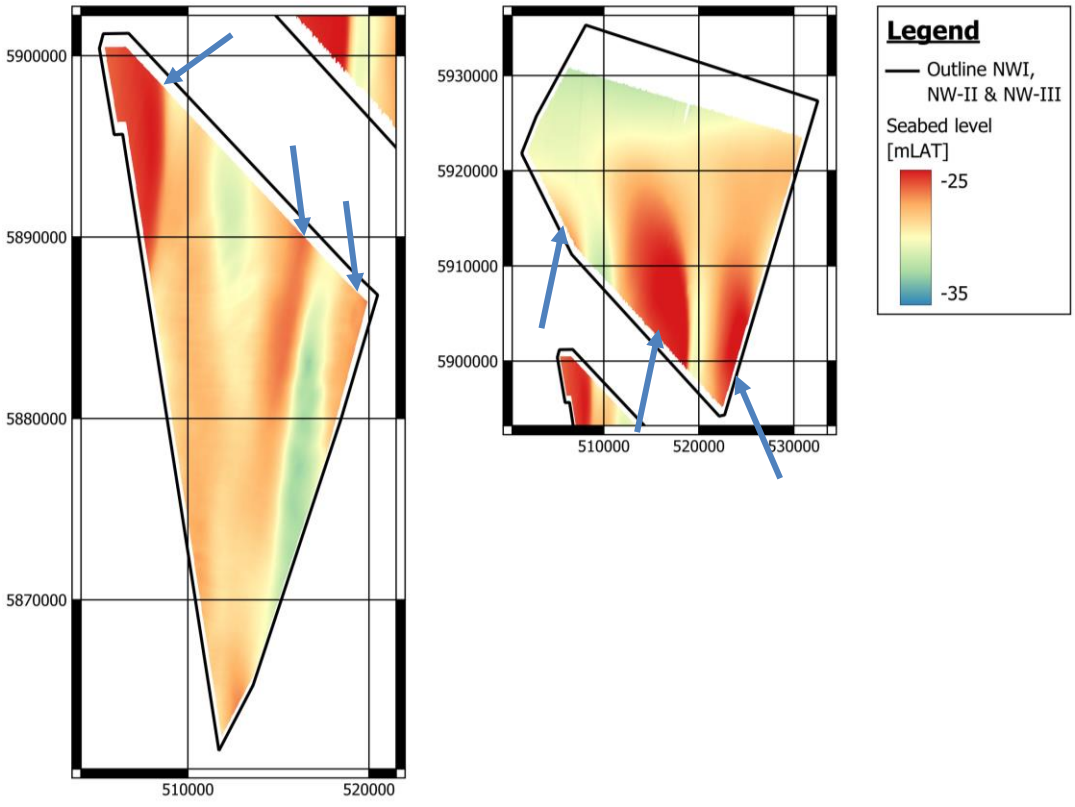

Figure 2-8: Stationary seabed NW-I (left panel) and NW-II/III (right panel). Large sandbanks are present in the area, indicated with arrows.

Sand waves

Sand waves are the largest dynamic bed features present in NW-I, no sand waves occur in NW-II/III. With wave lengths of *O*(100) m, wave heights of *O*(1) m, and migration rates of *O*(1) m/yr or even O(10) m/yr, sand wave migration can cause bed level differences of several meters over the wind farm's lifetime.

The identification of sand waves in the NWWFZ is shown in Figure 2-9. It can be seen that sand waves are present in most of the NW-I site but absent at the NW-II & NW-III site. The sand wave density is highest at the most southern part of the NW-I site, whereas they are absent at the northern part of the NW-I site. The sand wave height varies generally between 1 m – 3 m, and the sand wavelength generally varies between 200 m – 400 m.

The sand waves migrate with rates between 1 m/yr – 3 m/yr, with higher rates in the southern part and lower rates in the northern part of NW-I. The migration directions vary between NNW and NE.

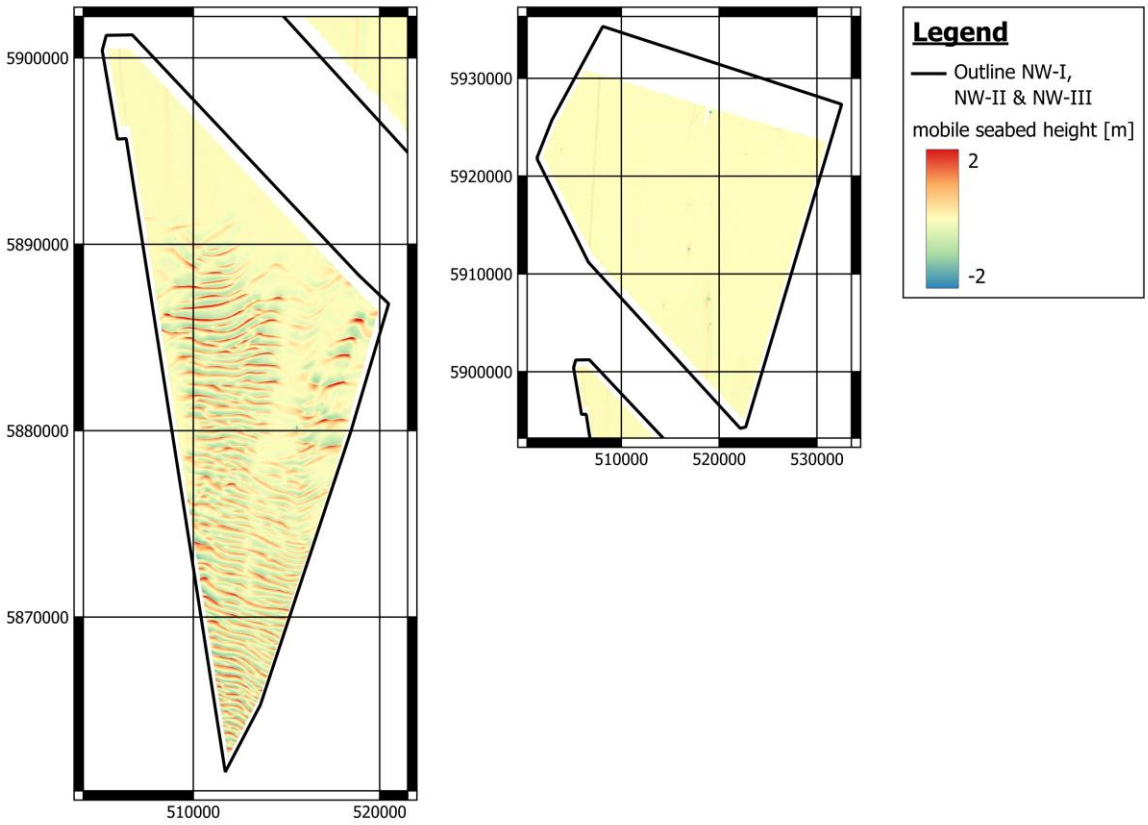

Figure 2-9: Mobile seabed NW-I (left panel) and NW-II/III site (right panel). The mobile seabed consists of the sand waves and megaripples only.

Megaripples

Megaripples are small scale bedforms which are present over almost the whole area of NW-I and NW-II/III. These bed features usually have length in the order of O(10)m and heights in the order of O(0.1)m. Additionally, they have higher migration speeds which cause them to pass over wind turbine foundations several times in its lifetime. Due to the small scale of these features, they do not pose a real threat to the foundations and cables but need to be considered when looking at the future seabed level.

The zones in the NWWFZ where megaripples are identified are shown in Figure 2-10. The figure shows that megaripples are present across the whole field of NW-I. These megaripples have and average height of about 0.25 m with slightly higher crests than troughs.

For the NW-II/III site, Figure 2-10 shows three main areas where megaripples are present. These are in:

1) The northwest where smaller features are present with an average height of 0.06 m.
2) The southeast on top of the sandbank with an average height of 0.09 m.
3) The southeast with an average height of 0.11 m.

The remaining area of NW-II and NW-III does not show any signs of megaripples.

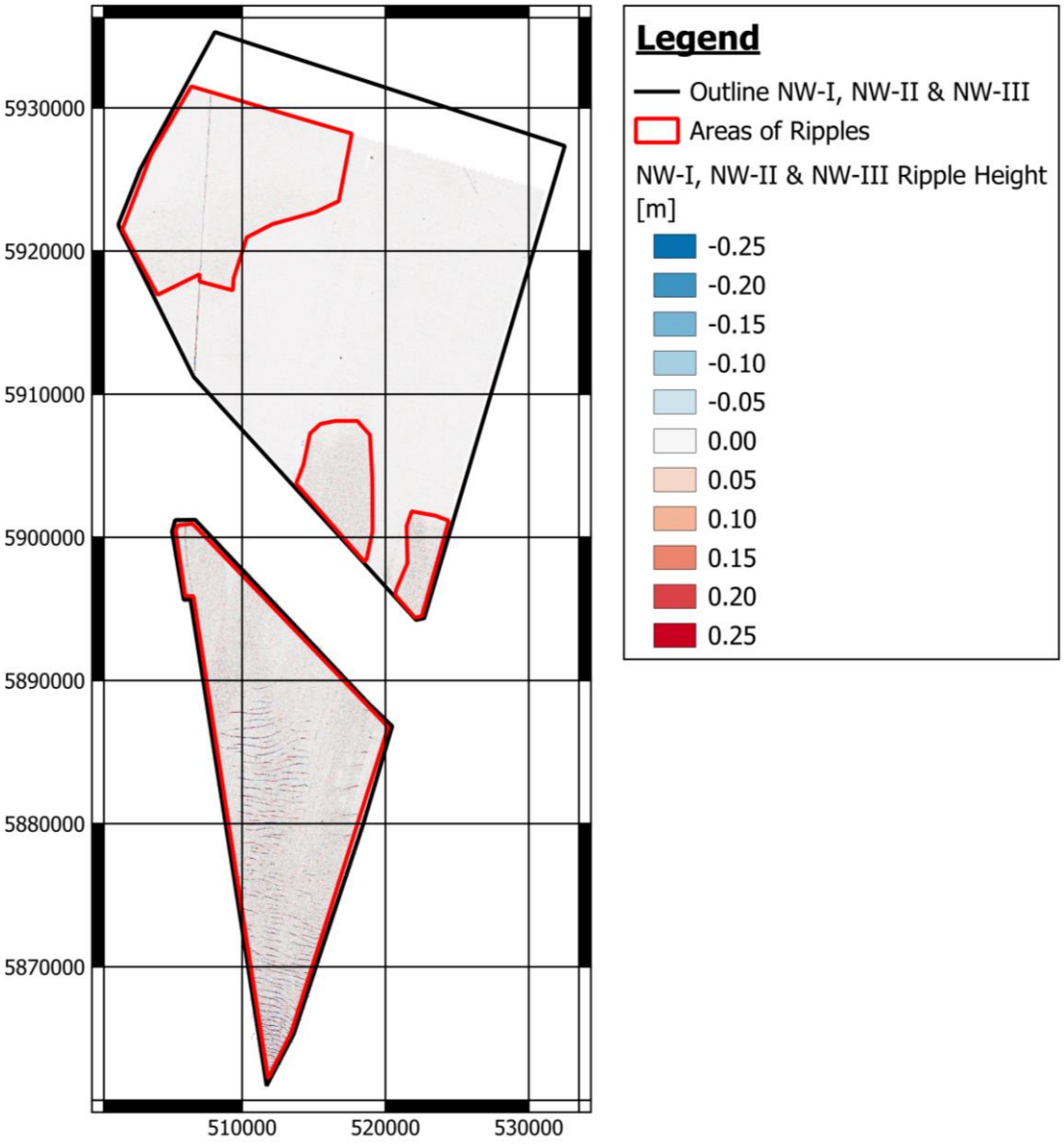

Figure 2-10: Spatial distribution of (mega)ripple fields across the NW-I and NW-II/III sites.

Lowest and highest bed levels

The Lowest Sea Bed Level (LSBL) and Highest Sea Bed Level (HSBL) between 2023 and 2073 are predicted based on the mobility of the seabed. These levels are evaluated with respect to the 2023

bathymetry to indicate the maximum bed level changes (both positive and negative) that can be expected during the lifetime of the wind farm. The magnitude of these changes are visualized for NW-I in Figure 2-11 and for NW-II/III in Figure 2-12.

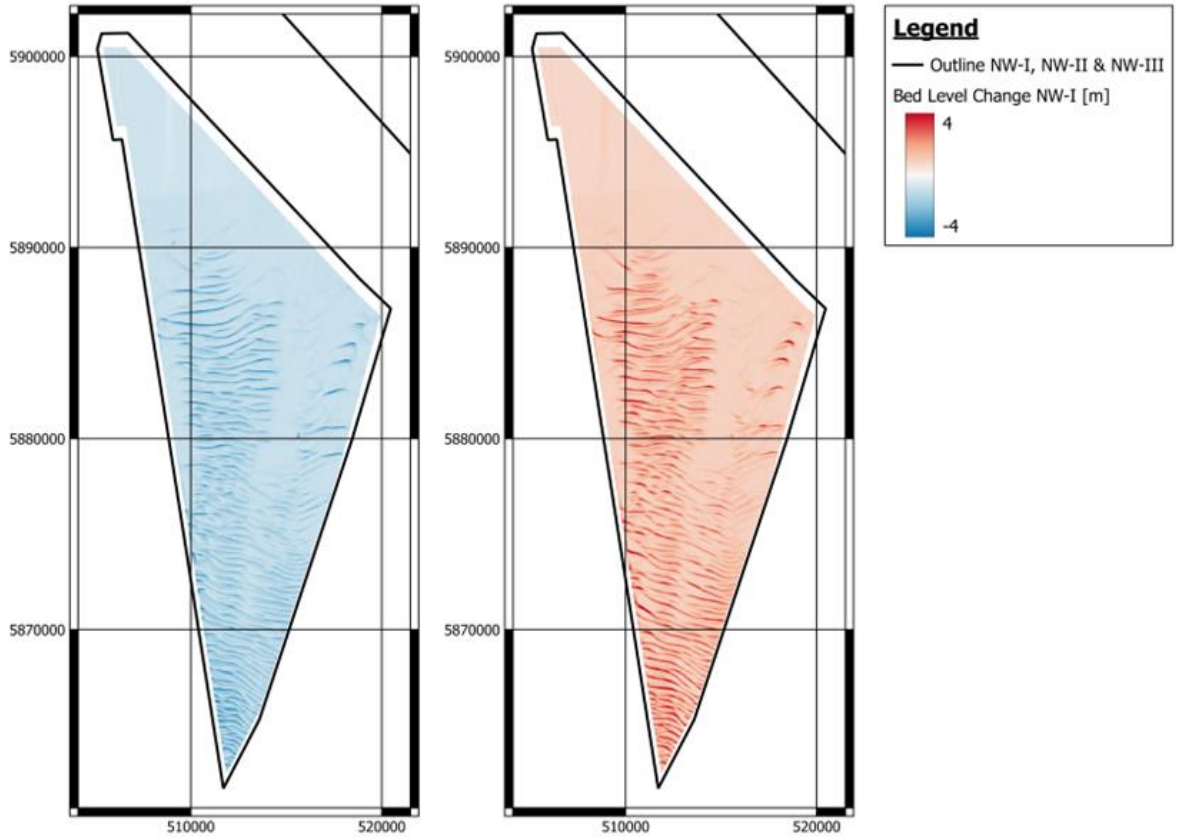

Figure 2-11: Spatial plots of the changes in bed level between the most recent bathymetry and the LSBL (left) and HSBL (right) between 2023 - 2073 including uncertainties.

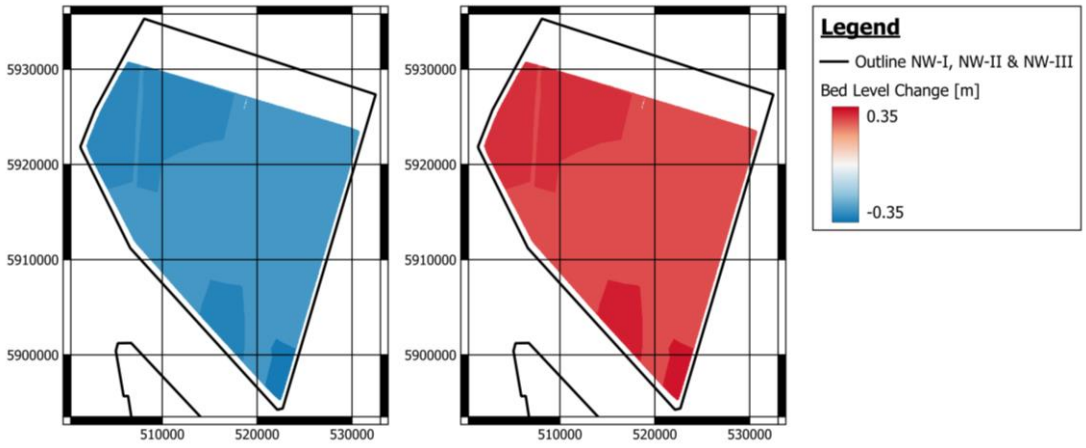

Figure 2-12: Spatial plots of the difference in bed level between the most recent bathymetry and the LSBL (left) and HSBL (right) in 2073 including uncertainties.

2.6 Sediment mobility

Sediment becomes mobile when the forces on the sediment caused by the flow are larger than the resistance of the sediment to the flow. The forces on the sediment are often expressed in the Shields

number (θ) and the resistance of the material in the critical Shields number (θ_{cr}). The ratio between the actual Shields number and the critical Shields number is called the mobility number (MOB). This value indicates how mobile the sediment is under a given flow load. When this number exceeds a value of 1, the sediment becomes mobile.

The sediment mobility can be calculated for the current velocity, the wave load, and the combination of the two. Figure 2-13 shows the sediment mobility caused by all three factors for 2003 at a relatively shallow location in NW-II/III. See Svašek Hydraulics (2024) for more information.

The red-dotted line in Figure 2-13 indicates the mobility threshold of MOB = 1. The currents exceed the sediment mobility threshold in almost every tidal cycle. Wave conditions exceed the mobility threshold less frequently, but can increase mobility significantly with higher wave conditions. As a result, the total mobility is caused by constant sediment mobility due to currents combined with high instantaneous mobility caused by high wave action. It can be concluded that the NWWFZ is current-dominated, as most of the mobility is caused by the frequent exceedance of the mobility threshold due to currents.

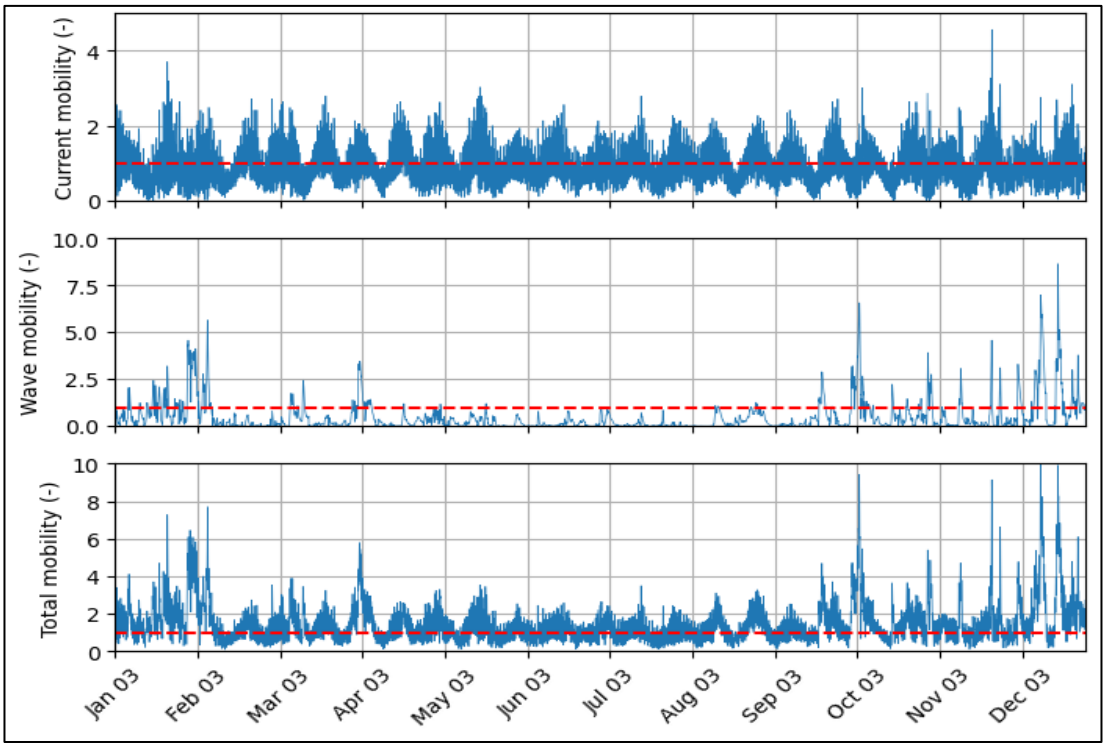

Figure 2-13: Seabed mobility at NWK2 for 2003, due to currents (top panel), waves (middle panel) and the combination of the two (bottom panel). Red dotted line indicates the mobility threshold.

3 SCOUR AND SCOUR MITIGATION STRATEGIES

3.1 Introduction

Scour is the process of erosion resulting in seabed lowering caused by an obstruction of a water flow due to the presence of a structure. The lowering of the seabed is often undesirable and can lead to structural failure. For monopiles, scour can lower the pile fixation level. For gravity-based structures, scour can lead to undermining. The severity of the scour and the potential failure modes caused by scour differ between different types of structures. This chapter explains the process of scour and potential scour mitigation strategies. Chapter 4 addresses the predicted scour depth around monopiles at the NWWFZ and the implications for different foundation types.

The method of dealing with scour can depend on the magnitude of the scour for the considered structure. Scour can either be mitigated or accepted. A mitigation strategy requires a scour protection that can be placed directly or as a reaction to the observed scour. Chapter 5 explains scour protections in more detail. An acceptance strategy requires adapting the foundation design to cope with the lowering seabed. The contractor can choose this strategy when the costs of the adaptations of the foundation is less than the costs of a potential scour protection. Some foundation types are more suitable for this strategy, as discussed in Chapter 4.

This study analyses three different strategies of dealing with scour:

1) Strategy A: Free scour development
2) Strategy B: Immediate scour protection
3) Strategy C: Monitor and react

Strategy A corresponds with the acceptance strategy, which requires adapting the foundation design. Strategy B corresponds with a mitigation strategy, which requires scour protection. Strategy C can either be an acceptance strategy or a mitigation strategy, depending on the development of the scour around the foundation type.

These strategies are considered both with and without migrating bedforms. Section 3.3 evaluates the strategies for a scenario where bedform migrations are omitted from the analysis. ‘Bedform migration’ relates to the sand wave migration expected in NW-I (see Chapter 2).). The height of these sand waves require adapted scour mitigation strategies. Megaripples are also present in NW-I and NW-II/III (Svašek Hydraulics, 2024). The height of these megaripples is sufficiently low that no additional flexibility of the scour mitigation is required. This is explained in section 3.4 and applies to most of NW-II/III. The explanation focuses mainly on monopiles, the most common foundation type. Section 3.5 gives recommendations for strategies applicable to the NWWFZ.

3.2 General description of scour

3.2.1 Scour characteristics and classification

Gradients in sediment transport cause the deposition or erosion of sediment. Spatially-varying hydrodynamic conditions or sediment properties can cause these gradients. When a temporary or permanent structure is placed onto a seabed, its presence disrupts the natural flow. This disruption can result in gradients in sediment transport, which can, in turn, result in either sediment deposition (sedimentation) or sediment erosion. Localized erosion (around a structure) is referred to as scour. For offshore wind farm foundations, the seabed lowering due to scour can influence the stability of the structure and is, therefore, often more important than sedimentation.

Scour can occur in both wave-dominated and current-dominated conditions. The deepest scour holes often appear in current-dominated conditions, which is mostly attributed to the persistency of

the horseshoe vortex in these conditions. In contrast, wave-dominated conditions can suppress the horseshoe vortex (Sumer et al., 1997). Generally, when the structure is subject to waves and currents in deep waters, the scour hole will deepen in current-dominated conditions and backfill in wave-dominated conditions (Sumer et al., 2013).

The process of seabed lowering around offshore structures is further classified into four different definitions (JIP HaSPro, 2023):

- *Local scour:* the scour around one individual structure or around one component of the structure. This can, for example, be a single monopile or one leg of a jacket structure;
- *Global scour:* the scour around multiple, closely placed structures where scour from the individual structures interact with one another and combine. This can, for example, be the scour around a jacket structure with multiple legs;
- *Edge scour*: the scour on the interface between the scour protection and the erodible bed;
- *General seabed level change*: the general changes in the seabed levels that are not influenced by the presence of the structure. This can, for example, be due to the migration of bedforms.

3.2.2 Scour around offshore structures

As discussed above, offshore structures block natural flow and cause disruption. Natural flows are defined as the flow caused by the tide, meteorological effects, and waves.

The structure's blocking effect causes the flow to accelerate and decelerate when passing it. The acceleration occurs towards the sides of the structure, where the flow streamlines contract to pass it. The flow subsequently decelerates as the streamlines diverge behind the structure. Figure 3-1 visualises this process.

The flow around offshore structures is unsteady and non-uniform, both due to flow reversal due to the tide and turbulent flow around the structures. It can be expected that the scour hole is at its deepest downstream of the structure in the direction of the peak ebb and peak flood directions. The shape of the scour hole depends mainly on the shape of the foundation.

Local scour

The governing process for developing the local scour hole varies between structure types. For offshore monopiles, this process is the horseshoe vortex. This turbulent structure forms at the bed of the upstream side of the monopile due to a downflow caused by a vertical pressure drop. This vortex sheds around the pile and propagates downstream through vertical vortices, causing high bed shear stresses, as visualized in Figure 3-1. Higher flow velocities amplify these vertical vortices, but the oscillating motion of waves can hinder them. The impact of waves on the seabed depends on the local water level, where the waves have less effect on the seabed in deeper waters than in shallow waters. Furthermore, the vertical vortices around the structure are less restricted by the water depth in deeper waters than in shallower waters. These arguments indicate that, in general, higher scour depths are predicted in deeper water, and lower scour depths are predicted in shallower water.

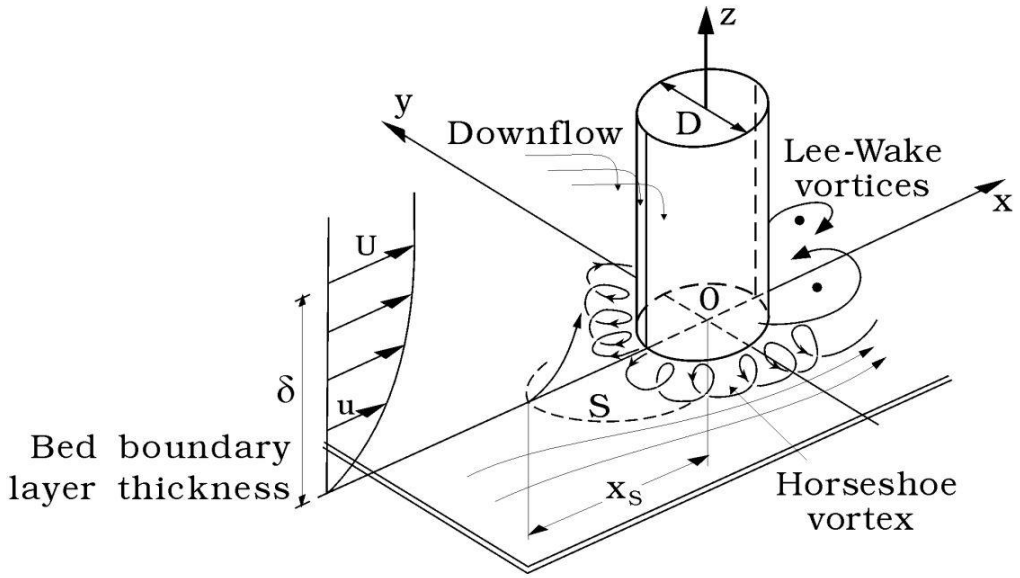

Figure 3-1: Definition sketch of the flow processes around a pile (Sumer et. al., 2002).

Global scour

More complex structures composed of several individual foundation elements, such as jacket structures, are also subject to global scour. Each foundation element of the structure is subject to local scour. However, the structure as a whole also causes a flow disruption on a larger scale. This disruption varies in magnitude depending on the porosity of the structure (how much flow can 'pass through' the structure). This, in turn, creates a global scour pattern together with the local scour around each pile. Figure 3-2 visualizes local scour superpositioned on global scour.

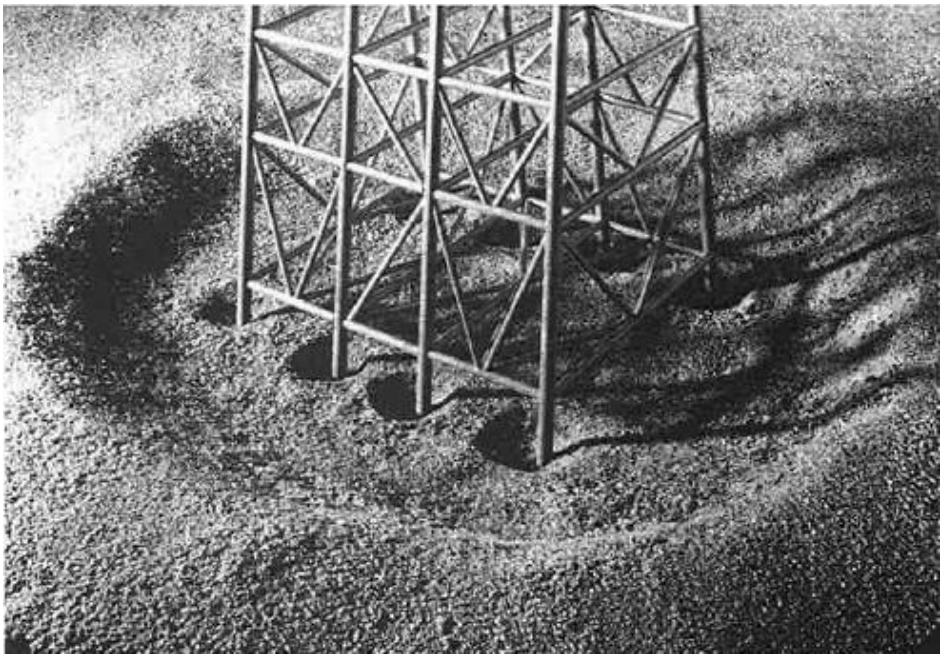

Figure 3-2: Representation of global and local scour development around a jacket structure. The figure is copied from Ferradosa (2012) and originally published in Angus & Moore (1982).

Edge scour

Edge scour is the scour on the interface between the scour protection and the unprotected bed. Two effects can cause edge scour. First, the downstream distance where the flow remains disrupted due to the structure can be longer than the placed scour protection. Second, the thickness of the scour protection itself can be sufficiently large to have a blocking effect on the flow and cause scour on its own. The edge scour holes are expected to be the deepest downstream of the structure in the primary ebb and flood directions. However, edge scour can occur all around the scour protection. An example of edge scour is visualized in Figure 3-3.

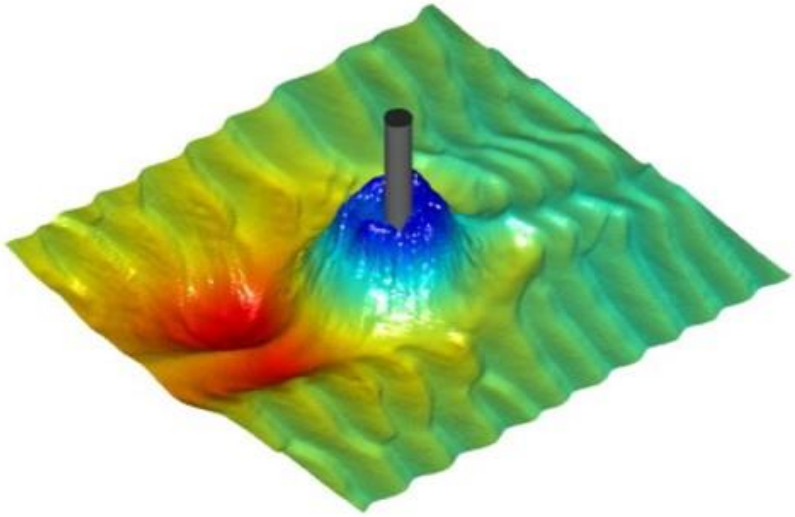

Figure 3-3: Edge scour visualized in a 3D-bathymetry around an individual monopile in the offshore windpark Egmond aan Zee. In order to more clearly show the bed level elevations, the vertical axis is stretched five times relative to the horizontal axis (Petersen et. al., 2015).

3.3 Scour mitigation without bedform migration

The seabed at the NWWFZ is dynamic and never entirely without morphological development. However, the morphological development caused by bedform migration depends on the size of the migrating bedforms. The bedform migration in NW-II/III is predicted to be limited as only relatively small megaripples migrate in the area. This study considers a location to be 'without bedform migration' when less than 1 meter of seabed change due to bedform migration is expected during the foundation's lifetime. This is consistent with the threshold in the Handbook of Scour and Cable Protection Methods (JIP HaSPro, 2023). This section highlights the design considerations for scour mitigation strategies A, B, and C when this criterion is fulfilled. The sub-sections below summarize Chapter 3.3 from JIP HaSPro (2023). For more details, the reader is referred to the Handbook.

3.3.1 Strategy A: Free scour development

Free scour development is an acceptance strategy where the foundation is installed on top of the unprotected seabed, and the scour development process is unhindered by interventions. Figure 3-4 illustrates this process. The structure's foundation must be designed to cope with the lowering seabed. For monopiles, this means that the embedded length must be increased.

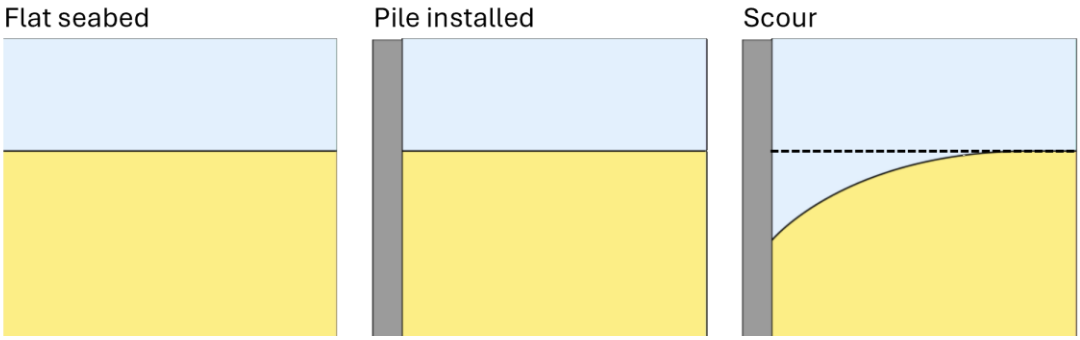

Figure 3-4: Strategy A: No scour protection and allowing free scour development excluding bedform migration (JIP HaSPro, 2023). The black dotted line indicates the original bed level.

The design considerations for strategy A are:

- The predicted scour depth. Lower predicted scour depths are more favourable for strategy A, as less excess material is required to adapt the foundation. The scour depths are lower at locations where the seabed material is hardly erodible (either in the top-layer or in a layer high in the bed) or where the hydrodynamic loading is small relative to the soil resistance.
- The foundation type. Some foundation types are less prone to failure due to scour (e.g., monopiles) than others (e.g., gravity-based or suction bucket structures).
- The connecting power cables. Power cables are often installed before the scour hole has developed towards an equilibrium. This means that the point where the cable touches the seabed, the touchdown point, might be subject to erosion after installation. As this point is often vulnerable to damage, this should be accounted for in the design of the cables.

3.3.2 Strategy B: Immediate scour protection

Immediate scour protection indicates that the scour protection is installed before the scour hole can develop significantly. Figure 3-5 illustrates this for a two-layered scour protection including a filter layer (green) and an armour layer (red). The filter layer (or in some cases the armour layer) can be placed prior to the installation of the monopile if the rock size is sufficiently small for the monopile to be driven through.

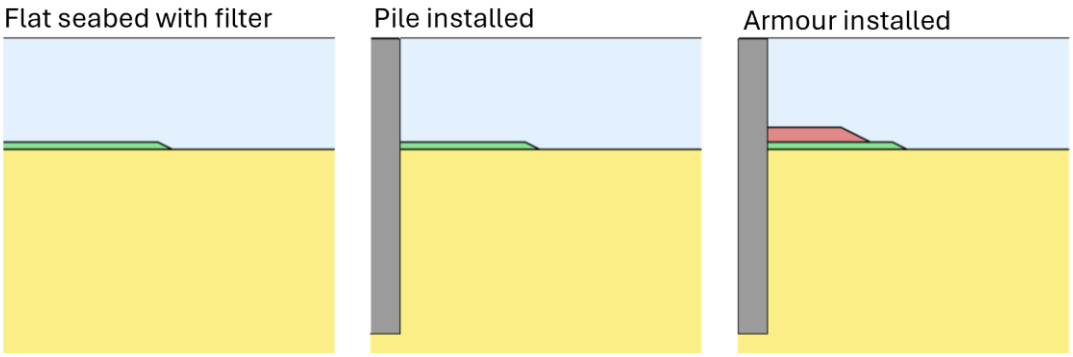

Figure 3-5: Strategy B: Immediate scour protection (JIP HaSPro, 2023).

The design considerations for strategy B are:

- The predicted scour depth. Higher predicted scour depths make a mitigation strategy more attractive as the adaptations to the design are (likely) more costly. The scour depths are higher at locations where the hydrodynamic loading is large enough to meet the soil resistance.

- The certainty of the scour prediction. Scour predictions around offshore structures are inherently uncertain. The choice not to protect the foundation can pose risks, and depending on the variability in environmental and soil conditions, it might be safer to design a scour protection system.
- The foundation type. Some foundation types allow no or limited scour; see strategy A.
- The installation window. An immediate scour protection must be installed relatively quickly to prevent the scour hole from forming. Furthermore, the installation must be done in hydrodynamically calm periods to ensure the scour protection is not damaged before commissioning.

3.3.3 Strategy C: Monitor & react

The scour hole can freely develop until a pre-defined depth within the monitor & react strategy. A scour protection is placed if the scour hole develops past this depth. The scour protection is now more sheltered as it is placed in the readily formed scour hole. The more sheltered position of the scour protection reduces the load on the stones. This, in turn, allows for a lighter material to be used for scour protection. Figure 3-6 illustrates this process.

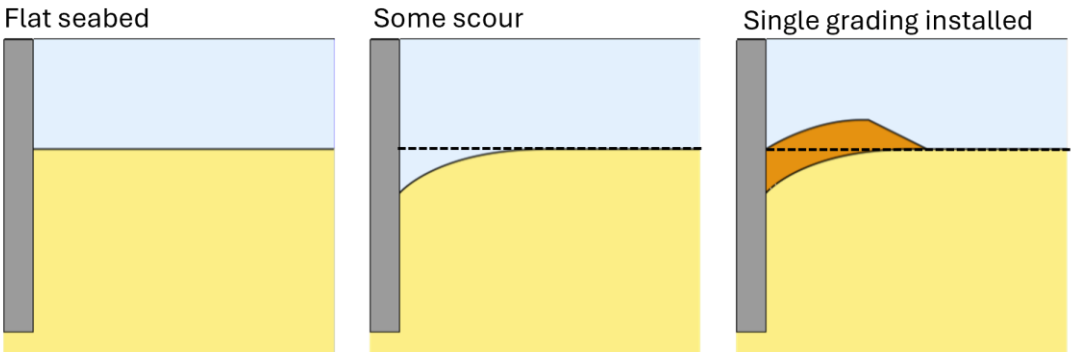

Figure 3-6: Strategy C: No scour protection, allowing some scour development and delayed installation of scour protection (JIP HaSPro, 2023). The black dotted line indicates the original bed level.

The design considerations for strategy C are:

- The availability of installation equipment. The installation date of the scour protection is more difficult to predict and can differ between foundation locations. Furthermore, the weather windows for installation can be unfavourable when the protection needs to be placed.
- The foundation type. Some foundation types only allow for limited scour hole development; see strategy A.
- The costs of frequent monitoring. This alternative requires frequent monitoring of the scour hole development at several foundations, especially within the first few months after placement. The initial measurements will result in confidence in the predictive formulas for scour depths and timescales and the prediction bandwidth can be reduced when observations are in line with the predictions. This means that the frequency of the monitoring can likely decrease as time progresses.
- The design conditions. As the scour protection is placed inside an irregular, steeply sloping scour hole, the installation of multiple layers can be complicated. It is thus preferred to apply only one scour protection layer, as opposed to a separate filter and armour layer. However, this must be possible given the design conditions and the stability of the scour protection (see Chapter 5).

3.4 Scour mitigation with bedform migration

This study considers a location to be subject to bedform migration when the expected seabed changes during the lifetime of the structure exceed 1 meter, which is consistent with JIP HaSPro (2023) and previous wind farm studies (Deltares, 2022; 2023). Therefore, this study includes the sand waves in NW-I but not the (mega)ripples, see Section 2.5. Depending on the bedform migration, the seabed change can either be a rise or a lowering. It is the responsibility of the designer to account for these changes. It can also be a design decision to purposely place the monopiles on specific positions of the bedforms to decrease scour mitigation costs or steel consumption costs. This section discusses the impact of bedform migration on the different scour mitigation strategies.

3.4.1 Strategy A: Free scour development

Due to the slow migration rates of bedforms, the timescale of the bed level changes due to bedform migration is longer (slow) than the typical timescales for scour development (fast). The scour hole can, therefore, generally follow the changing seabed due to bedform migration. Figure 3-7 shows this process.

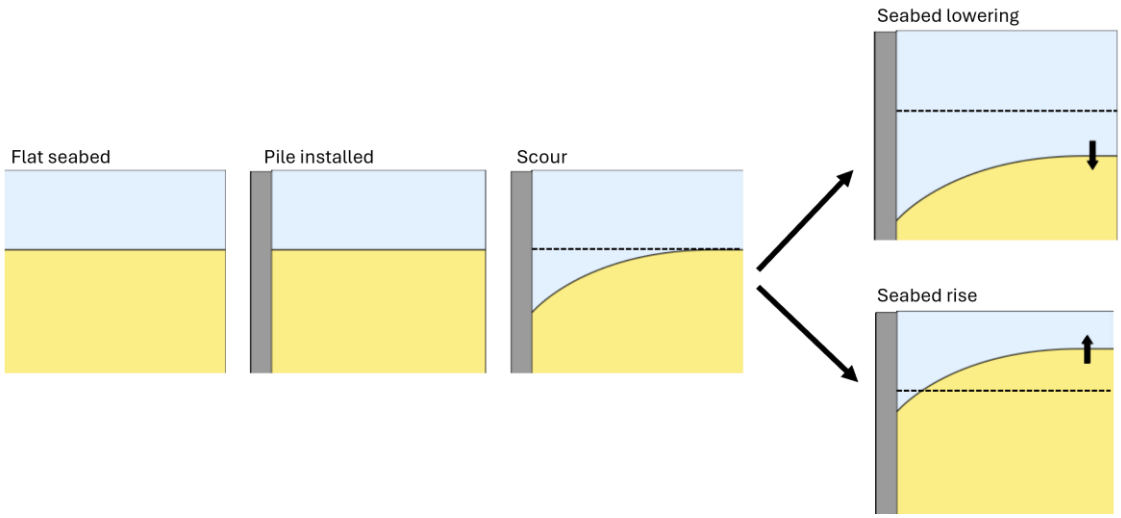

Figure 3-7: Strategy A: No scour protection, allowing free scour development with a lowering seabed (top right) and a rising seabed (bottom right) (JIP HaSPro, 2023). The black dotted line indicates the original bed level.

The migration of the bedforms also changes the spatial distribution of the hydrodynamic parameters. Flow velocities are typically higher on the crests of bedforms than in the troughs. This change in the local hydrodynamic climate around the foundations can influence the scour hole's depth, shape, and development timescale. However, this is expected to be of limited influence due to the relatively deep water depths at the NWWFZ.

The bed level changes due to bedform migration typically have a slight dampening effect on the scour hole. A bed lowering due to migration from a crest to a trough would result in lower flow velocities, potentially yielding lower scour depths. Therefore, it is expected to be a conservative estimate to add the bed level changes due to the bedform migration to the predicted scour hole depths when considering the fixation level of monopiles.

3.4.2 Strategy B: Immediate scour protection

The consequences of migrating bedforms differ for strategy B depending on whether the seabed is lowering or rising. Figure 3-8 illustrates the scenario with a rising seabed. It is unlikely that sand will pile up on the armour layer of the scour protection due to the high flow load. Therefore, relatively few changes occur close to the pile. Further away from the pile, the sand can start to accumulate due to the reduced flow load.

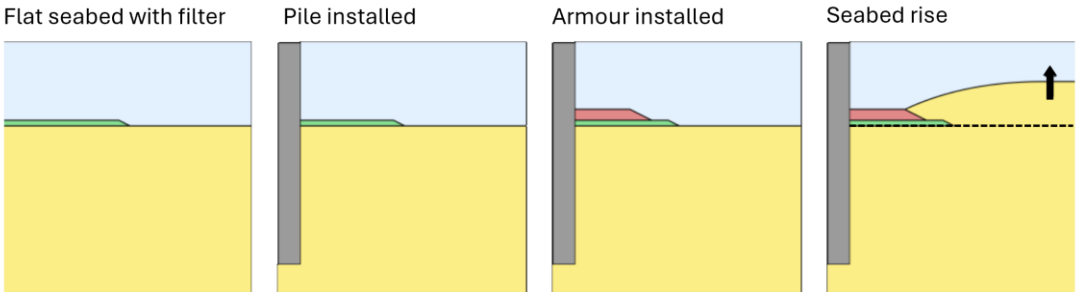

*Figure 3-8: Strategy B: Immediate scour protection with **rising** seabed. In this morphodynamic scenario, the foundation is hardly affected because of local scour development couteracting the rising seabed (JIP HaSPro, 2023). The black dotted line indicates the original bed level.*

Figure 3-9 shows the process of seabed lowering around a monopile with immediate scour protection. As the scour protection prevents any material from eroding close to the pile, the effects of the lowering seabed are found some distance away. The scour protection design should allow for this seabed lowering combined with edge scour. The scour protection's edge can be protected with, e.g., a falling apron (Chapter 5). Subsequent seabed rise after a lowering will embed the falling apron and have a similar effect to immediate seabed rise, as discussed previously.

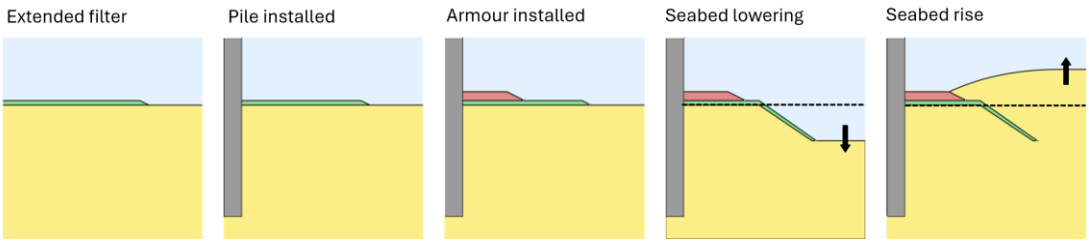

*Figure 3-9: Strategy B: Immediate scour protection with **lowering** seabed. This strategy is relying on flexible behaviour of the protection at the edges in order to maintain the seabed level close to the pile and to ensure the integrity of the scour protection. Subsequent rising of the seabed is not expected to harm the protection. The black dotted line indicates the original bed level.*

The local hydrodynamic conditions can change when the seabed lowers or rises. For example, after seabed lowering, the scour protection may protrude like a sill, potentially being exposed to larger and more focused wave action.

3.4.3 Strategy C: Monitor & react

The effects of bedform migration on strategy C are a combination of the impact on strategies A and B. When strategy C is used, and no scour protection is placed initially, the effects of bedform migration are virtually identical to those of strategy A, see Figure 3-7. In this scenario, it might be more challenging to determine when to place a scour protection as the measurements are influenced by both the scour hole development and the bedform migration.

Under strategy C, after placing a scour protection as a reaction to the occurring scour, the same design considerations as with strategy B are in play. The influences of bedform migration again depend on whether a seabed lowering or a seabed rise occurs. When considering a seabed rise, the scour protection placement will get even more sheltered. Figure 3-10 shows this sheltering effect.

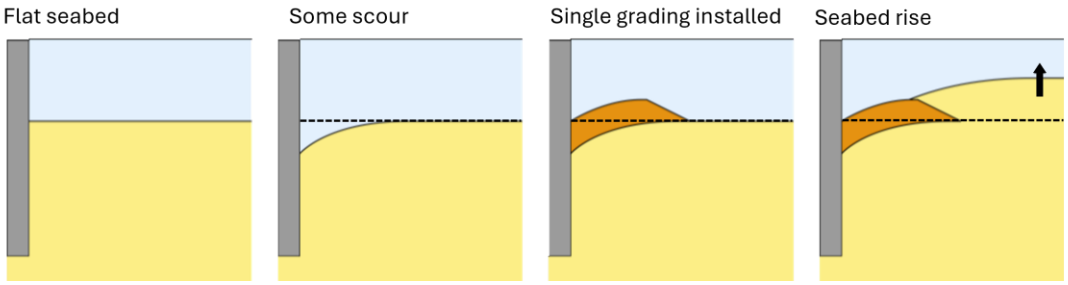

*Figure 3-10: Strategy C: Monitor and React with **rising** seabed. In this morphodynamic scenario, the foundation is hardly affected because of the local scour development counteracting the rising seabed (JIP HaSPro, 2023). The black dotted line indicates the original bed level.*

When considering a seabed lowering, the flexibility of the scour protection is essential. This can be achieved by e.g. a falling apron, see Figure 3-11. This design should allow for edge scour (Chapter 5).

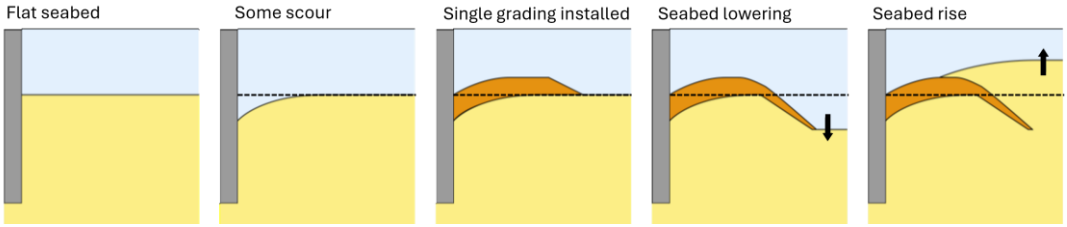

*Figure 3-11: Strategy C: Monitor and React with **lowering** seabed. This strategy is relying on the flexible behaviour of the protection at the edges in order to maintain the seabed level close to the pile and to ensure the integrity of the scour protection. Subsequent rising of the seabed is not expected to harm the protection (JIP HaSPro, 2023). The black dotted line indicates the original bed level.*

3.5 Recommendations for strategies in Nederwiek

It is explained in Section 2.5 that significant bedform migration is only expected in the form of sand wave migration in NW-I. Therefore, scour mitigation strategies with bedform migration should be considered when placing foundations in the areas with sand waves in NW-I. The scour mitigation strategies without bedform migration should be considered for NW-II/III, even though a slight effect of the (mega)ripples can be expected in some areas.

Scour mitigation strategy A (free scour development) best suits stable, shallow areas. Shallow areas are more prone to backfilling induced by waves, yielding lower scour depths. The most suitable locations are on the crests of the sandbanks, which are present in both NW-I and NW-II/III. Aside from shallow areas, low-current areas tend to yield lower scour depths. This can be the case for the northern sections of NW-II/III. However, scour mitigation strategy A is only feasible in shallow and low-current areas if the expected scour development is limited. When using scour mitigation strategy A in NW-I, special care should be taken when placing the foundation in an area with expected seabed lowering due to bedform migration.

The highest reduction in steel consumption can be achieved by employing scour mitigation strategy B (immediate scour protection) in combination with a placement in shallow areas. This will increase the load on the scour protection and requires sufficient flexibility of the scour protection. Whether this strategy is the most economical depends on the balance between the costs of the scour protection and the savings in steel consumption. Note that if this strategy is used on the crests of sand waves in NW-I, special care should be taken that the scour protection has sufficient flexibility to account for the expected seabed lowering.

Scour mitigation strategy C (monitor & react) is most feasible using single-layered scour protection. This scour protection requires that the hydrodynamic load is relatively low. Therefore, deeper areas might be the most suitable for this strategy. An additional consideration is to place the foundation in

an area where seabed rise due to sand waves is expected. This seabed rise will result in more sheltering of the scour protection, further limiting the load on the scour protection.

4 SCOUR PREDICTIONS

4.1 Introduction

Considerable research has been conducted regarding scour around offshore foundations. Most research has focussed on scour around monopiles because this is the most popular foundation type. This study delivers a preliminary estimate of the to-be-expected scour at the NWWFZ. The scour analysis will be performed quantitatively for monopiles. This quantitative analysis is then qualitatively extended to other foundation types.

The scour predictions for monopiles use a time-dependent scour model. This model calculates the equilibrium scour hole depth and characteristic timescale of scour to calculate the development of the scour hole through time. The working principles of this model, together with the model input and assumptions, are described in Section 4.2. The assumptions made within the methodology are validated against field data from nearby offshore (monopile) wind farms in Section 4.3.

The scour analysis is done probabilistically to highlight the uncertainty in these predictions at this stage. The resulting 5%, 50%, and 95% non-exceedance scour depths are visualized and explained in Section 4.4. The chapter ends with the site-specific conclusions in Section 4.5.

It is noted that the predicted scour depths are indicative and are suitable for a feasibility-level analysis only. This is reflected in the model generalizations, assumptions, and a wide confidence interval in the chosen input parameters. In the project's design phase, it may be possible to reduce the bandwidth of the prediction as more detailed model inputs become available, along with the choice of the foundation locations.

4.2 Scour modelling approach

4.2.1 Scour prediction model

The scour prediction for monopiles uses a time-dependent scour prediction model with a probabilistic approach. The assessment is on a feasibility level, which means that results can indicate 1) whether scour mitigation is necessary and 2) the timescales it takes for a certain scour depth to develop. The probabilistic approach will account for both variations in hydrodynamic forcing and uncertainties in equilibrium scour depth and time scale, which will be explained further below. In total, 1000 simulations with stochastic parameters are performed per location.

The model concept used is similar to the Dynamic Sediment Modelling Tool used in the study at IJmuiden Ver WFZ (Deltares, 2023). Figure 4-1 shows the model's workflow. It works as follows:

- The time-varying hydrodynamic conditions are discretized in timesteps Δt in the order of hours;
- For each timestep, the hydrodynamic conditions are translated into:
    - the sediment mobility based on Soulsby (1997), which is defined as the ratio between the actual Shields parameter and the critical Shield parameter;
    - the relative velocity, which is defined as the contribution of the current flow velocity to the total flow velocity (wave + current) according to JIP HaSPro (2023).
- The sediment mobility determines whether the sediment is mobile; values below a certain threshold (often 0.5) state that the sediment is not mobile.
- The relative velocity determines whether the flow is wave-dominated or current-dominated. This, in turn, determines which equilibrium scour hole depth formula is applicable. The Breusers formula, including the depth-correction factor, is used for current-dominated conditions. This choice is further highlighted below. The formula from Raaijmakers & Rudolph (2006) is used for the wave-dominated conditions.

- The equilibrium scour hole depth for the given timestep is calculated based on the above. Also, the scouring (or backfilling) timescale will be calculated based on Raaijmakers & Rudolph (2006).
- Scouring will occur if the equilibrium scour hole depth is deeper than the present scour hole (S_n). Backfilling will occur if the equilibrium scour hole depth is shallower than the present.
- The scour hole depth in the next timestep (S_{n+1}) is calculated based on the following formula: $S_{n+1} = S_{eq,n+1} + (S_n - S_{eq,n+1}) \exp\left(-\frac{dt}{T}\right)$.

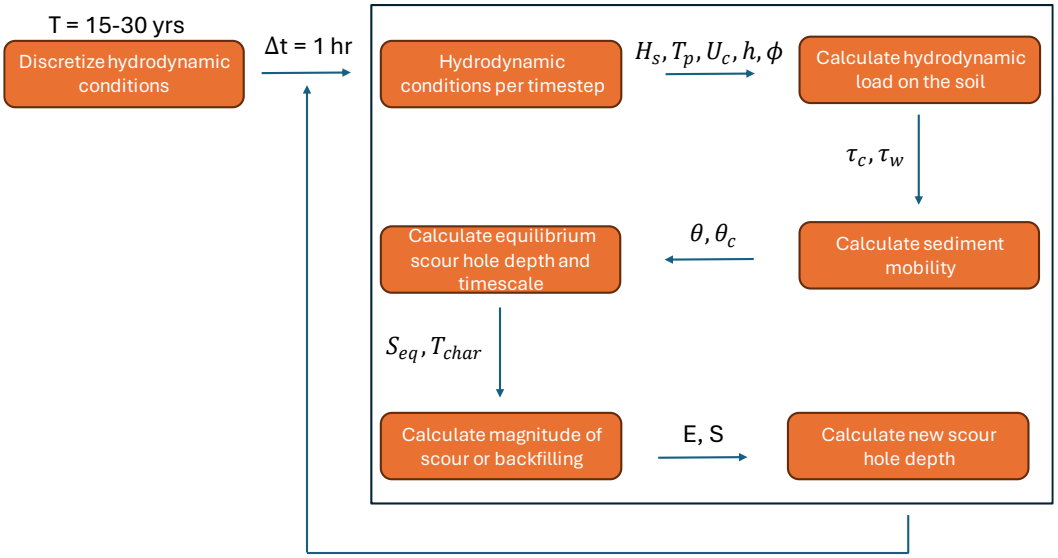

Figure 4-1: Workflow of the time-dependent scour prediction model. Definitions of parameters: T = simulation time, Δt = timestep, H_s = significant wave height, T_p = peak wave period, U_c = current velocity, h = water depth, ϕ = angle between wave and current vectors, τ_c = current bed shear stress, τ_w = wave bed shear stress, θ = actual shields parameter, θ_c = critical shields parameter, S_{eq} = equilibrium scour hole depth, T_{char} = characteristic timescale of scour, E = erosion, S = sedimentation.

The model is forced with time-varying hydrodynamic conditions with a sufficient length to reach the equilibrium scour depth in less dynamic parts of the project area. Based on several sensitivity computations, a period of 15 years is estimated to be sufficient for NW-I and 30 years for NW-II/III, see Appendix A. Different time series are generated from the DHI MOOD time series for the probabilistic analysis to account for variations in scour development due to variations in wave forcing (DHI 2023a; 2023b). The total time series has a length of 43 years.

The model is set up on a 1x1 km grid for computational efficiency, with a resolution of the same order as that of the hydrodynamic data. The results will later be interpolated to a 20x20 m grid in the NWWFZ.

The equilibrium scour hole depth for current-dominated conditions is calculated using the Breusers formula (Eq 4-1). This formula is used for the following reasons:

- The hydrodynamic conditions in the NWWFZ are often current-dominated (see Section 2.2.3), which increases the need for suitable uncertainty in the formula for current-induced scour;
- Its level of detail suits the preliminary stage of the analysis best;
- A comparison with observations at North Sea field sites shows a good, somewhat conservative fit.

$$\frac{S_{eq}}{D} = C \cdot \mathrm{K_u} \cdot \mathrm{K_s} \cdot \tanh\left(\frac{h}{D}\right) \qquad \text{Eq 4-1}$$

Where:

- C: Calibration constant [-]
- K_u: Velocity correction factor [-]
- K_s: Shape correction factor (1 in this study) [-]
- h: Water depth [m]
- D: Pile diameter [m]

The calibration constant 'C' in the Breusers formula has been studied well for both the best-fit and maximum scour depth. Harris et al. (2010) suggest using a value of C = 1.3 for field applications, which is in-line with DNV guidance. Hoffmans & Verheij (2021) indicate a value of C = 2.4 as an upper limit for the maximum equilibrium scour hole depth. In this study, the parameter C is translated to a stochastic normal distributed parameter by stating that $C_{50\%}$ = 1.3 and $C_{99\%}$ = $C_{50\%}$ + 3σ = 2.4. Which results in a mean value of 1.3 and a standard deviation of 0.35. Section 4.3 highlights the applicability of this method further in the context of field measurements at different offshore wind farms.

The Raaijmakers & Rudolph (2008) formula is used for wave-dominated conditions (Eq 4-2 - Eq 4-3). This formula is similar to the Breusers formula: multiplication of a constant C with the tanh(h/d), but with an additional factor representing the wave dynamics (K_w). This constant is a function of the Keulegan-Carpenter number and the relative velocity. The relative velocity is low because this formula is only applied in wave-dominated conditions. Due to the large pile diameter of D = 12 m, the Keulegan-Carpenter number is also relatively low. As a result, K_w is in the range of 0.01 to 0.3 and significantly reduces the predicted equilibrium scour hole depths. This means that for the current-dominated situation at Nederwiek, the present scour depth is always far from equilibrium when wave-dominated conditions occur. The impact of the additional scaling with C is low. Therefore, using this calibration constant as a stochastic parameter in the scour analysis is deemed unnecessary.

$$\frac{S_{eq}}{D} = 1.5 \cdot \mathrm{K_w} \cdot \mathrm{K_h} \cdot \tanh\left(\frac{h}{D}\right) \qquad \text{Eq 4-2}$$

$$K_w = 1 - \exp(-1 * (0.012 \cdot KC + 0.57 \cdot KC^{1.77} \cdot U_{rel}^{3.76})) \qquad \text{Eq 4-3}$$

Where:

- KC: Keulegan Carpenter number ($\frac{U_{wave}T_p}{D}$) [-]
- K_h: Height correction factor (1 in this study) [-]
- U_{rel}: Relative flow velocity ($\frac{U_{current}}{U_{current}+U_{wave}}$) [-]
- h: Water depth [m]
- D: Pile diameter [m]

4.2.2 Data availability

The hydrodynamic data that is used in the scour analysis originates from DHI (2023a; 2023b). The raw data employs different numerical grids for the wave- and current-related parameters. Data for both waves and currents is interpolated to a regularly spaced 500x500 m grid to ensure each simulation has both data types. Figure 4-2 visualizes the grid using the water depth.

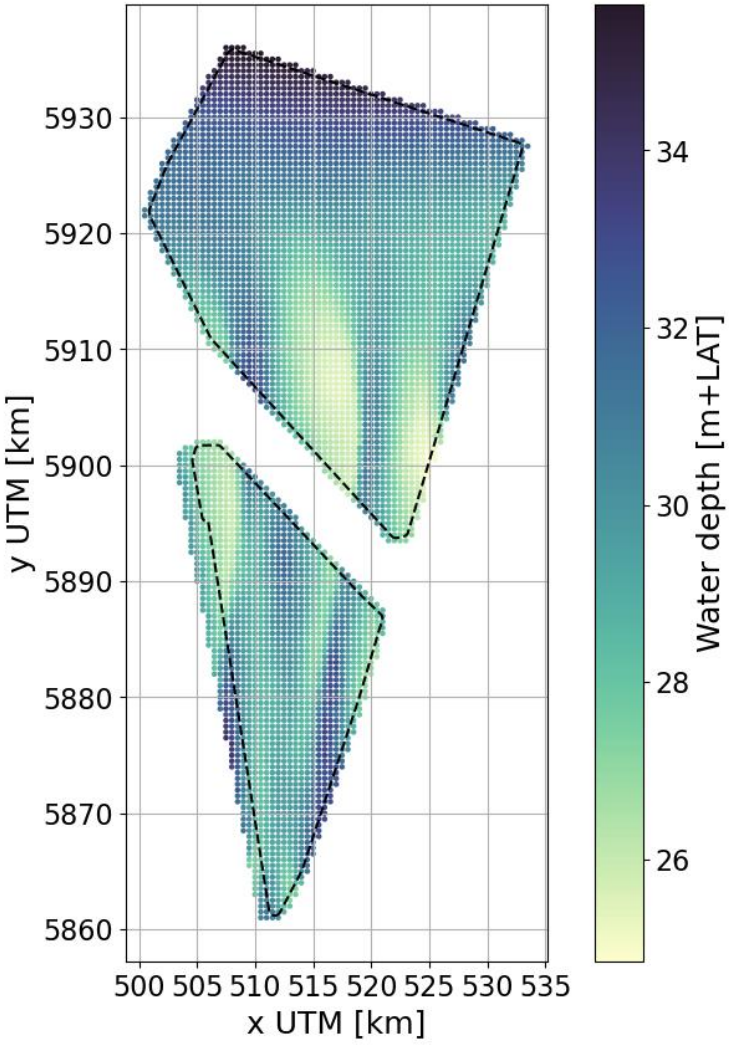

Figure 4-2: Resolution of the input data from DHI (2023a; 2023b)

The time series data is available between 01/01/1980 – 31/12/2022, resulting in 43 years of hydrodynamic data. Table 4-1 summarizes the available parameters.

Table 4-1: Available hydrodynamic parameters in the 43-year timeseries (DHI, 2023a; 2023b).

Name	Symbol	Unit
Significant wave height	H_{m0}	[m]
Peak wave period	T_p	[s]
Peak wave direction	PWD	[°N]
Current speed	UV	[m/s]
Current direction	CD	[°N]
Water level	H	[m]
Water depth	D	[m]

4.2.3 Stochastic parameters

The model is dependent on a broad range of parameters, varying from physical parameters (D_{50}, hydrodynamic conditions, densities, etc.), model parameters (mobility threshold, relative velocity threshold), and empirical parameters (coefficient in Breusers formula, timescale calibration factors). In general, part of the uncertainty of the physical parameters can be captured by using either conservative or stochastic empirical parameters. This study employs the latter. The coefficient in the Breusers formula has the most significant impact on the equilibrium scour hole depth for current-dominated conditions, which is the prevailing condition at the NWWFZ. The timescale calibration factors and hydrodynamic forcing have the most significant impact on the temporal development of the scour hole. It is thus decided that, for this feasibility level analysis, it is sufficient to include only four stochastic parameters:

- The Breusers coefficient
- The timescale calibration factor for scour
- The timescale calibration factor for backfilling
- The hydrodynamic forcing

Table 4-2 summarizes the ranges of the parameters.

Table 4-2: Ranges of the different stochastic parameters used in the scour simulations. Terminology: STD = Standard Deviation.

Name	Symbol	Distribution	Min	Max	Mean	STD
Breusers coefficient	C	Normal	0.1	2.5	1.3	0.35
Timescale calibration factor scour	T_{scour}	Uniform	1	20	10.5	5.5
Timescale calibration factor backfilling	$T_{backfill}$	Uniform	1	20	10.5	5.5
Starting year	Y	Uniform	0	42	21	12
Starting month	M	Uniform	1	12	6.5	3.2

4.2.4 Non-stochastic parameters

The parameters that are not described in Table 4-2 are considered to be constant per simulation. A spatially varying depth-averaged value is used for the median grain size diameter. Figure 2-7 visualizes the spatial distribution of this parameter.

Other parameters, such as the water/sediment density, pile diameter, and model parameters, are considered constant in space. In reality, these parameters can vary both spatially and through time. However, the current methodology captures this uncertainty in the calibration factor of the equilibrium scour hole depth. Table 4-3 summarizes the values of the static parameters used in the simulations.

Table 4-3: Non-stochastic parameters used in the scour prediction simulations. The relative velocity threshold is the threshold below which the conditions are considered wave dominated and above which they are considered current dominated. The mobility threshold is the threshold when the sediment becomes mobile. The hydraulic roughness factor is the factor with which the median grain size is multiplied to determine the roughness height in hydraulically rough flow.

Name	Symbol	Value	Unit
Pile diameter	D	12	[m]
Median sediment grain diameter	d_{50}	100 – 250	[mm]
Sediment density	ρ_s	2650	[kg/m^3]
Water density	ρ_w	1025	[kg/m^3]
Time step	Δt	3600	[s]
Simulation duration NW-II and NW-III	T	30	[years]
Simulation duration NW-I	T	15	[years]
Relative velocity threshold	$U_{rel,\ th}$	0.5	[-]
Mobility threshold	MOB_{th}	0.5	[-]
Hydraulic roughness factor	N	2.5	[-]

4.2.5 Simulation period

It is unnecessary to simulate the entire 43-year time period from the time series. This is because the equilibrium scour hole depth is expected to have formed in a shorter period than 43 years. The required simulation duration to accurately calculate the maximum scour hole depth was therefore assessed. It was found that for NW-I, a period of 15 years is sufficient at all locations. For NW-II/III, it was found that 15 years is enough in the high-velocity areas towards the south and that 30 years is sufficient for the low-velocity regions of the north. It was therefore decided to use a simulation period of 15 years in NW-I and a simulation period of 30 years in NW-II/III. See Appendix A for more information.

4.2.6 Grid resolution

The hydrodynamic data is available on a 500 x 500 m grid. This grid resolution is too coarse to accurately capture the spatial variation in the hydrodynamic conditions induced by sand waves, which have a wavelength between 200 and 400 m, see Section 2.5. The scour simulations will thus only capture the larger scale bathymetrical changes such as sandbanks. It is assumed that a spatial resolution of 1000 x 1000 m grid is sufficient to capture the large-scale bathymetrical changes. This is also necessary to keep the simulations' computational time within reasonable limits. Figure 4-3 visual s the simulation resolution.

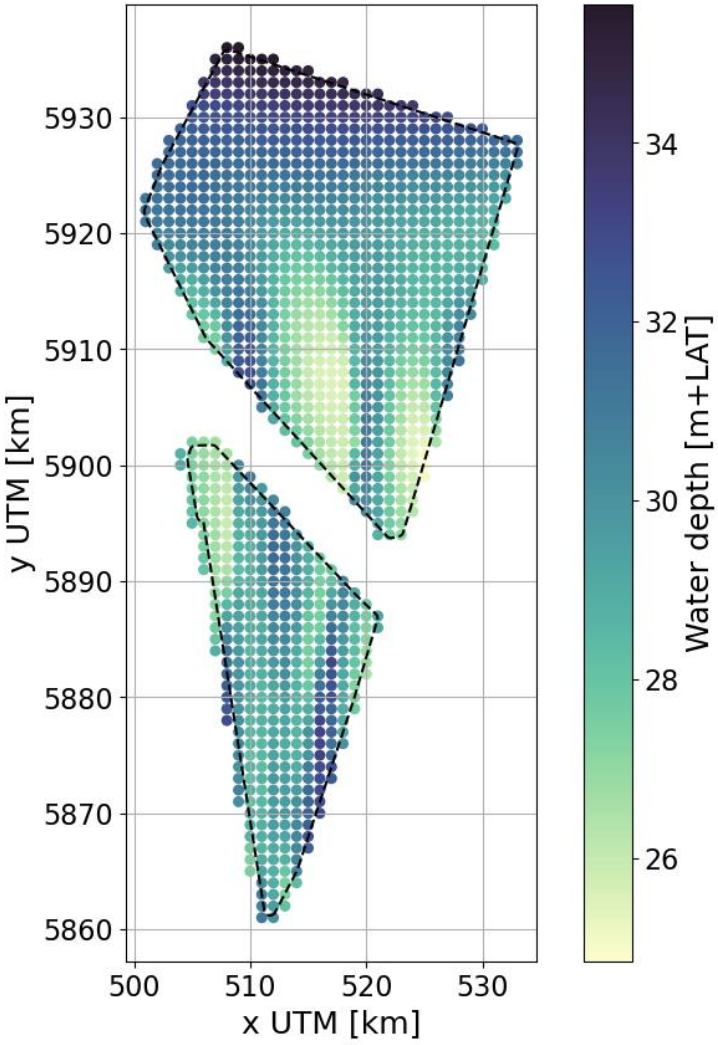

Figure 4-3: Resolution of the scour simulations (1 x 1 km).

4.3 Scour at similar sites

Scour around monopiles is often expressed as a non-dimensional ratio between the scour depth and the pile diameter (S/D) or the water depth (S/h). Melling (2015) used this method to perform a large-scale comparison between scour depths at 16 offshore wind farms. This data is supplemented with validation data and uncertainty ranges from the IJV and TNW wind farm studies (Deltares, 2022; Deltares, 2023). Figure 4-5 shows the locations of the wind farms most relevant to the NWWFZ.

Assuming that the observations presented in Melling (2015) and Deltares (2022, 2023) are close to equilibrium, they are compared to the 95% confidence interval of the equilibrium scour hole depth as predicted with the Breusers formula using the normal distribution for C as described in Section 4.2 in Figure 4-4. It is noted that the scour depth is constantly varying due to the changing hydrodynamic conditions. Therefore, the maximum scour hole depth during the structure's lifetime is essential for stability. This parameter is often denoted as S_{max} and is challenging to capture in field measurements. This means that the points shown in Figure 4-4 are not necessarily the maximum scour hole depths for which the structure should be designed. Nevertheless, the large amount of data points in Figure 4-4 is expected to account for this uncertainty.

The blue dots in Figure 4-4 represent the data points used in Melling (2015, figure 5.10) from 16 offshore wind farms. The black dotted lines roughly indicate the maximum and minimum h/D ratios

around the NWWFZ. These lines are constructed with a maximum water depth of 40 m and a minimum water depth of 20 m, combined with a pile diameter of D = 12 m. Within the applicability range at the NWWFZ, the 95% confidence interval using the Breusers formula aligns with the data. Thus, the Breusers formula is suitable for the analysis at the NWWFZ to give a realistic but conservative bandwidth, which is notably more larger than what has been used for predictions at previous sites (e.g., IJV and TNW).

It is noted that the field measurements are taken at wind farms, which are not all comparable to the NWWFZ. Most of the nearby wind farms comprise monopile foundations smaller than 12 m and placed in shallower waters. Therefore, the absolute magnitude of the water depth 'h' and the pile diameter 'D' can differ between sites while maintaining equal values for the ratio 'h/D'. However, this comparison aims to show that the bandwidth, as predicted using the Breusers formula, is sufficient to describe the variation observed in almost all available data points within the h/D range of the NWWFZ. This gives confidence that the uncertainty ranges that will be predicted for the NWWFZ are sufficiently large to cover a broad range of uncertain parameters and neglected processes, such as soil stratification, marine growth, turbulence effects, tidal backfilling, etc.

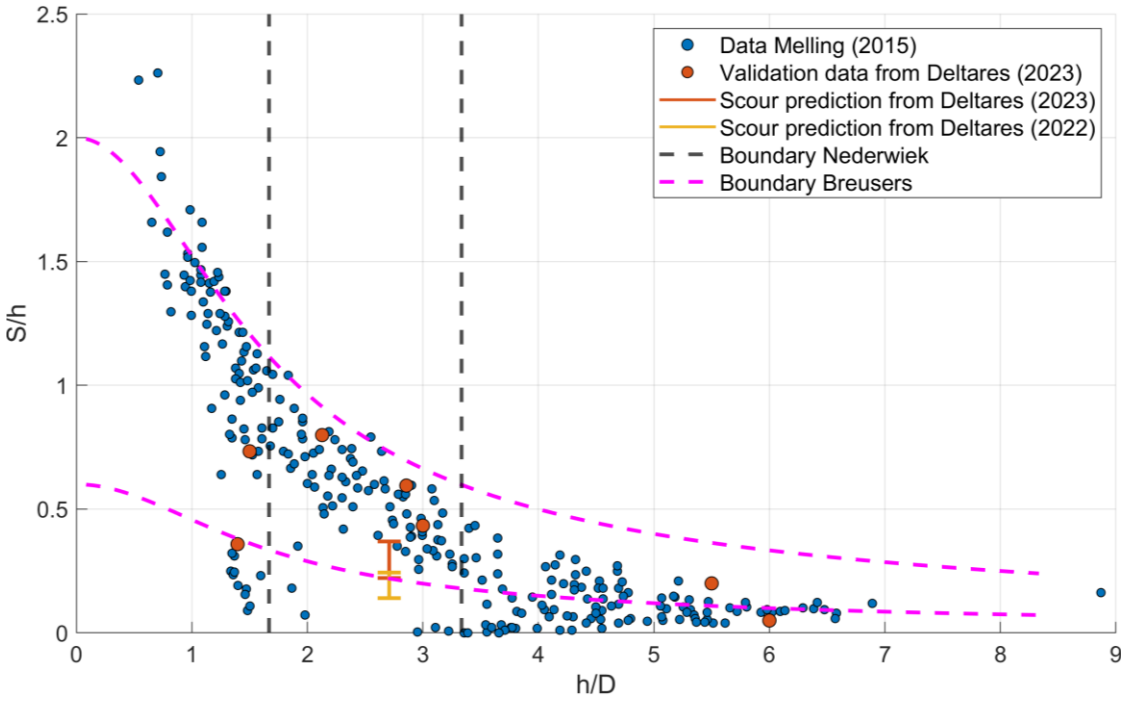

Figure 4-4: Performance of the Breusers formula to predict the scour hole depth compared to many offshore wind farms. The blue dots represent field data points from Melling (2015) for 16 different offshore monopiles. The black dotted lines represent the applicability range at the NWWFZ. The pink dotted lines represent the 95% confidence interval using the Breusers formula with a mean constant of 1.3 and a standard deviation of 0.35.

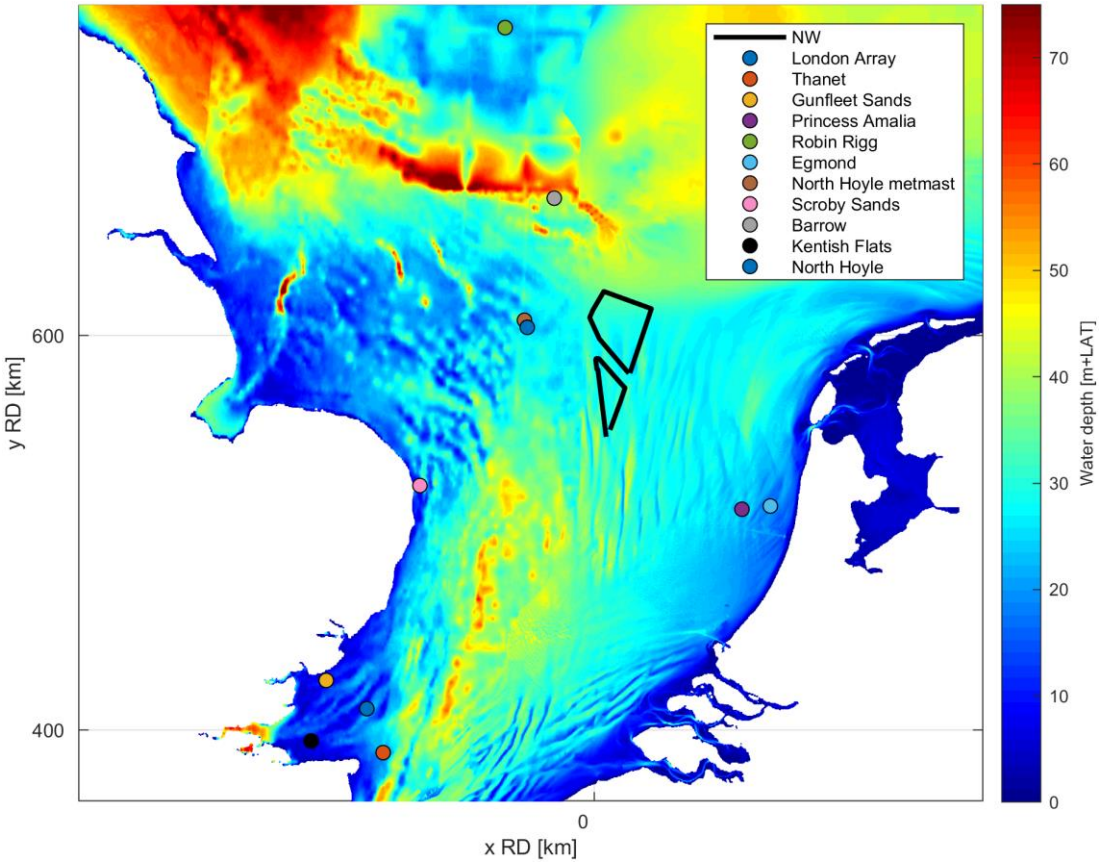

Figure 4-5: Locations of the most important nearby wind farms of which data is used in Figure 4-4.

4.4 Scour at different types of construction

4.4.1 Introduction

This section includes a relatively extensive analysis regarding the predicted scour depths at the NWWFZ for monopile foundations. The study is extended with a qualitative description of scour for other foundation types. This qualitative description is mostly a relevant summary of Chapter 4 of Deltares (2023). Where applicable, the summary is supplemented with site-specific information for the NWWFZ.

4.4.2 Monopiles

The methodology regarding the scour modelling for monopiles is explained in Section 4.2. This section focusses on the results.

Non-exceedance scour depths

For each location, the 5%, 50%, and 95% non-exceedance scour depths are calculated for each timestep in the simulation. These lines form the median and the 90% confidence interval of the time-dependent simulation; see Figure 4-6 for an example. The maximum scour hole depth during the simulation time is determined for these three lines. These maximum depths are described as $S_{max,5\%}$, $S_{max,50\%}$, and $S_{max,95\%}$. Table 4-4 summarizes the maximum scour hole depths for these three non-exceedance values for the individual Nederwiek sites and the total NWWFZ.

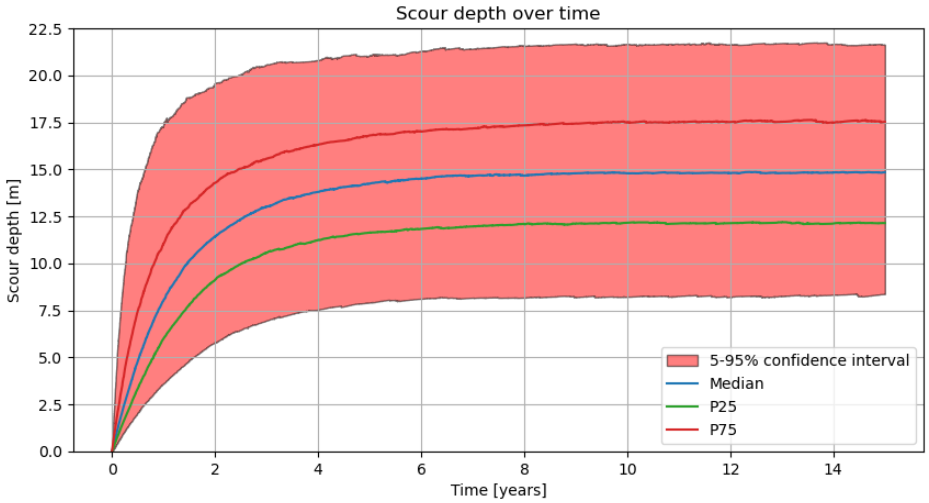

Figure 4-6: Example ensemble of 1000 Monte Carlo iterations of the time-dependent scour predictions for X=516000, Y=5872000 in NW-I.

Table 4-4: Predicted scour depths across the NWWFZ. The percentage values indicate the non-exceedance values. Indicated scour depths are the maximum scour depth during the entire simulation. The simulations are based on monopiles with a pile diameter of D = 12 m. $S_{n\%}$ stands for the n% non-exceedance scour depth.

Location	$S_{5\%}$ [m]	$S_{5\%}$/D [-]	$S_{50\%}$ [m]	$S_{50\%}$/D [-]	$S_{95\%}$ [m]	$S_{95\%}$/D [-]
Total	5.0 – 8.4	0.4 – 0.7	10.7 – 14.9	0.9 – 1.2	18.2 – 21.8	1.5 – 1.8
NW-I	7.0 – 8.4	0.6 – 0.7	13.1 – 14.9	1.1 – 1.2	20.1 – 21.8	1.7 – 1.8
NW-II/III	5.0 – 8.1	0.4 – 0.7	10.7 – 14.4	0.9 – 1.2	18.2 – 21.4	1.5 – 1.8

Spatial distribution

The spatial distribution of $S_{max,5\%}$, $S_{max,50\%}$, and $S_{max,95\%}$ are shown in Figure 4-7, Figure 4-8, and Figure 4-9 respectively. Please note the different colour scales between the three figures. All three non-exceedance values show the same spatial distribution but with different magnitudes. The predicted scour hole depths mainly depend on the local hydrodynamics (currents, waves) and are usually related to the water depth and foundation dimensions. This relationship is further explained in Chapter 3.

Figure 4-7, Figure 4-8, and Figure 4-9 show that the scour depths in NW-I are generally higher compared to NW-II/III. This can be attributed to the higher flow velocities and lower wave dominance due to lower waves at NW-I compared to NW-II/III (as is shown in Figure 2-4). As the flow and waves within NW-I are relatively uniform, the highest scour depths are found at the deepest waters between the sandbanks. The lowest scour depths are found on the crests of the sandbanks. It is stressed that the influence of sand waves is not included in the hydrodynamic conditions.

The flow and the waves within NW-II/III are less uniform. Lower flow velocities and slightly higher waves are found in the area's north compared to the south. The bed levels generally decrease from the southeast towards the northwest. As a result, the lowest scour depths occur in the northeast corner of the area, where the waves are the most dominant, the water depth is average, and the flow velocities are low. The flow velocities decrease towards the northwest corner, and the water depth increases. The latter results in a lower wave effect and, thus, less backfilling and slightly higher scour depths.

More towards the south of NW-II/III, the effect of the sandbanks becomes prevalent. The highest scour depths are located at the deeper points between the sandbanks, whereas the scour depth is

lower on the crests of the sandbanks. Note that uncertainties due to bedform migration are not yet included in this analysis.

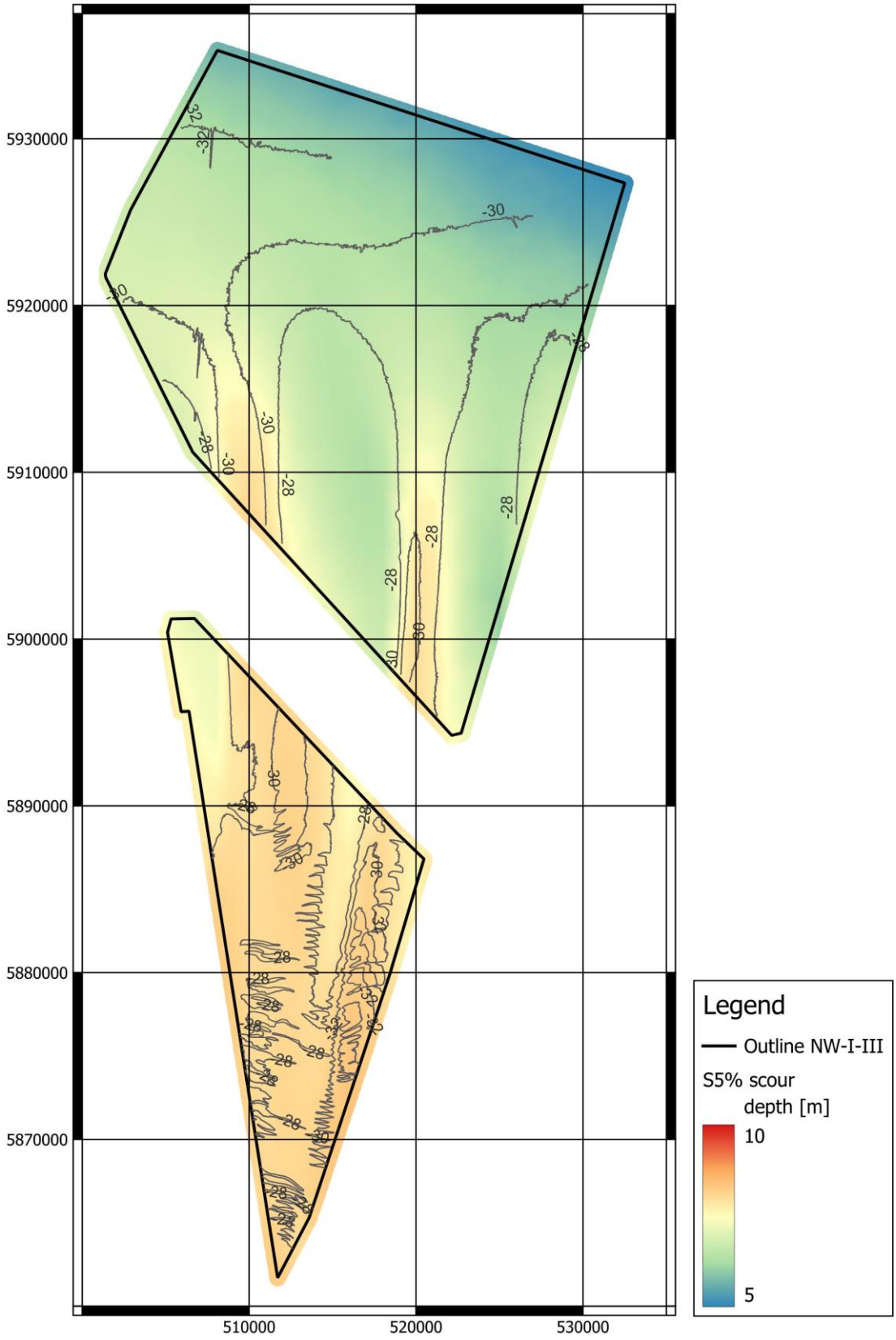

Figure 4-7: 5% non-exceedance scour depths predicted at the NWWFZ. Scour depths are the maximum scour depths during the simulations. Simulations are performed for monopiles with D = 12 m.

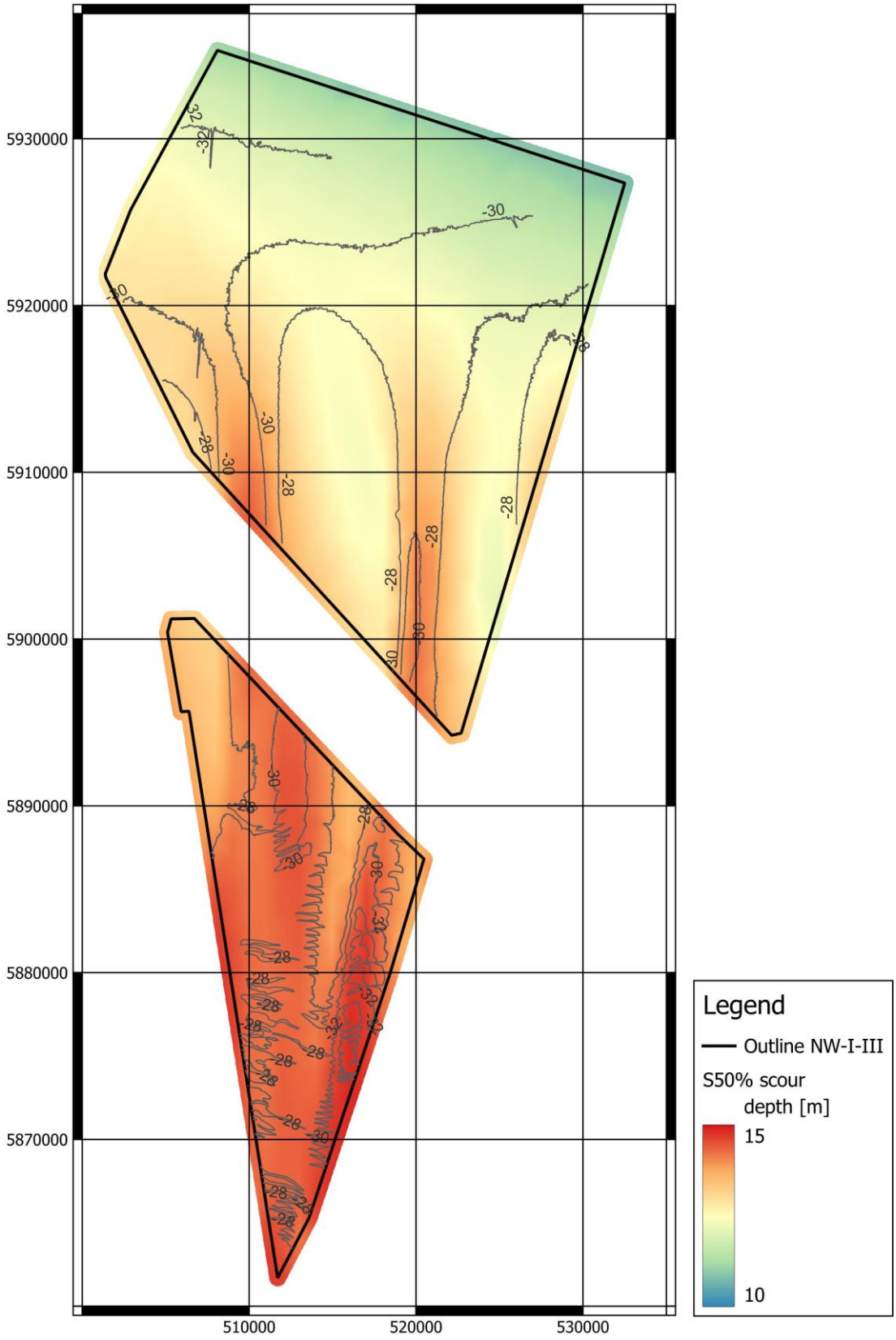

Figure 4-8: 50% non-exceedance scour depths predicted at the NWWFZ. Scour depths are the maximum scour depths during the simulations. Simulations are performed for monopiles with D = 12 m.

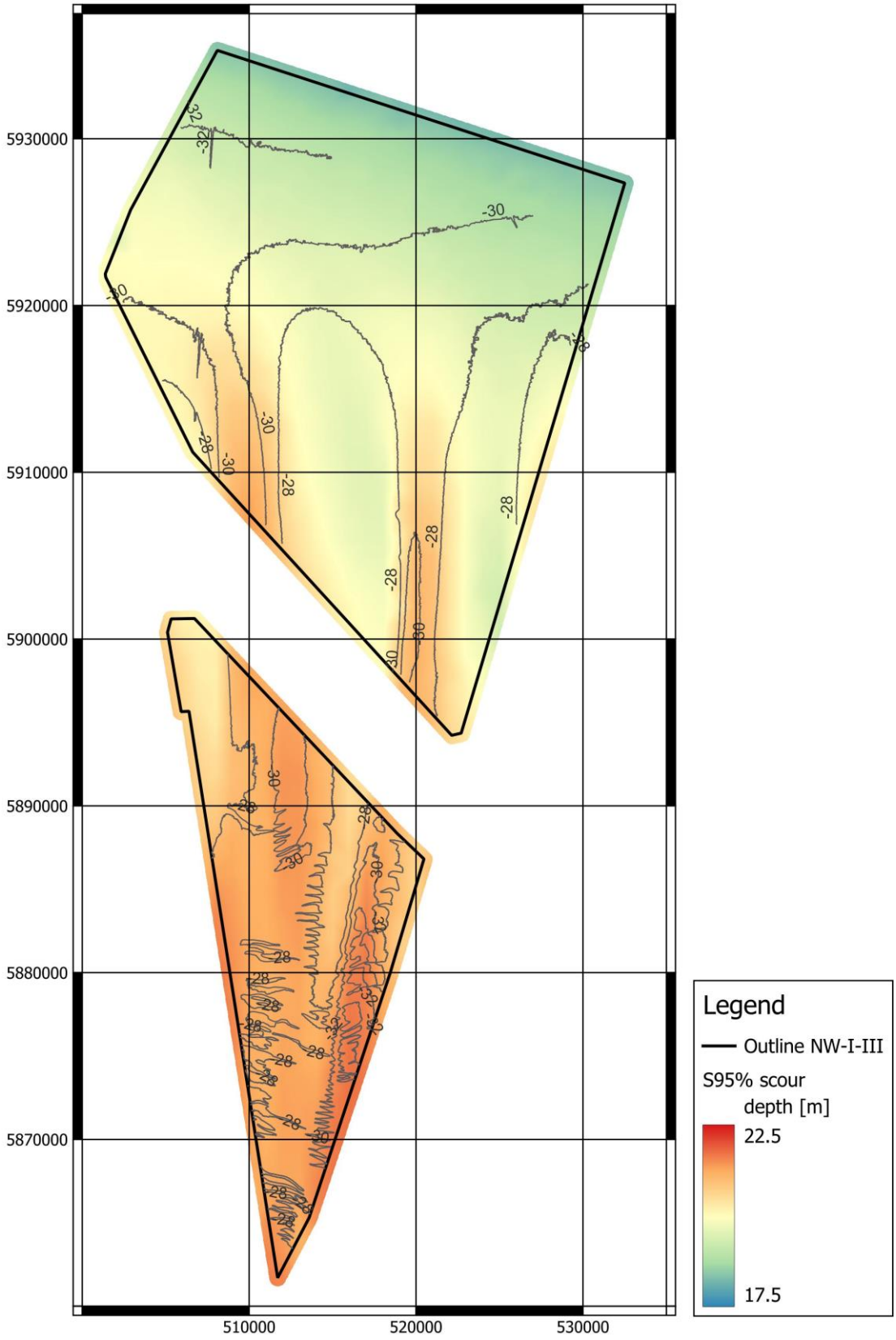

Figure 4-9: 95% non-exceedance scour depths predicted at the NWWFZ. Scour depths are the maximum scour depths during the simulations. Simulations are performed for monopiles with D = 12 m.

Timescale of scour

Section 4.2 already discussed that the predicted timescales of scour can vary between locations in the NWWFZ. The scour holes will develop quicker in NW-I due to the more frequent high flow velocities. Equilibrium scour hole depths are predicted to be reached 5 to 10 years after construction. The scour hole development in NW-II/III varies spatially, with slower scour development towards the north and faster scour development towards the south. The equilibrium scour hole depths are generally reached between 5 to 25 years in NW-II/III.

The 95% non-exceedance scour depths signify a strong initial scour development for all locations. Scour depths of several meters can develop in a matter of months. The 5% non-exceedance scour depths signify a slower scour development, with scour depths of several meters developing in timescales in the order of years. It is recommended to take this uncertainty into account when considering scour mitigation strategies A (free scour development) and C (monitor & react). Table 4-5 shows the time it takes for the scour hole to develop to a depth of 1 to 5 meters.

Table 4-5: 5%, 50% and 95% non-exceedance time it takes for the scour hole to develop to a depth of 1 to 5 meters for NW-I and NW-II/III. The ranges are due to the spatial differences within the sites.

	NW-I			NW-II/III		
Scour depth [m]	5% exceedance time [days]	50% exceedance time [days]	95% exceedance time [days]	5% exceedance time [days]	50% exceedance time [days]	95% exceedance time [days]
1	60-125	25-50	5-10	105-735	40-285	5-50
2	125-260	50-100	10-20	225-1525	85-600	15-110
3	210-430	75-155	15-30	365-2540	135-935	25-170
4	310-610	110-215	20-40	540-3660	185-1305	35-240
5	415-870	140-285	25-50	770-10060	245-1730	45-315

Lateral scour hole extent

The shape of the scour hole in offshore current-dominated conditions depends mainly on the tidal flow. Asymmetrical tidal flow, both in current velocities and current directions, will likely create an asymmetrical scour hole. Therefore, the lateral scour hole extent is not uniform around the structure.

The distance from the monopile to the deepest point of the scour hole is important for the stability of the monopile foundation. It dictates the volume of soil supporting the foundation and can be calculated based on the expected scour hole slope and can be calculated based on the expected scour hole slope. The deepest points of the scour hole are expected downstream of the pile in the peak flood and peak ebb current directions. Considering the asymmetry of the tide it is expected that the peak flood (located northeast) scour hole maximum is larger than that of the ebb flow (located southwest) in most of the NWWFZ.

Typical values of the scour hole slope found in literature lie between 1:2 and 1:3 (Boon et al., 2004; Deltares, 2023; Rudolph et al., 2008). However, prototype scenarios have measured gentler slopes (e.g., Rudolph et al., 2008). This indicates that the lateral scour hole extents around the NWWFZ can vary significantly. An extensive analysis of the local soil behaviour is advised to correctly predict the lateral scour hole extent for the considered locations. Using the typical slopes of 1:2 and 1:3 and the expected scour hole depths ($S_{50\%}$) from Table 4-4, the lateral scour hole extent at the NWWFZ varies between 20 – 45 m.

Non-erodible layers

There is evidence of a large-scale non- or less-erodible layer within the range of the maximum scour depth in the NWWFZ. Figure 2-6 shows the spatial variation in the depth of this layer. When the predicted scour is expected to reach this layer, additional research regarding its erodibility is advised.

4.4.3 Piled jacket structures

Figure 4-10 (left) shows an example of a piled jacket structure. As the structure consists of multiple elements, the structure is subject to both local and global scour. Figure 4-10 (right) shows an example of the scour pattern around a piled jacket structure. The foundation piles are embedded and can thus be used with all three scour mitigation strategies.

Scour around piled jacket structures is not as well researched as scour around monopiles. Some data have been published, and some general design formulae exist (e.g., Bolle et al., 2012; Welzel et al., 2019), but these results are structure-specific. Scour assessments for jacket structures are often done by predicting the scour around the individual structural elements near the bed.

The local scour depth can be estimated in the order of several meters, and the global scour can be estimated between 1 and 3 meters (Deltares, 2023). However, it is again stressed that these estimates largely depend on the structure type. Generally, the larger the structure, the larger the flow obstruction and the larger the expected scour depths. The smaller individual pile diameters of a piled jacket structure are expected to reduce the overall flow obstruction compared to the monopile. This might yield lower overall scour depths and be a feasible alternative to the monopile.

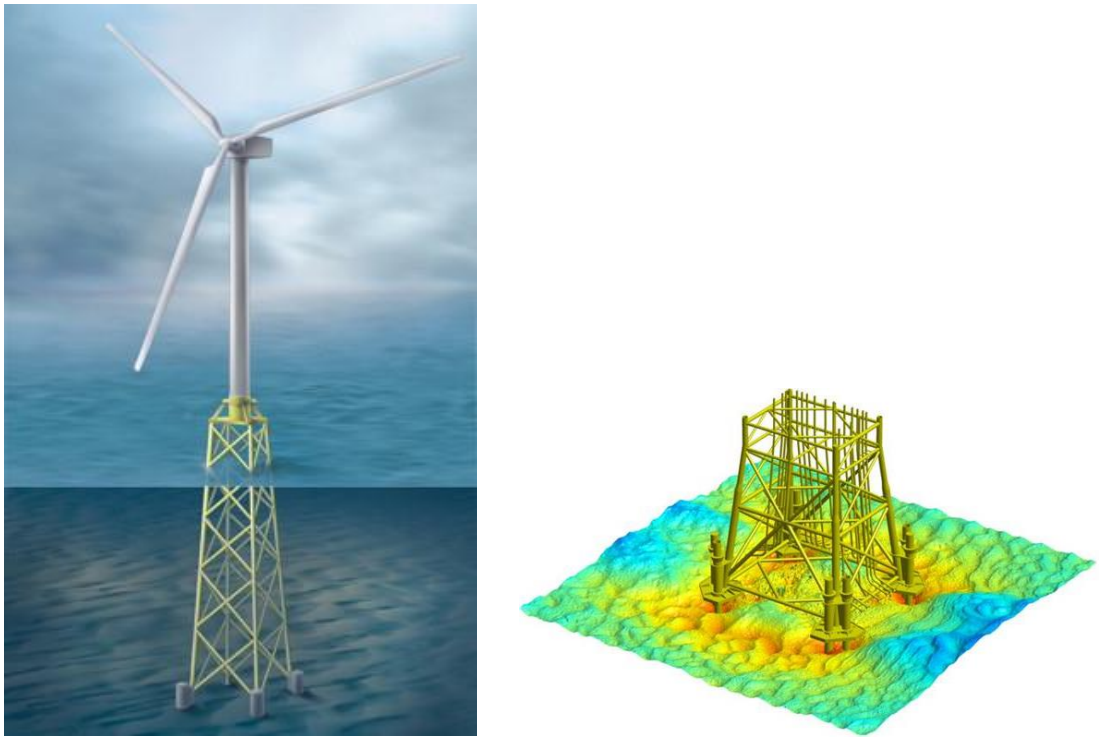

Figure 4-10: Left: an example of a jacket structure as a foundation for a wind turbine (image from Dong et. al., 2012). Right: 3D-bathymetry after a scour test showing the global scour hole in green and the local scour hole in red (Deltares, 2023).

4.4.4 Suction bucket jackets

Figure 4-11 (left) shows a (schematic) example of a suction bucket foundation. Suction bucket foundations can be either a multi-bucket structure (Figure 4-11) or a mono-bucket structure. Both structure types are subject to local scour. Only when a multi-bucket installation is used, is the

structure also subject to global scour. Figure 4-11 (right) shows an example of the scour pattern around a multi-bucket foundation.

The suction buckets are anchored into the seabed by pumping out the water inside the buckets, creating suction. This process often does not fully submerge the bucket, leaving a stick-up height of the buckets above the seabed. This section of the bucket, combined with other connecting structures close to the seabed, obstructs the flow and thus causes scour. Local scour depths of up to approximately 5 m are found in literature (Deltares, 2023). However, it is recommended to perform a more thorough analysis of the predicted scour depths when considering suction bucket type foundations. As a general rule-of-thumb, the larger the obstruction to the flow, the larger the expected scour.

Suction bucket structures have a limited penetration depth and are thus susceptible to destabilization due to scour. The previous sections showed that relatively deep scour holes can occur throughout the NWWFZ. As such, it is recommended to use mitigation strategy B (immediate scour protection) for suction bucket type foundations.



Figure 4-11: Left: schematic of a suction bucket foundation (photo: Tractabel). Right: an example of local (and some global) scour patterns around a Suction Bucket Jacket design (Deltares, 2023).

4.4.5 Gravity based structures

Figure 4-10 (left) shows an example of a gravity-based structure. Gravity-based structures rely on weight to keep them stable. Figure 4-12 (right) shows an example of the scour pattern around a gravity-based structure. Gravity-based structures can vary in design, making it challenging to predict scour depths without prior knowledge of the design.

Due to their reliance on contact with the seabed, gravity-based structures are vulnerable to undermining due to scour. As such, it is recommended to use scour mitigation strategy B (immediate scour protection) for gravity-based foundations.

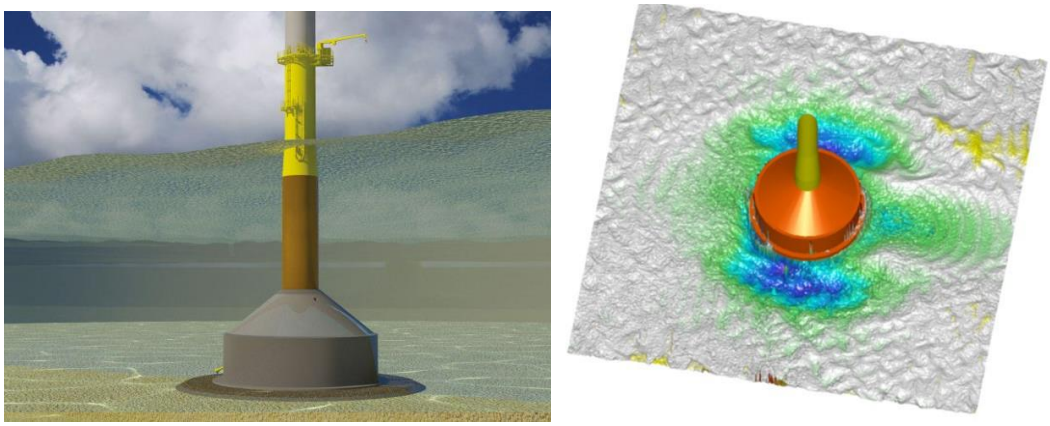

Figure 4-12: Left: schematic of a gravity based foundation foundation (photo: BAM). Right: 3D-bathymetry of the scour pattern with clear contraction scour at the sides and undermining at the upstream side and both transverse sides (Deltares, 2023).

4.5 Summary of site-specific conclusions

4.5.1 NW-I

The hydrodynamic conditions in NW-I are relatively uniform spatially. The scour depth in NW-I is mostly influenced by the varying water depths. Lower scour depths are found on the crest of the sandbank in the northwest, and higher scour depths are found in the deeper areas. Table 4-6 summarizes the predicted 5%, 50%, and 95% non-exceedance scour depths. Figure 4-13 visualizes the spatial distribution of the 50% non-exceedance scour depths in NW-I**.** With typically expected scour slopes of 1:2 – 1:3, the lateral extent of the scour holes in NW-I using the 50% non-exceedance scour depth varies between 25 and 45 m.

Table 4-6: Predicted scour depths in NW-I.

Location	$S_{5\%}$ [m]	$S_{5\%}$/D [-]	$S_{50\%}$ [m]	$S_{50\%}$/D [-]	$S_{95\%}$ [m]	$S_{95\%}$/D [-]
NW-I	7.0 – 8.4	0.6 – 0.7	13.1 – 14.9	1.1 – 1.2	20.1 – 21.8	1.7 – 1.8

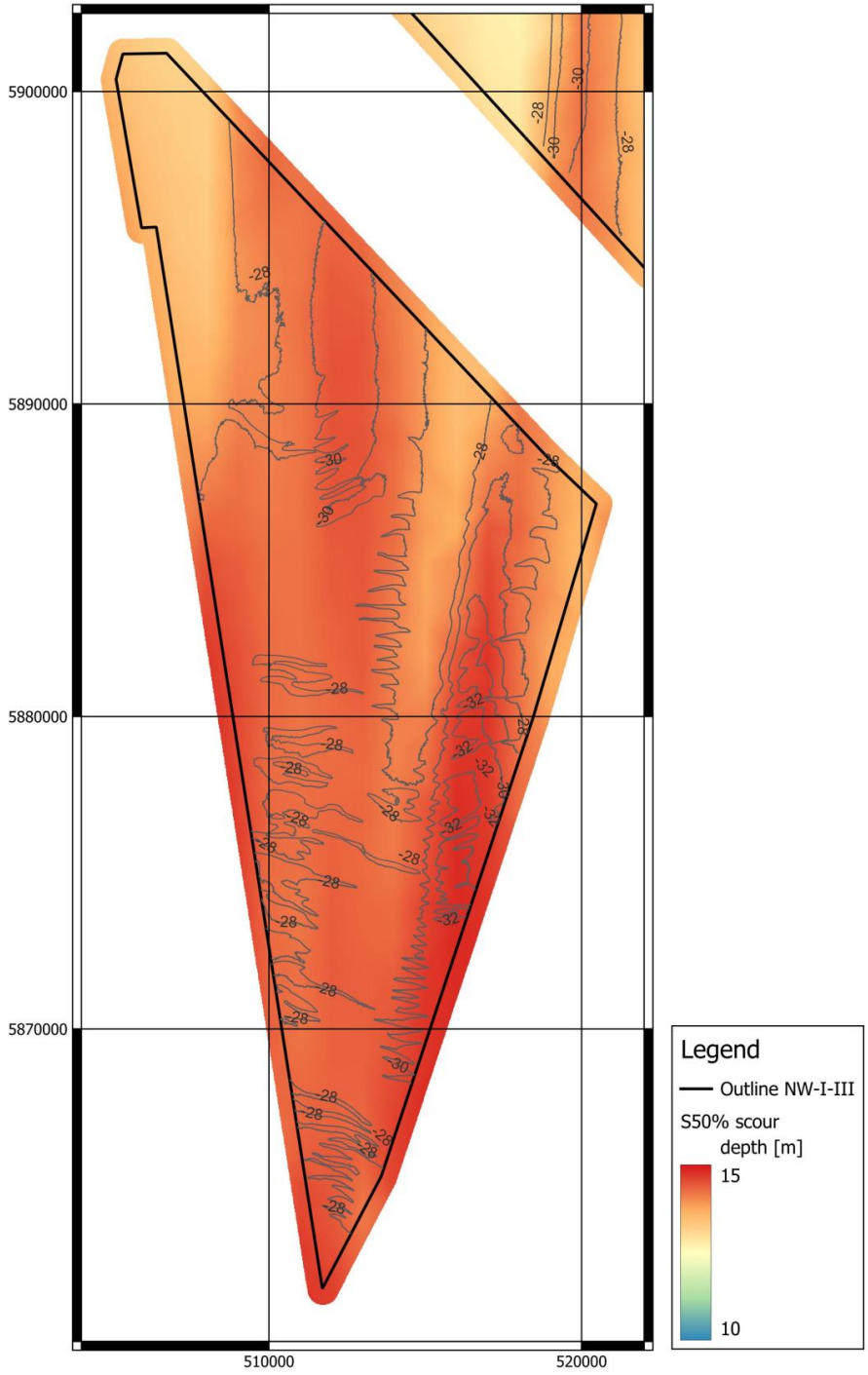

Figure 4-13: 50% non-exceedance maximum scour hole depth predicted for monopiles with D=12 m in NW-I.

The time scales of the scour development are also relatively uniform in NW-I. The equilibrium scour hole depth is predicted to be reached between 5 – 10 years. Table 4-7 summarizes the predicted time for the scour hole to reach depths between 1 and 5 meters.

Table 4-7: Predicted (in days) time to reach scour depths between 1 and 5 m at NW-I.

	NW-I		
Scour depth [m]	5% non-exceedance time [days]	50% non-exceedance time [days]	95% non-exceedance time [days]
1	60-125	25-50	5-10
2	125-260	50-100	10-20
3	210-430	75-155	15-30
4	310-610	110-215	20-40
5	415-870	140-285	25-50

There is evidence of a large-scale non- or less-erodible layer within the range of the maximum scour depth in the NWWFZ. Figure 2-6 shows the spatial variation in the depth below the seabed of this layer. When the predicted scour is expected to reach this layer, additional research regarding its erodibility is advised.

The predicted scour depths at NW-I are expected to be too large to employ scour mitigation strategy A (free scour development). This means only strategy B (immediate scour protection) and strategy C (monitor & react) are feasible. When using strategy B, all scour foundation types are feasible at NW-I. A monopile or piled jacket structure can be considered when using strategy C.

4.5.2 NW-II/III

The hydrodynamic conditions in NW-II/III vary mainly between the southern and the northern sections. These varying conditions create a complex interaction between flow velocities, wave conditions, and water depths to influence the scour potential per location. The highest scour potential is found in the south of NW-II/III. This is primarily the result of the high flow velocities and relatively low wave heights in the south. The scour depths are maximum in the throughs between the sandbanks.

The scour depths decrease towards the north of NW-II/III. Lower flow velocities and slightly higher waves are found in the area's north compared to the south. The bed levels generally decrease from the southeast towards the northwest. As a result, the lowest scour depth occurs in the area's northeast corner, where the waves are highest, the water depth is average, and the flow velocities are low. Table 4-8 summarizes the predicted 5%, 50%, and 95% non-exceedance scour depths. Figure 4-14 visualizes the spatial distribution of the 50% non-exceedance scour depths in NW-II/III. With typically expected scour slopes of 1:2 – 1:3, the lateral extent of the scour holes in NW-II/III using the 50% non-exceedance scour depth varies between 20 and 45 m.

Table 4-8: Predicted scour depths in NW-II/III.

Location	**$S_{5\%}$ [m]**	**$S_{5\%}/D$ [-]**	**$S_{50\%}$ [m]**	**$S_{50\%}/D$ [-]**	**$S_{95\%}$ [m]**	**$S_{95\%}/D$ [-]**
NW-II/III	5.0 – 8.1	0.4 – 0.7	10.7 – 14.4	0.9 – 1.2	18.2 – 21.4	1.5 – 1.8

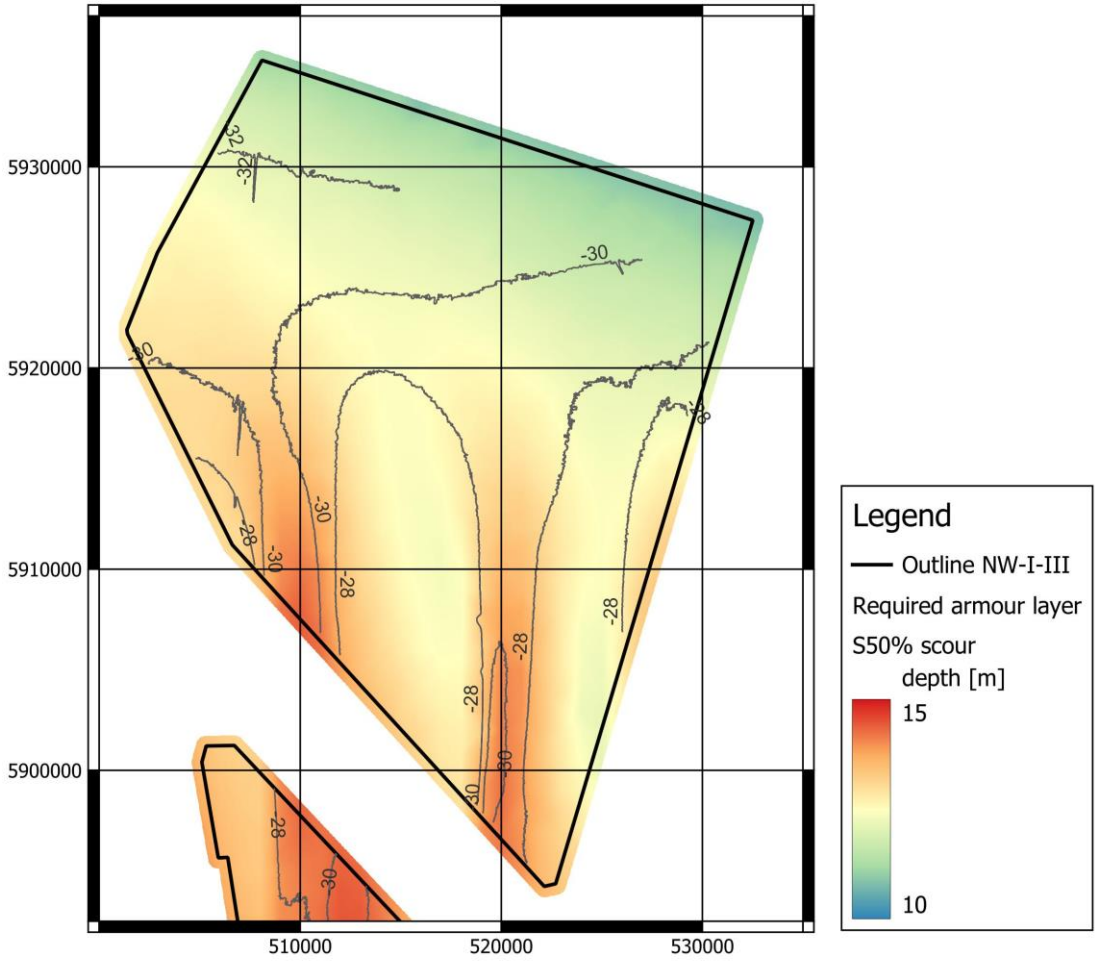

Figure 4-14: 95% non-exceedance maximum scour hole depth predicted for monopiles with D=12 m in NW-II/III.

The time scales of the scour development also are not spatially uniform in NW-II/III. The scour hole is predicted to develop the fastest in the south of the area and the slowest in the north. This is mainly caused by the slower flow velocities in the north compared to the south. The equilibrium scour hole depth is predicted to be reached between 5 – 25 years. Table 4-9 summarizes the expected time it takes for the scour hole to reach depths between 1 and 5 meters.

Table 4-9: Predicted time (in days) it takes to reach scour depths between 1 and 5 m at NW-II/III.

	NW-II/III		
Scour depth [m]	5% non-exceedance time [days]	50% non-exceedance time [days]	95% non-exceedance time [days]
1	105-735	40-285	5-50
2	225-1525	85-600	15-110
3	365-2540	135-935	25-170
4	540-3660	185-1305	35-240
5	770-10060	245-1730	45-315

There is evidence of a large-scale non- or less-erodible layer within the range of the maximum scour depth in the NWWFZ. Figure 2-6 shows the spatial variation in the depth of this layer. When the predicted scour is expected to reach this layer, additional research regarding its erodibility is advised.

The predicted scour depths at NW-II/III are expected to be too large to employ scour mitigation strategy A (free scour development). This means only strategy B (immediate scour protection) and strategy C (monitor & react) are feasible. When using strategy B, all scour foundation types are feasible at NW-I. A monopile or piled jacket structure can be considered when using strategy C.

5 SCOUR PROTECTION METHODS

5.1 Introduction

This chapter introduces several scour protection methods and their applicability at the individual NWWFS. Scour protection is necessary when scour mitigation method B (immediate scour protection) is chosen or when scour mitigation method C (monitor & react) is chosen. The scour protection aims to protect the seabed around the foundation against erosion. This mitigates the risk of destabilization of the structure due to scour. The design of a feasibility-level scour protection follows this chapter in the form of loose rocks in Chapter 6.

The design requirements of scour protection mainly focus on its stability. Section 5.2 highlights these stability requirements. Section 5.3 follows with a more in-depth description of loose rocks, the most popular protection type, ending with the less conventional mattress-type protections in Section 5.4. Alternative scour protection methods are discussed in Section 5.5. This chapter ends with the site-specific conclusions in Section 5.6. The primary focus of this chapter is the required grain size of the armour layer of the scour protection. Other aspects of the scour protection, such as the filter layers and horizontal extend of the scour protection, are not considered.

This chapter mainly summarizes the relevant information in chapters 4, 9, and 11 from JIP HaSPro (2023) and chapter 5 from Deltares (2023) for the NWWFZ. Information from either study is supplemented with notes on the applicability of the described methods specifically for the NWWFZ. More detailed information regarding scour protections can be found in CIRIA, CUR, CETMEF (2007), and Pilarczyk (2000).

5.2 Design requirements for a scour protection

The primary function of the scour protection is to protect the foundation from destabilization due to scour. The scour protection is considered unstable when this function is not fulfilled. Three main stability requirements are defined to ensure the scour protection is sufficiently stable. These are the external stability requirement, the interface stability requirement, and the flexibility requirement. Figure 5-1 visualizes these requirements.

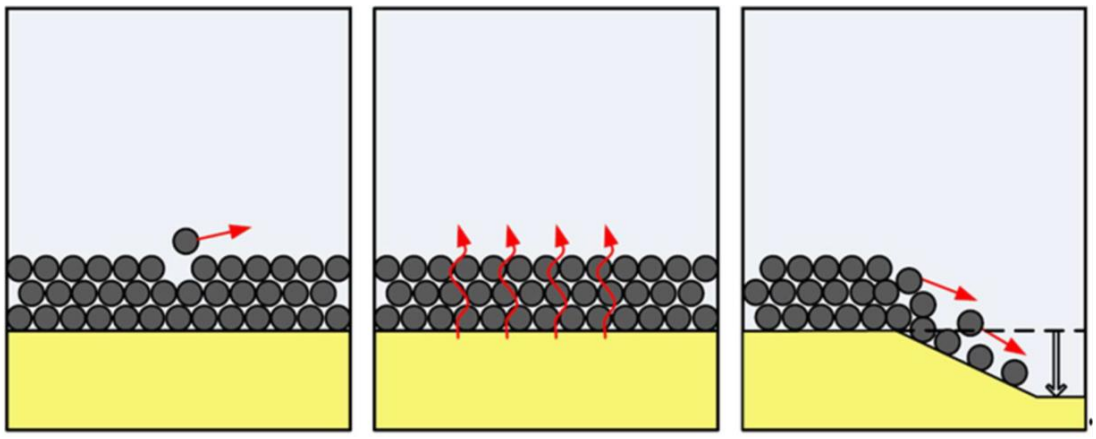

Figure 5-1: Schematisation of the stability requirements. Left: external stability. Middle: interface stability. Right: flexibility (JIP HaSPro, 2023).

5.2.1 External stability requirement

The external stability requirement states that the top layer of the protection should be sufficiently stable under the design load. Extreme hydrodynamic conditions exert an extreme force on the scour protection. The resistance of the protection material should be sufficiently high that no significant

scour can occur during the design conditions. Furthermore, depending on the design choices, the deformation of the scour protection should be limited. There are generally two choices:

- A statically stable protection
- A dynamically stable protection

The protection elements in a statically stable protection are designed to remain stationary under the design load. This means that no deformation of the protection occurs. Statically stable protections often require larger protection elements. This can make the protection both more expensive and more challenging to install. Larger protection elements can also increase the edge scour around the scour protection, which will be further discussed with the flexibility requirements.

Dynamically stable bed protections allow for deformation to occur during the design conditions. A certain minimum protection thickness is defined to protect the seabed material. This can reduce the size of the protection elements, potentially making the protection less expensive and easier to install and possibly decreasing the edge scour.

Figure 5-2 shows an example of a statically stable protection (left) and a dynamically stable protection (right) with loose rocks.

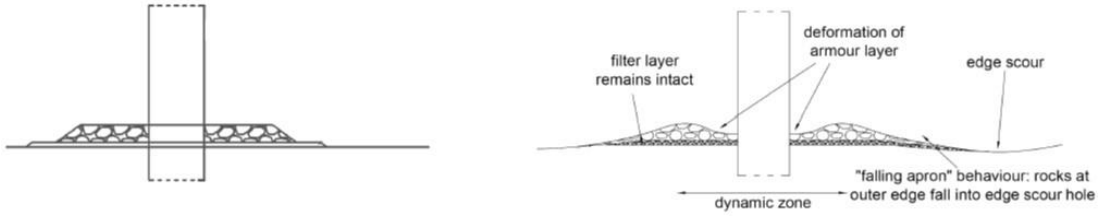

Figure 5-2: Scour protection around a monopile. Left: statically stable. Right: dynamically stable (JIP HaSPro, 2023).

5.2.2 Interface stability requirement

The interface stability requirement signifies that the seabed material is not removed through the pores of the scour protection. This means that the scour protection should be impermeable for the seabed material or that the hydraulic load exerted on the seabed through the scour protection is sufficiently small that no suction removal occurs. The former is a geometrically closed filter, whereas the latter is a geometrically open filter. This suction removal through a geometrically open filter is called winnowing. Winnowing mainly occurs adjacent to the upstream sides of the pile. When designing a geometrically open filter, it is crucial to maintain a sufficient layer thickness to reduce the hydraulic loads on the seabed so that winnowing is limited.

When considering a geometrically closed filter layer, the pores between the protection material should be sufficiently small that the bed material cannot pass through. This is often done using a filter layer. The dimensions of the filter layer depend on the grain size of the seabed material, the grain size of the armour layer, and the grading width of all materials. An alternative to the filter layer is a geotextile that is impermeable to the seabed material.

Note that the interface stability criterion should be satisfied for all layers of the scour protection.

5.2.3 Flexibility stability requirement

The scour protection does not necessarily span the entire area of flow disruption due to the construction. Furthermore, depending on the thickness of the scour protection, the scour protection itself obstructs the flow. Both factors cause scour at the interface between the scour protection and the unprotected seabed. This is called edge scour. Edge scour has a similar effect on scour protections as a lowering seabed level due to bedform migration. The scour hole at the edge of the

scour protection can cause destabilization of the scour protection. The scour protection should thus be able to handle the predicted edge scour formation.

A falling apron is often used to mitigate destabilization due to edge scour. The filter layer (or armour layer if a single-graded protection is used) is extended past the required scour protection width within a falling apron. This additional material will roll down the slope of the scour hole, which develops around the edge. This stabilizes the edge scour hole against further erosion. Figure 5-1 (right) shows an example of a falling apron.

It is noted that edge scour does not necessarily occur around the entire scour protection, in contrast to a lowering seabed due to bedform migration, which happens uniformly over the scour protection. This should be considered when fulfilling the flexibility requirement.

5.3 Scour protections consisting of loose rock

5.3.1 Introduction

The most common type of scour protection consists of loose rock. The rock formation of loose rock protections can be separated into two categories: double-layered protections and single-layered protections. Both rock formations can be designed to be either dynamically stable or statically stable.

5.3.2 Double-layered scour protections

Double-layered scour protections have two separate layers satisfying different stability criteria. The top or armour layer is designed to fulfil the external stability criterion. This means the stones should be large enough to withstand the hydrodynamic force of the design conditions. The layer on top of the seabed, or filter layer, is designed to satisfy the interface and flexibility stability criteria. This means that either the pores of the filter layer are sufficiently tiny that it is impermeable for the seabed material, or the scour protection height sufficiently reduces the flow load on the seabed material.

Furthermore, the filter layer is often extended past the armour layer to form a falling apron. However, it is also possible for the armour layer to fulfil this function. Double-layered protections are difficult to place on already-formed scour holes. Therefore, this type of rock protection is less suited in the case of scour mitigation strategy C.

5.3.3 Single-layered scour protections

Single-layered protections consist of only one rock grading. This single grading should fulfil all three stability requirements. The stone size should be sufficiently large to resist the design load, but the pores should also be small to prevent winnowing. Single-layered protections are easier to install than double-layered ones, as only one wide grading has to be installed. This type of protection is more feasible for scour mitigation strategy C (monitor & react), as it can be placed more easily in an already formed scour hole compared to double-layered scour protections. Do note that this approach can require more stones to fill up the scour hole compared to placement on a flat bed (strategy B, immediate scour protection).

5.3.4 Statically stable scour protections

Statically stable scour protections allow no deformation under the design load. These types of protections are often on the conservative side. Large stones are required to mitigate any deformation under design conditions. This poses a challenge for the design: large stones increase the scour protection height, increasing the load on the scour protection and the potential edge scour. Furthermore, larger stones make it more challenging to fulfil the internal stability criterion. This makes single-layered protections less feasible for a statically stable design.

5.3.5 Dynamically stable scour protections

Dynamically stable scour protections allow for deformations under severe conditions. The scour protection is designed to some maximum allowable deformation. In Chapter 6, the required stone sizes for a feasibility-level, dynamically stable scour protection with a maximum deformation of 0.5 m are calculated for the entire NWWFZ. The size of the stones needed for dynamically stable scour protections is generally smaller than for statically stable scour protections. This smaller stone size means the total layer thickness is smaller, reducing the hydrodynamic load on the scour protection. Furthermore, the internal stability criterion is more easily satisfied. Dynamically stable scour protections require more maintenance than statically stable ones to ensure the deformation limit has not been reached.

When a dynamically stable scour protection is designed as a single-layered protection, the allowable deformation can be slightly higher. This is because the scour protection consists of only one grading, meaning that if the layer thickness reduces at some point in the scour protection, the same stone size still protects the bed.

5.4 Scour protections consisting of mattresses

Figure 5-3 shows an example of a scour protection mattress in the form of a block mattress. Uniform elements with a large width and length but a limited thickness characterize mattress-type protections. Contrary to loose rock protections, the material within a mattress is connected. This connection between the material inside the mattress creates additional strength. For the block mattress in Figure 5-3, the force required to move one individual block is relatively large, as it requires the adjacent blocks to be moved as well. This does require the reinforcement to be sufficiently strong to circumvent the lifting of the blocks as result of local pressure differences.



Figure 5-3: Geotextile-bonded block mattress (JIP HaSPro, 2023).

The connection between elements within a mattress differs depending on the mattress type. For block mattresses, the connection is made by either a cable between the rocks or by a geotextile on which the rocks are mounted. For gabion mattresses, the connection is made by entrapping loose rock within a wire mesh. This wire mesh prevents individual rock transport, meaning transport is only possible if the entire wire mesh moves.

Mattresses are characterized by their flexibility, permeability, and relatively small height compared to loose rock protections. The flexibility allows the mattress to follow gradients in the bed, allowing the mattress to follow some edge scour. The expected edge scour is generally lower than loose rock protections due to the relatively small height of the mattresses. The permeability indicates the need for a proper filter to satisfy the internal stability criterion. Specifically for gabion mattresses, the

internal stability criterion can be fulfilled with the rock grading inside the wired meshes. For block mattresses, either a filter layer or a geotextile is required.

An issue with mattress-type protection is the relatively small installation tolerance. The mattresses should be tightly connected to ensure no gaps persist between adjacent mattresses. These gaps can be prevented by applying an overlap between mattresses, connecting adjacent mattresses, or applying a two-layered mattress system. The same issue holds at the interface between the mattresses and the structure, where a sand-tight connection might be necessary. This limited installation tolerance makes mattress-type protections less suitable for scour mitigation strategy C (monitor & react) due to the difficulty of placing inside the already formed scour hole.

The reader is referred to JIP HaSPro (2023) and CIRIA, CUR, CETMEF (2007) for further reading on mattress-like protections.

5.5 Alternative scour protection methods

Besides loose rock protections and mattress-like protections, plenty of different scour protection methods exist. This section provides a non-exhaustive list of alternative scour protection methods. These alternative methods are generally less conventional in the offshore industry, meaning less design guidance is available. Some guidance from inland usage might be transferable to offshore usage, and JIP HaSPro (2023) gives some novel guidance. The reader is referred to JIP HaSPro (2023), CIRIA, CUR, CETMEF (2007), and Pilarczyk (2000) for more information regarding alternative scour protections.

Alternative scour protection methods that can be considered for the scour protection at the NWWFZ are:

- **Artificial vegetation**: placing a mat with densely packed artificial vegetation reduces the flow velocities at the seabed, decreasing the bed shear stresses and scour. Furthermore, sediment can be entrapped in the vegetation, stimulating sedimentation.
- **Ballast-filled mattresses**: an impermeable shell is filled with ballast (or any other heavy substance) and is placed at the seabed to prevent the underlying material from eroding. The advantages of a ballast-filled mattress are similar to the other mattress types.
- **Rock-filled mesh bags or gravel/sandbags:** a mesh bag or jute bag is filled with sand, rocks or gravel and placed at the seabed to protect the underlying seabed material. The working principle is similar to mattress-like constructions but is more flexible due to the flexible bags.

5.6 Site specific conclusions

5.6.1 NW-I

Loose rock protections are feasible in NW-I. Special care should be taken around the areas where a seabed lowering is expected due to migrating sand waves, especially around the crests of the sand waves. A seabed lowering requires sufficient flexibility of the scour protection. This can be achieved by designing a falling apron. Furthermore, the scour protection will stick out like a sill when the surrounding seabed lowers. This increases the load on the scour protection, which should be accounted for in the design of the armour layer, see Hoffmans & Verheij (2021) for more information.

It is advised to employ mitigation strategy C only when a single-layered rock protection will suffice. The single-layered protection is easier to install inside an already-formed scour hole compared to double-layered scour protections. The applicability of single-layered and double-layered rock protections depends on both the flow load and the internal stability criterion at the considered

locations. The decision between a statically stable or a dynamically stable scour protection depends solely on the flow load. These considerations are up to the designer.

Mattresses are expected to have some flexibility to deal with the seabed lowering due to sand waves. When using mattress-like scour protections, special care should be taken regarding the sand-tightness of the construction.

5.6.2 NW-II and NW-III

Loose rock protections are feasible in NW-II/III. There are no additional flexibility requirements as there are no migrating bedforms in NW-II/III. The required flexibility of the rock protection depends entirely on the predicted edge scour. It is advised only to employ mitigation strategy C when a single-layered rock protection will suffice. The single-layered protection is easier to install inside an already-formed scour hole compared to double-layered protections. The applicability of single-layered and double-layered rock protections depends on both the flow load and the internal stability criterion at the considered locations. The decision between a statically stable or a dynamically stable scour protection depends solely on the flow load. These considerations are up to the designer.

Mattresses are expected to have some flexibility when dealing with edge scour. When using mattress-like scour protections, special care should be taken regarding the sand-tightness of the construction. Furthermore, installing a mattress-like scour protection towards the north of NW-II/III might be difficult due to the higher water depths.

6 FEASIBILITY LEVEL SCOUR PROTECTION

6.1 Introduction

The design approach of dynamically stable, loose rock scour protection at the NWWFZ is demonstrated in this chapter. This design aims to provide the reader with a general estimate of the required rock gradings for the armour layer that can be used for a feasibility analysis. This is not to say that scour protections other than loose rock are not feasible for the NWWFZ. This study focuses on loose rock protection as it is the most popular scour protection type.

It is stressed that the results are valid for a feasibility-level design only and should not be used for detailed design purposes. The presented design can never substitute a detailed scour protection design for the NWWFZ.

This chapter starts with the model approach in Section 6.2, followed by the input parameters in Section 6.3. The latter includes an explanation of the chosen design loads, the boundary conditions and estimations, and the rock gradings considered. The required armour layer thicknesses are discussed in Section 6.4, followed by the site-specific conclusions in Section 6.5.

6.2 Model approach

The deformation model from JIP HaSPro (2023) is used to calculate the required gradings of the armour layer of a dynamically stable loose rock scour protection. This model is based on an extensive physical model test database focused on scour protections for offshore monopiles. However, due to the model's novelty, it has (to the authors' knowledge) not yet been applied in prototype scenarios. The results from the deformation model are therefore validated with more standard methods from Schiereck (2017), such as the Shields method.

The scour protection deformation (S) within the model is linked to the rock mobility at the top of the scour protection and the total Keulegan-Carpenter number (KC). Eq 6-1 and Eq 6-2 show the formulas.

$$\frac{S}{D_{pile}} = f(KC_{tot}) \cdot c_1 \cdot MOB_{top}^{c_2} \qquad \text{Eq 6-1}$$

$$f(KC_{tot}) = 1 + \frac{c_3}{1 + \exp[-c_4 \cdot KC_{tot} + c_5]} \qquad \text{Eq 6-2}$$

The minimum median stone diameter in the rock grading characterizes the required rock grading. This stone diameter is used implicitly in multiple parameters that are used to calculate MOB_{top}. Therefore, the deformation is calculated with the minimum median diameter of various gradings that are commonly used in offshore applications. The required grading is calculated as the smallest rock for which the deformation is less than or equal to 0.5 m ($S \leq 0.5$).

The values of $c_{1\text{-}5}$ are dependent on the chosen subset of the physical modelling data. In this study, the dataset which omits high scour protection deformations (> 4 layers) and high KC-numbers (> 4.2) is chosen. A deformation of more than four rock layers is too large, with the deformation limit considered to be 0.5 m. Furthermore, the KC numbers calculated from the design load are relatively small due to the large pile diameter (2 – 3). The reduced set is therefore deemed the most fitting for the scenario at the NWWFZ, even though fewer data points are used.

Aside from the variation between datasets, JIP HaSPro (2023) provides various non-exceedance values for the fitting parameter c_1. In this study, the 90% non-exceedance value is used. Table 6-1 shows the resulting values for $c_{1\text{-}5}$.

Table 6-1: Fitting constants used in the deformation model from JIP HaSPro (2023).

C_1	C_2	C_3	C_4	C_5
0.1136	1.6976	5.000	0.5918	4.5000

6.3 Input parameters

6.3.1 Input parameters and boundary conditions

A simplified extreme value analysis is performed to derive the design conditions for the scour protection design. The deformations due to the hydrodynamic loads are calculated for the entire 43-year hydrodynamic time series at several locations in the NWWFZ. These calculations found that the wave height was the governing parameter for the calculated deformations. Therefore, the basis for this analysis is the 50-year return period (RP50) wave height. The design current velocity and water depth are adjusted to the design wave condition. The designer should perform a joint probability between wave height, current velocity, and water depth in a more detailed design stage of the scour protection.

The RP50 wave height is derived from the 43-year dataset from DHI (2023a; 2023b). The 43-year data is fitted using a 3-parameter Weibull fit to extrapolate to the 50-year return period conditions. The corresponding wave period is derived based on the wave steepness; see Appendix B for more information.

DHI (2023a; 2023b) performed a joint probability between water levels, wave heights, and current velocities on three locations. The current velocities correlated to the RP50 wave height are in the order of magnitude of the 1-year return period current velocity (RP1). It was, therefore, decided to use the RP1 current velocities together with the RP50 wave conditions. These RP1 current velocities are derived from the 43-year dataset DHI (2023a; 2023b). It was further chosen to use the Mean Low Water (MLW) conditions as a conservative estimate for the water depth. Please note that this (relatively simple) analysis yields unidirectional extremes. Therefore, no directional information is available, and the conservative assumption is made that the design current and design wave follow the same direction. For more information, see Appendix B.

The hydrodynamic data is available on a grid with a resolution of roughly 500 m in x and y directions. The design conditions on this grid are interpolated to a finer grid with 20 m resolution. This allows for a higher resolution bathymetry to be used within the analysis. Please note that this analysis does not include the feedback on the hydrodynamic conditions of bed features with a length smaller than 500 m. The higher resolution bed only affects the local depth in the computation and, in addition, the bed shear stress and sediment mobility.

Figure B-4 shows the resulting design wave height, peak wave period, water level, and current velocity.

Table 6-2 summarizes the other input parameters.

A scour protection thickness of 1.5 m is assumed in this study for both single-layered and double-layered scour protections. It is noted that, in reality, the scour protection thickness depends on the designed armour layer grading, scour protection design choices, and (if applicable) the filter layer. For more information regarding the design thickness of the scour protection, see Hoffmans (2012).

Table 6-2: Input parameters used in the feasibility-level scour protection design.

Parameter name	Symbol	Value	Unit
Total scour protection thickness	t	1.5	[m]
Water density	ρ_w	1025	[kg/m^3]
Bed roughness	K_s	$2 \cdot D_{50}$	[m]
Pile diameter	D	12	[m]

6.3.2 Rock gradings

Several rock gradings are considered to be applicable at the NWWFZ. It was chosen to use the same rock gradings as were considered for the IJV and TNW sites to remain consistent with previous scour studies at Dutch wind farm zones (Deltares, 2022; Deltares, 2023). These gradings are considered because they are applied at nearby wind farms. Most of them are standard gradings. Table 6-3 gives an overview. The minimum value of the median rock diameter is used in the calculations.

The inch-gradings in Table 6-3 can be considered for single-layered protections if the grading width is sufficiently large to satisfy the internal stability criterion. Single-layered protections might be preferable to double-layered protections; for example, when using scour mitigation strategy C (monitor & react), see Chapter 5. Therefore, the 2-8" and 3-9" gradings are also considered with a high-density variant (HD). It is noted that these high-density variants are more expensive compared to the normal-density variants (ND). The higher density makes the rock more stable, allowing the HD gradings to be more efficient as a scour protection. The consideration of the pros and cons of high-density gradings is up to the designer.

Table 6-3: *Considered rock gradings in this indicative assessment; ND refers to normal density rock, whereas HD refers to high density rock. For the median rock diameter, the minimum diameter that qualifies for this grading is taken. Note that these rock gradings span typical adopted rock gradings in neighbouring wind farms. Most considered rock gradings are standard rock gradings as described in the New European Rock Manual (CIRIA / CUR / CETMEF, 2007); the 10-200 kg and 3-9 inch* gradings are non-standard gradings, but often applied in offshore applications *(Deltares, 2023)*

Grading	Minimum median diameter D_{50} [mm]	Particle density [kg/m^3]
60-300 kg ND	469	2650
40-200 kg ND	402	2650
10-200 kg ND	355	2650
10-60 kg ND	258	2650
3-9" HD	125	3050
3-9" ND	125	2650
2-8" HD	100	3050
2-8" ND	100	2650

6.4 Feasibility level armour layer gradings

The deformation model from JIP HaSPro (2023) is used with 90% non-exceedance values. The results thus yield the 90% non-exceedance grading required for a stable dynamic scour protection around the NWWFZ with a maximum allowable deformation of 0.5 meters. Of the gradings discussed in the

previous section, the smallest grain size that fulfils this stability requirement is chosen. Please note that this is not necessarily the most economical grading, as the high-density rocks can be more expensive than the normal density rocks. The results are indicative only and cannot and should not replace a detailed scour protection design

Figure 6-1 visualizes the required gradings around the NWWFZ. The figure shows that shallow locations often require more heavy protection than deeper ones. This is most evidently visible on the crest of the sandbanks, where the largest stones are required for the armour layer. It is noted that it is unlikely that a contractor will vary the gradings used as an armour layer as much as Figure 6-1 portrays. In reality, the contractor will likely choose one grading to protect foundations in a large area.

A 2-8” or 3-9” grading of high-density rock can effectively protect most of the NWWFZ. This mainly applies to NW-I and the north-western sections of NW-II/III. These gradings are commonly employed as single-layer scour protections. If the grading width meets the internal stability criteria, these gradings can serve as a single-layer scour protection at Nederwiek. Only the shallower areas strictly require a double-layered scour protection based on external stability. Furthermore, a few locations in NW-I can be protected with normal density rock with a grading of 3-9”.

It can generally be said that the wave load increases from southwest to northeast in NW-II/III. Figure B-2 visualizes this pattern. The maximum design wave height and maximum design peak velocity are located at the northeast corner of NW-II/III. As a result, the northeast section of NW-II/III requires heavier protection than is expected at other locations at the same water depth.

The sand wave pattern in NW-I is visible in Figure 6-1. The reduced wave loading at the sand wave crests is underestimated because of the relatively coarse resolution of the hydrodynamic conditions compared to the wavelength of the sand waves. Therefore, the effect of sand waves might be slightly exaggerated in the figure. Nevertheless, placing a monopile foundation on the crest of a sand wave requires the scour protection to be heavier. This effect is expected to increase further when the sand wave migrates. The migration of the sand wave lowers the unprotected seabed around the monopile. This causes the scour protection to stick out like a sill and can increase the hydrodynamic load on the scour protection.

The 90% non-exceedance gradings are validated using the typical Shields method from Schiereck (2017) using a critical Shields parameter of 0.03. This (relatively low) Shields number allows for some deformation during the design storm. The required gradings from this method are generally slightly lower than those shown in Figure 6-1. This is expected, as Figure 6-1 shows the 90% non-exceedance values. The spatial patterns are similar. This gives confidence that the 90% non-exceedance gradings, calculated with the deformation model from JIP HaSPro (2023), are valid.

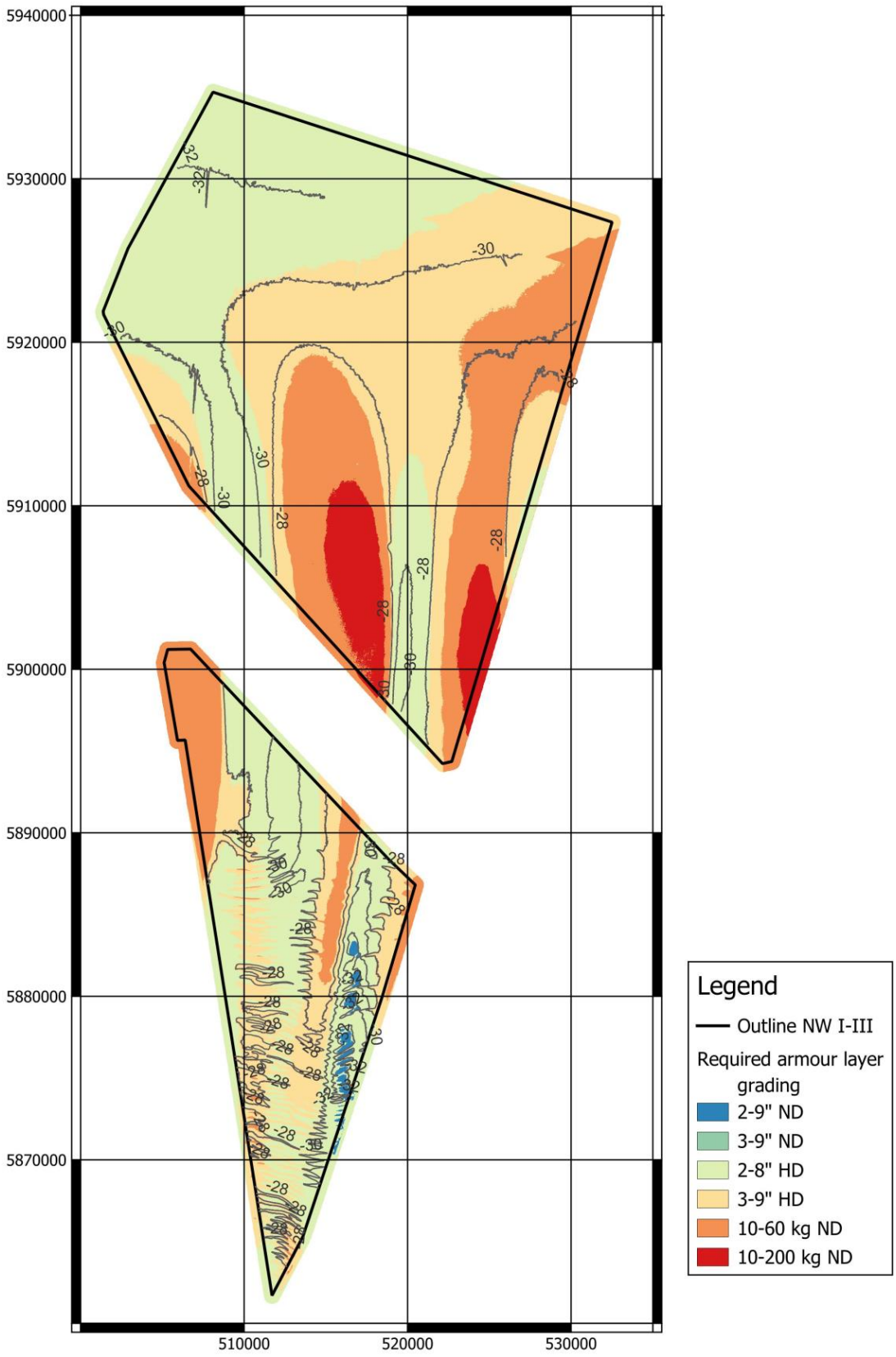

Figure 6-1: Required armour layer grading to achieve a maximum deformation of 0.5 m in the NWWFZ with 90% confidence.

6.5 Site specific conclusions

6.5.1 NW-I

Figure 6-2 shows the required armour layer grading in NW-I to achieve a maximum deformation of 0.5 m with 90% confidence**.** The shallowest areas are shown to require the heaviest gradings. This is applicable mainly on the crest of the sandbank in the northwest. The crests of the sand waves further towards the south require heavier protection compared to the throughs. Note that the migration of the sand waves will eventually increase the load on the scour protection if it is placed in an area with a lowering seabed.

A 2-8” or 3-9” grading of high-density rock can effectively protect most of NW-I. gradings are commonly employed as single-layer scour protections. If the grading width meets the internal stability criteria, these gradings can serve as a single-layer scour protection at NW-I. Based on external stability, a double-layered scour protection can be applied everywhere. The heaviest grading required is 10-60 kg on the crest of the sandbank.

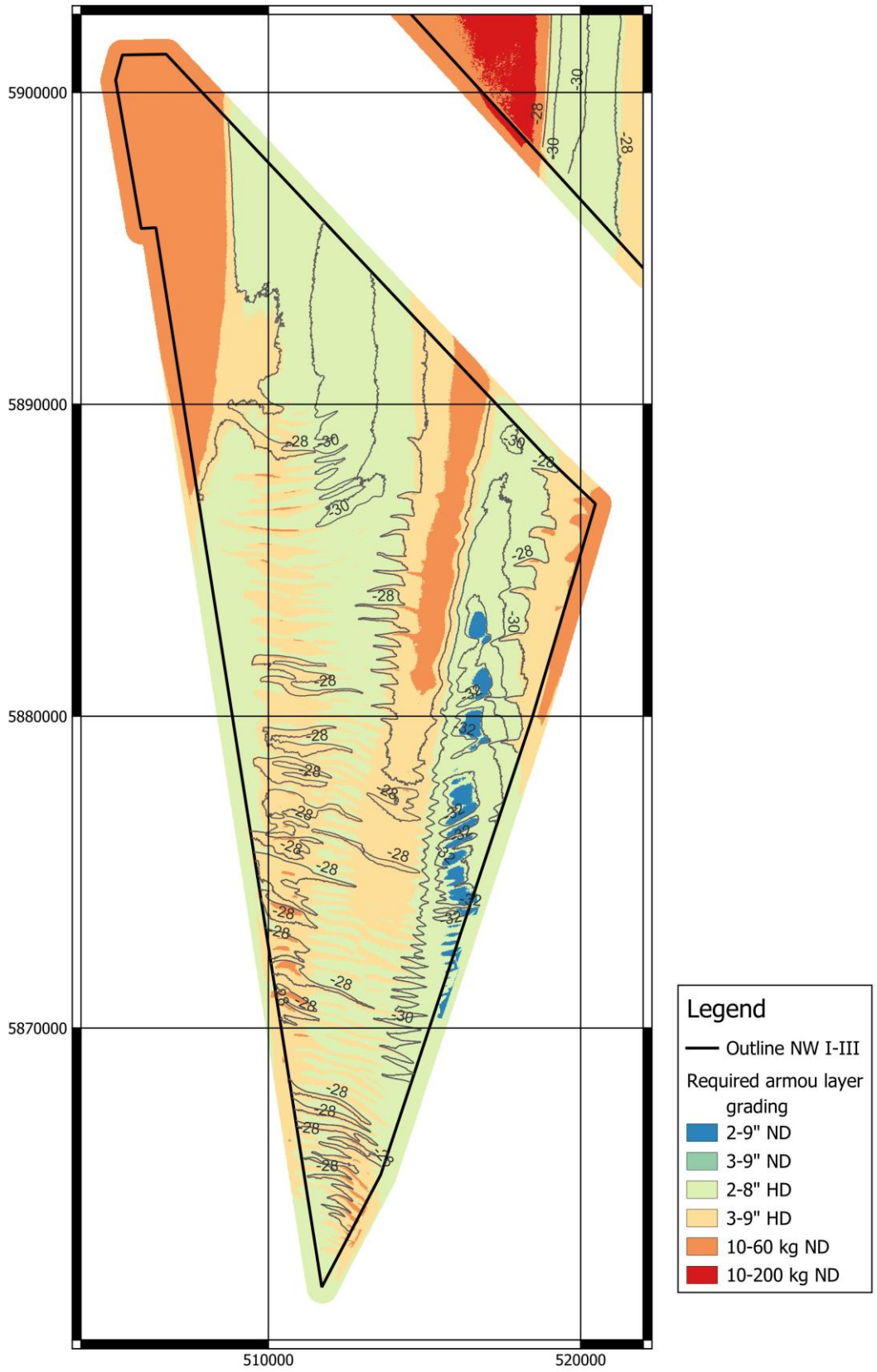

Figure 6-2: Required armour layer grading in a feasibility-level design to achieve a maximum deformation of 0.5 m with 90% confidence in NW-I.

6.5.2 NW-II/III

The required armour layer grading in NW-II/III to achieve a maximum deformation of 0.5 m with 90% confidence is shown in Figure 6-3**.** The heaviest gradings are required in the shallowest areas, most notably on the crests of the sandbanks in the south. The deeper regions typically require lighter gradings. However, the design wave conditions are higher and longer in the northeast compared to the southwest. This means that locations with an equal water depth require heavier protection in the northeast compared to the southwest. The area in the northwest requires a relatively light grading due to the more significant water depths.

The sand bank troughs and the deeper north-western area of NW-II/III can be protected by a 2-8” or 3-9” grading of high-density rock. These gradings are commonly employed as single-layer scour protections. If the grading width meets the internal stability criteria, these gradings can serve as a single-layer scour protection at NW-II/III. Based on external stability, a double-layered scour protection can be applied everywhere. The heaviest grading required is 10-60 kg on the crest of the sandbank. The heaviest grading required is 10-200 kg on the crest of the sandbank.

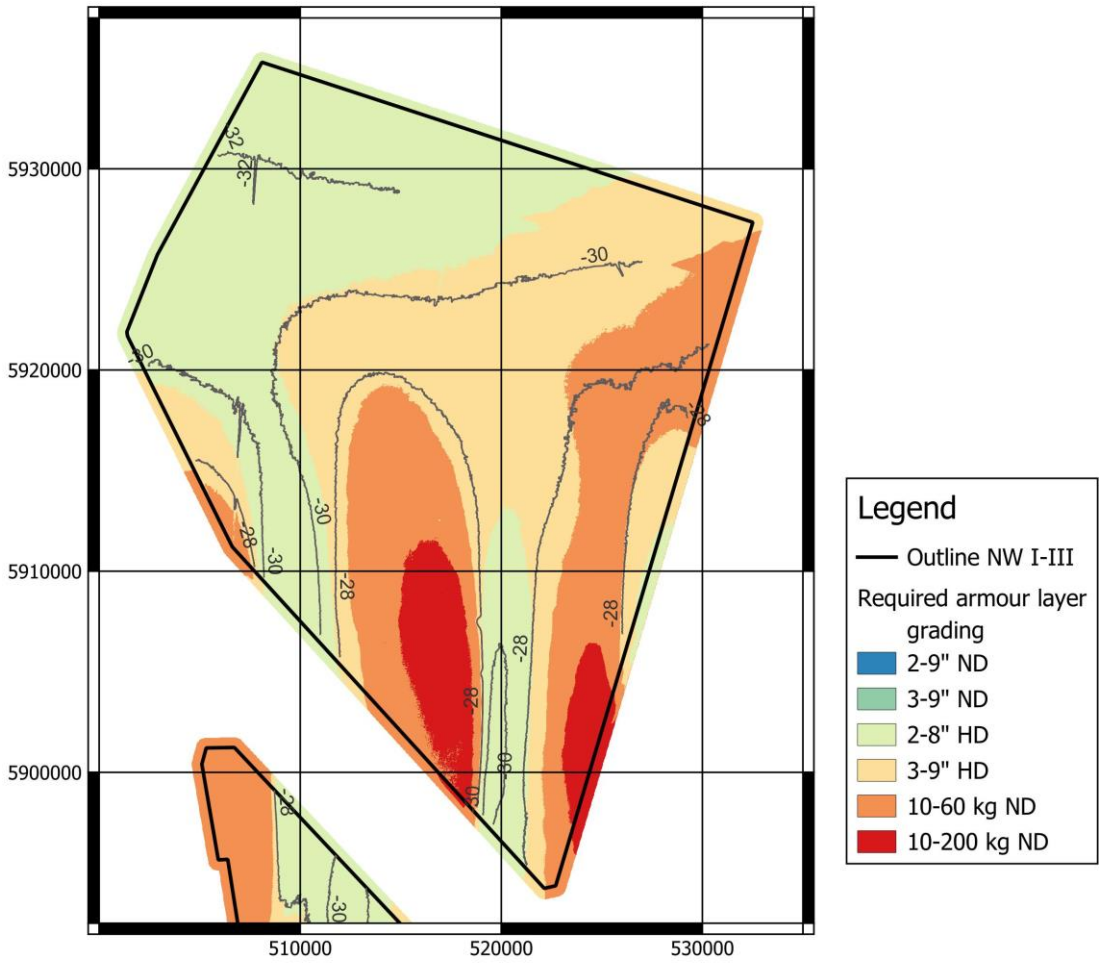

Figure 6-3: Required armour layer grading in a feasibility-level design to achieve a maximum deformation of 0.5 m with 90% confidence in NW-II/III.

7 CONCLUSIONS AND RECOMMENDATIONS

7.1 General Conclusions

The NWWFS study aims to improve the understanding of the seabed morphology, morphodynamics, and infrastructure-related scour potential at the Nederwiek Wind Farm Zone (NWWFZ). These objectives are separated into two reports. The first report focuses on the seabed morphology and morphodynamics at Nederwiek (Svašek Hydraulics, 2024). This report focuses on the infrastructure-related scour and potential scour protections at NWWFZ.

Scour is the process of seabed lowering caused by an obstruction of a water flow due to the presence of some structure. This lowering of the seabed is generally unwanted and can lead to structural failure. Three different scour mitigation strategies are analysed in this study:

- Strategy A: Free scour development
- Strategy B: Immediate scour protection
- Strategy C: Monitor and react

The predicted scour depths at the NWWFZ are expected to be too large to employ scour mitigation strategy A (free scour development). This means only strategy B (immediate scour protection) and strategy C (monitor & react) are feasible. When using strategy B, all scour foundation types are feasible at NW-I. A monopile or piled jacket structure can be considered when using strategy C.

There is evidence of a large-scale non- or less-erodible layer within the range of the maximum scour depth in the NWWFZ. Figure 7-1 shows the spatial variation in the depth of this layer The none erodible layer is relevant if free scour *is* allowed to develop (Strategy A). We advise to perform additional research regarding locations where, in such a case, maximum scour is expected to reach this layer.

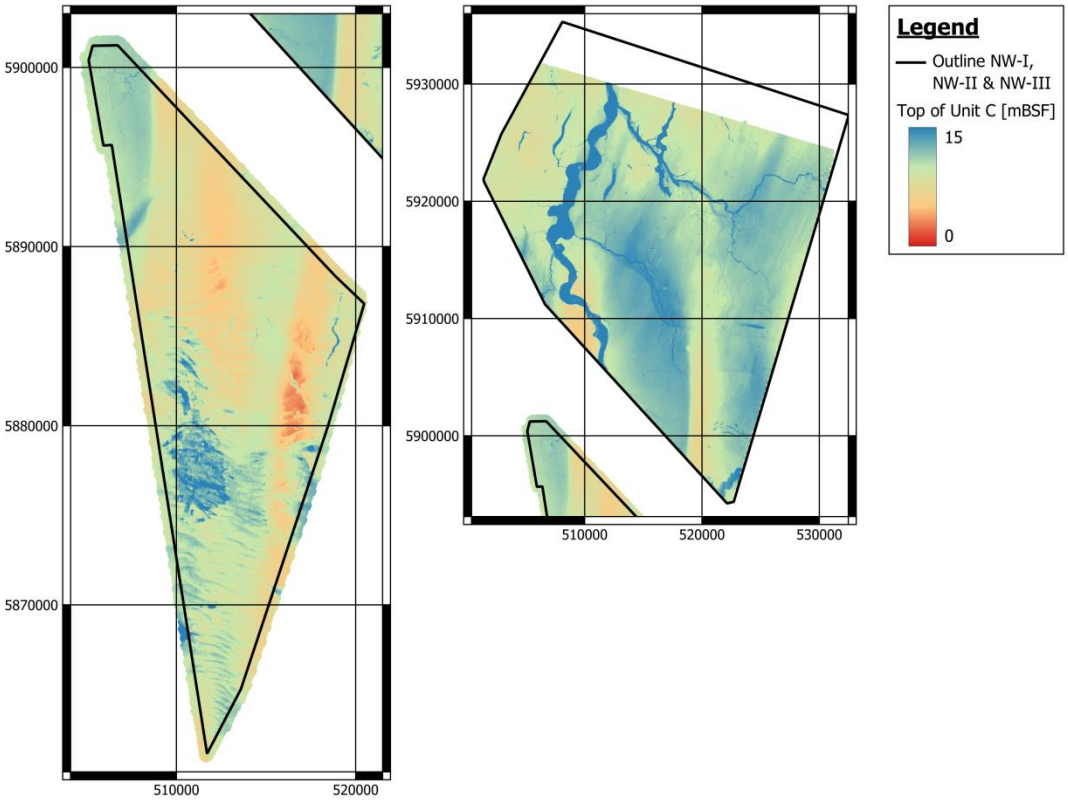

Figure 7-1: Depth of top of the less erodible layer (unit C) below the surface for NW-I (left) and NW-II/III (right).

The NWWFZ is characterized as flow-dominated, indicating that the scour is mainly caused by tidal flow velocities rather than waves.

A quantitative analysis of the general order of magnitude of the to-be-expected scour at the NWWFZ has been performed. These predicted scour depths are indicative and are suitable for a feasibility-level analysis. The scour prediction for monopiles uses a time-dependent scour prediction model with a probabilistic approach. The governing stochastic parameters are listed below. A normal distribution is assumed for the Breusers coefficient, of which the confidence interval shows a good fit with scour measurements at surrounding wind farms. This analysis is translated to a spatially varying scour map which is presented in the sections below.

- The Breusers coefficient
- The timescale calibration factor for scour
- The timescale calibration factor for backfilling
- The hydrodynamic forcing

A feasibility level armour layer of a scour protection has been designed in this study. Loose rock protections seem to be feasible scour protections throughout the NWWFZ. It is advised to employ mitigation strategy C only when a single-layered rock protection will suffice. The single-layered protection is easier to install inside an already-formed scour hole. Wider rock gradings, such as the 2-8" and 3-9" rock grading, are expected to only be applicable at the NWWFZ with high-density rock. These gradings are commonly used as single-layered scour protections. If the grading width meets the internal stability criteria, these gradings can serve as a single-layer scour protection in most of the NWWFZ, except for the shallow areas around the sandbanks.

7.2 Conclusions NW-I

Relatively uniform hydrodynamic conditions characterize NW-I. A sandbank is present in the north-west of the site. Migrating sand waves are present throughout the site, except the most northern sections. The applied scour mitigation strategies should account for these migrating sand waves. For strategy A, this means considering the possible additional seabed lowering in the foundation design. For strategies B and C, the scour protection requires additional flexibility to account for the lowering of the surrounding seabed.

Table 7-1 summarizes the predicted 5%, 50%, and 95% non-exceedance scour depths, both absolute and relative to the pile diameter. Figure 7-2 visualizes the spatial distribution of the 50% non-exceedance scour depths in NW-I. With typically expected scour slopes of 1:2 – 1:3, the lateral extent of the scour holes in NW-I varies between 25 and 45 m, based on the 50% non-exceedance scour depth.

Note that it is a conservative estimate in the determination of the fixation point of monopiles to take the sum of bed level lowering due to sand waves in conjunction with the scour depths as predicted without sand wave migration. It is expected that scour will be reduced when the seabed lowers. The scour hole is expected to be able to follow the development of the bedform migration due to the differences in timescales.

Table 7-1: Predicted scour depths in NW-I. The percentage values indicate the non-exceedance values. Indicated scour depths are the maximum scour depth during the entire simulation. The simulations are based on monopiles with a pile diameter of D = 12 m. $S_{n\%}$ stands for the n% non-exceedance scour depth.

Location	$S_{5\%}$ [m]	$S_{5\%}/D$ [-]	$S_{50\%}$ [m]	$S_{50\%}/D$ [-]	$S_{95\%}$ [m]	$S_{95\%}/D$ [-]
NW-I	7.0 – 8.4	0.6 – 0.7	13.1 – 14.9	1.1 – 1.2	20.1 – 21.8	1.7 – 1.8

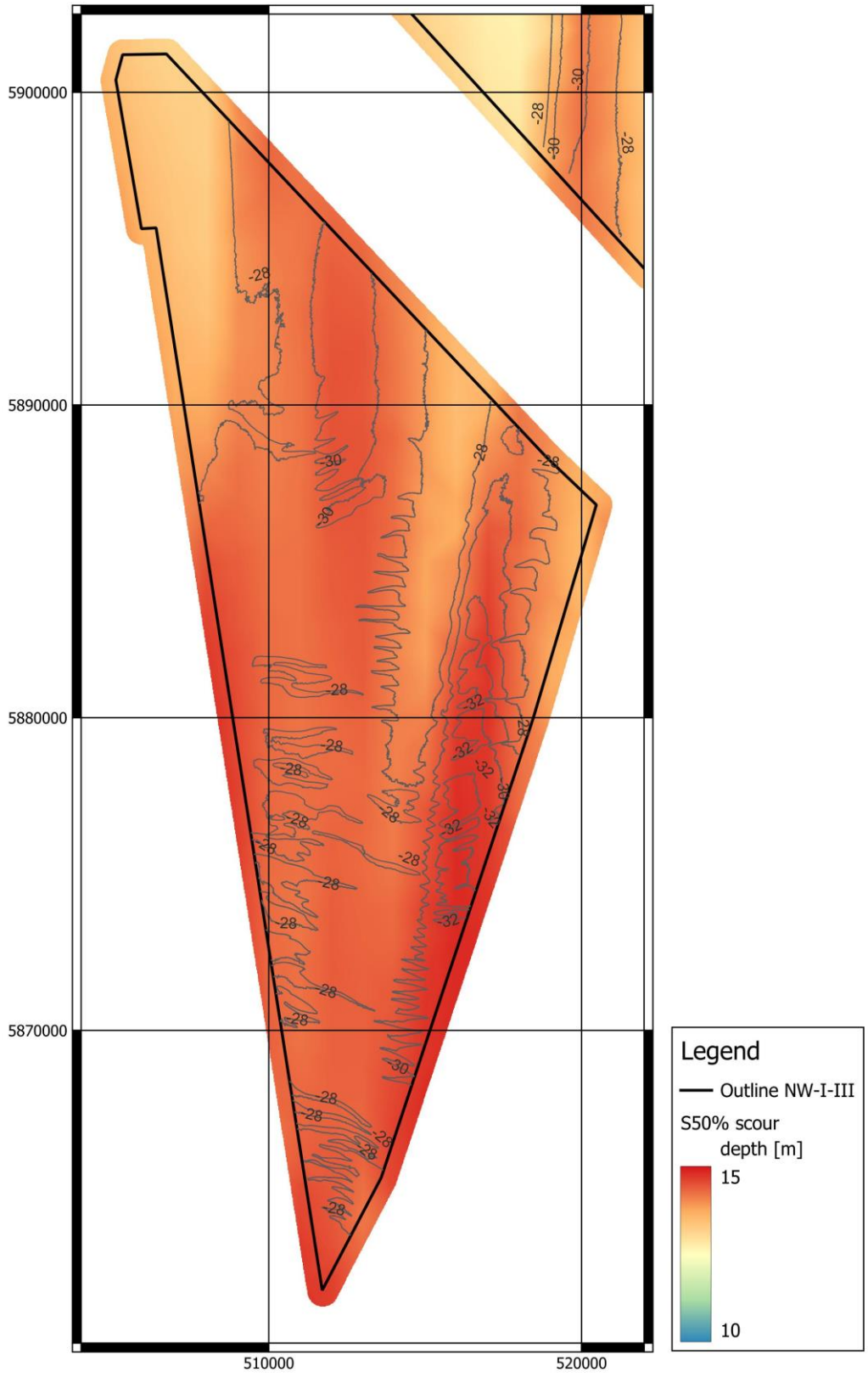

Figure 7-2: 95% non-exceedance maximum scour hole depth predicted for monopiles with D=12 m in NW-I. The map can be seen as the predicted scour depth at a location in NW-I if you were to place a monopile at that location.

The time scales of the scour development are relatively uniform in NW-I. The equilibrium scour hole depth is predicted to be reached between 5 – 10 years. Table 7-2 summarizes the expected time for the scour hole to reach depths between 1 and 5 meters.

Table 7-2: Predicted time it takes to reach scour depths between 1 and 5 m at NW-I.

	NW-I		
Scour depth [m]	5% exceedance time [days]	50% exceedance time [days]	95% exceedance time [days]
1	60-125	25-50	5-10
2	125-260	50-100	10-20
3	210-430	75-155	15-30
4	310-610	110-215	20-40
5	415-870	140-285	25-50

When designing a scour protection, special care should be taken around the areas where a seabed lowering is expected due to migrating sand waves. This is especially true around the crests of the sand waves. A seabed lowering requires sufficient flexibility of the scour protection. This can be achieved by designing a falling apron. Furthermore, the scour protection will stick out like a sill when the surrounding seabed lowers; see Hoffmans & Verheij (2021) for more information. This increases the load on the scour protection, which should be accounted for in the design of the armour layer.

Figure 7-3 shows the required armour layer grading in NW-I to achieve a maximum deformation of 0.5 m with 90% confidence**.** The shallowest areas, particularly along the crest of the sandbank in the northwest, require the heaviest grading. The crests of the sand waves further in the south of NW-I require heavier protection than the throughs.

The inch gradings in Figure 7-3 are most suitable for single-layered protections. If the grading width of these gradings satisfy the internal stability criterion, we expect that most of NW-I can be protected with a single-layered scour protection, but only if a high-density rock is used. A double-layered protection can be used everywhere. At least a 10-60 kg grading is required on the crest of the sandbank.

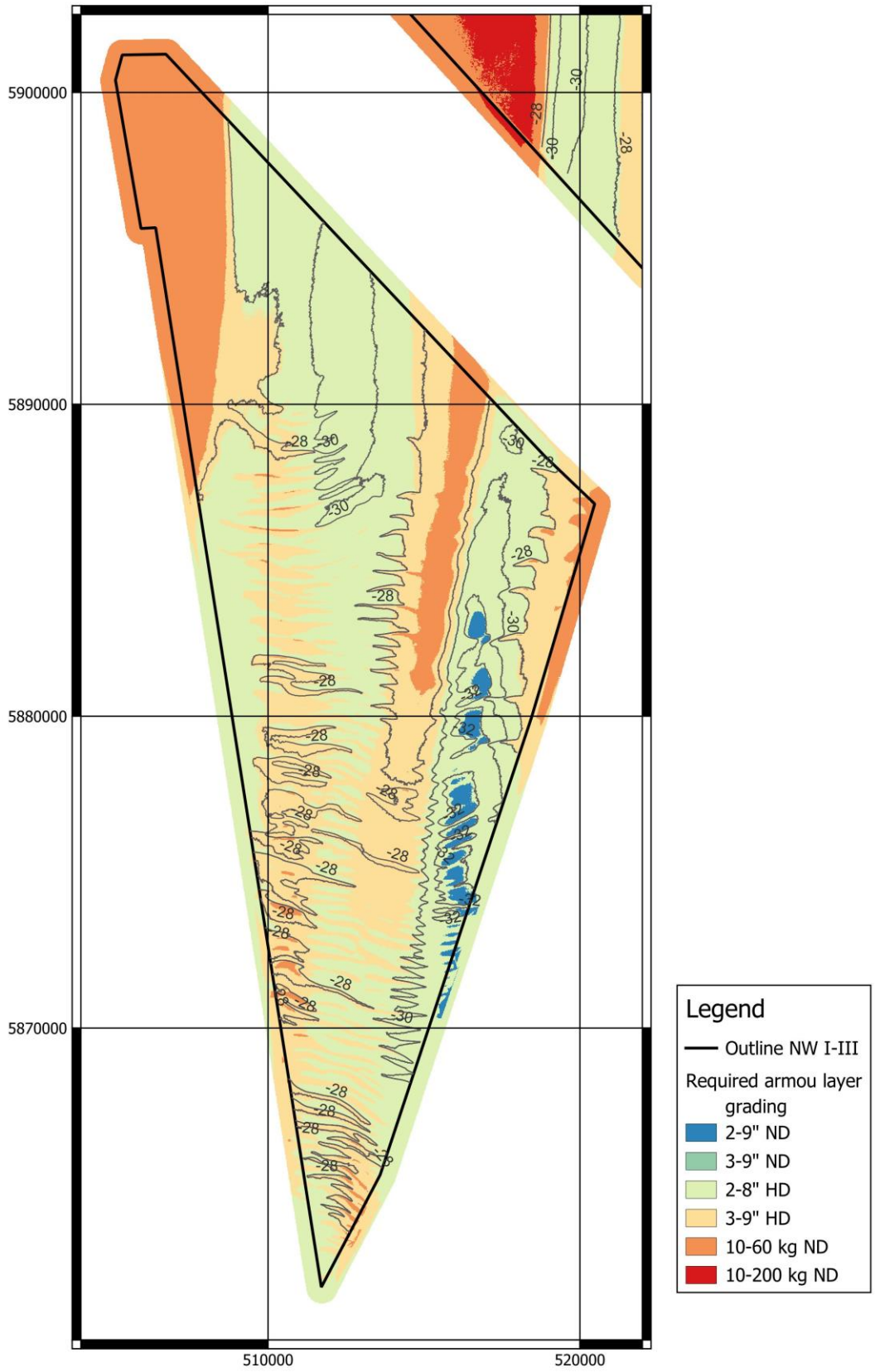

Figure 7-3: Required armour layer grading in a feasibility-level design to achieve a maximum deformation of 0.5 m with 90% confidence in NW-I.

7.3 Conclusions NW-II/III

NW-II/III is characterized by spatially varying hydrodynamic conditions. The flow velocities decrease from the south towards the north. Wave heights and wavelengths increase from the southwest to the northeast. The bed level generally decreases from the southeast to the northwest.

Two sandbanks are present in the southeast of the area. Sand waves are not present. Therefore, the scour and scour mitigation analyses do not consider bedform migration.

Table 7-3 summarizes the predicted 5%, 50%, and 95% non-exceedance scour depths, both absolute and relative to the pile diameter. Figure 7-4 visualizes the spatial distribution of the 50% non-exceedance scour depths in NW-II/III. With typically expected scour slopes of 1:2 – 1:3, the lateral extent of the scour holes in NW-II/III using the 50% non-exceedance scour depth varies between 20 and 45 m.

Table 7-3: Predicted scour depths in NW-II/III. The percentage values indicate the non-exceedance values. Indicated scour depths are the maximum scour depth during the entire simulation. The simulations are based on monopiles with a pile diameter of D = 12 m. $S_{n\%}$ stands for the n% non-exceedance scour depth.

Location	$S_{5\%}$ [m]	$S_{5\%}/D$ [-]	$S_{50\%}$ [m]	$S_{50\%}/D$ [-]	$S_{95\%}$ [m]	$S_{95\%}/D$ [-]
NW-II/III	5.0 – 8.1	0.4 – 0.7	10.7 – 14.4	0.9 – 1.2	18.2 – 21.4	1.5 – 1.8

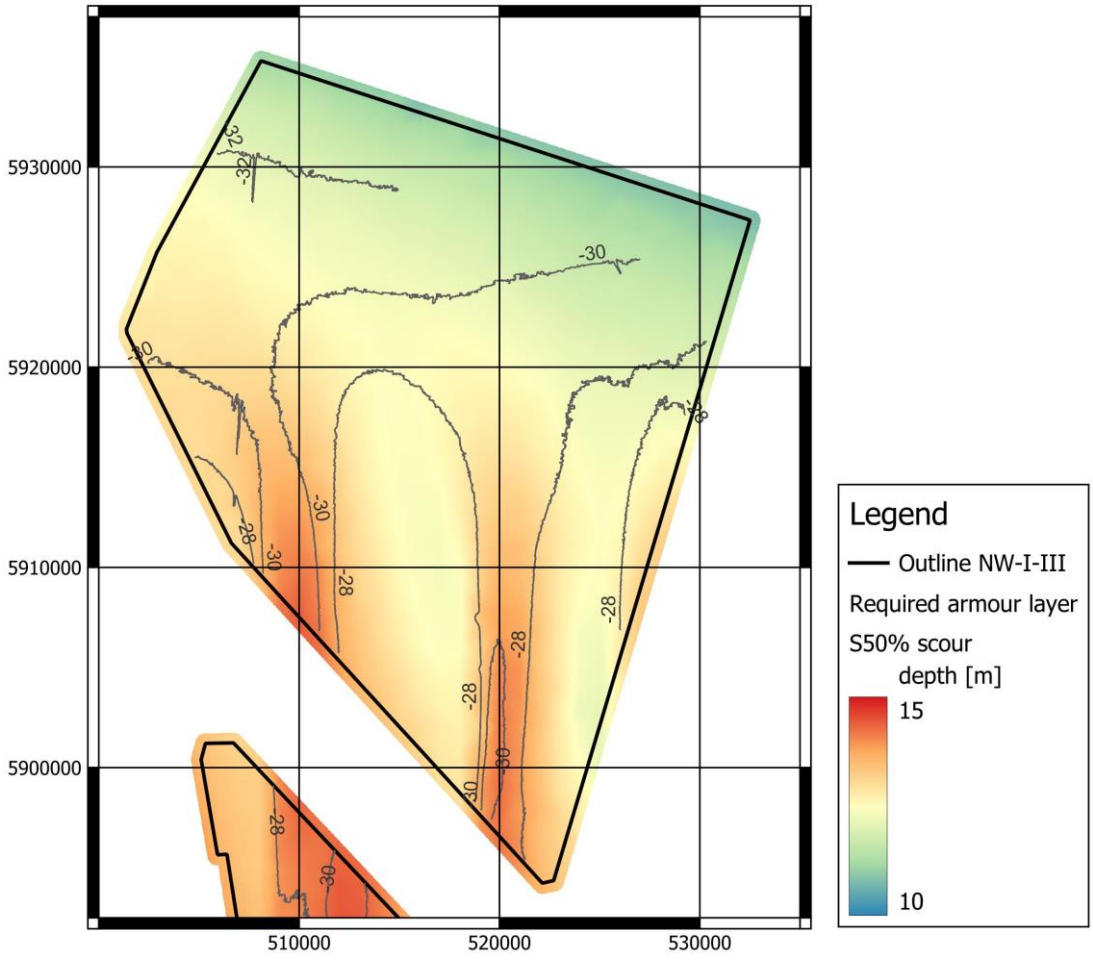

Figure 7-4: 95% non-exceedance maximum scour hole depth predicted for monopiles with D=12 m in NW-II/III. The map can be seen as the predicted scour depth at a location in NW-I if you were to place a monopile at that location.

The time scales of the scour development not spatially uniform in NW-II/III. The scour hole is predicted to develop the fastest in the south of the area and the slowest in the north. This is mainly caused by the slower flow velocities in the north compared to the south. The equilibrium scour hole depth is predicted to be reached between 5 and 25 years. Table 7-4 summarizes the expected time for the scour hole to reach depths between 1 and 5 meters.

Table 7-4: The predicted time to reach scour depths between 1 and 5 m at NW-II/III.

	NW-II/III		
Scour depth [m]	5% exceedance time [days]	50% exceedance time [days]	95% exceedance time [days]
1	105-735	40-285	5-50
2	225-1525	85-600	15-110
3	365-2540	135-935	25-170
4	540-3660	185-1305	35-240
5	770-10060	245-1730	45-315

Figure 7-5 shows the required armour layer grading in NW-II/III to achieve a maximum deformation of 0.5 m with 90% confidence. The heaviest gradings are needed in the shallowest areas, most notably on the crests of the sandbanks in the south. The deeper regions typically require lighter gradings. However, the design wave conditions are higher and longer in the northeast compared to the southwest. This means that locations with an equal water depth require heavier protection in the northeast than in the southwest. The area in the northeast requires a relatively light grading due to the deeper water depths.

The inch gradings in Figure 7-5 are most suitable for single-layered protections. If the grading width of these gradings satisfy the internal stability criterion, we expect that most of NW-II/III can be protected with a single-layered scour protection, but only if a high-density rock is used. A double-layered protection can be used everywhere. At least a 10-200 kg grading is required on the crest of the sandbank.

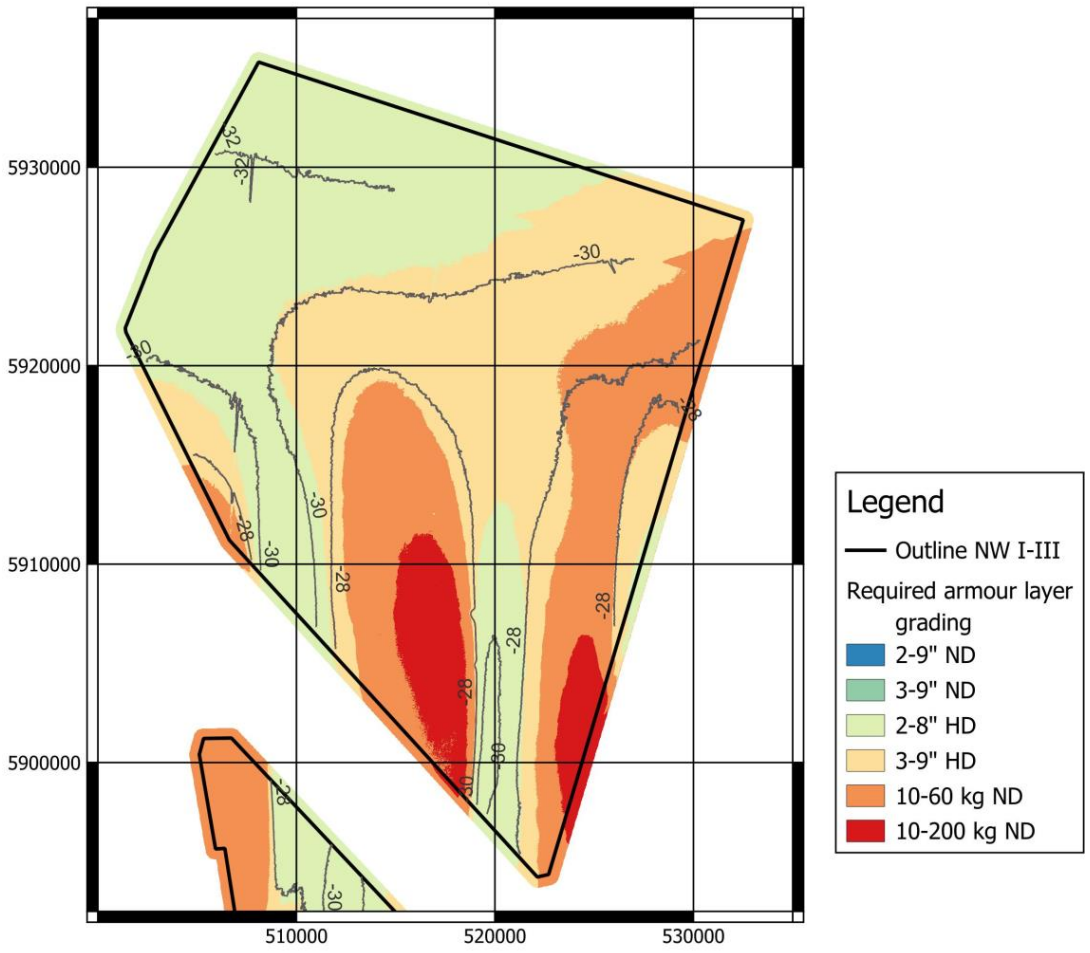

Figure 7-5: Required armour layer grading in a feasibility-level design to achieve a maximum deformation of 0.5 m with 90% confidence in NW-II/III.

8 REFERENCES

Angus, N. M., & Moore, R. L. (1982, May). Scour repair methods in the Southern North Sea. In Offshore Technology Conference (pp. OTC-4410). OTC.

Bolle, A., De Winter, J., Goossens, W., Haerens, P., & Dewaele, G. (2012, August). Scour monitoring around offshore jackets and gravity based foundations. In Proceedings of the Sixth International Conference on Scour and Erosion, Paris, France (pp. 27-31).

CIRIA, CUR, CETMEF (2007). The Rock Manual. The use of rock in hydraulic engineering.

Den Boon, J. H., Sutherland, J., Whitehouse, R., Soulsby, R., Stam, C. J. M., Verhoeven, K., ... & Hald, T. (2004, November). Scour behaviour and scour protection for monopile foundations of offshore wind turbines. In Proceedings of the European Wind Energy Conference (Vol. 14, p. 26). EWEC London UK.

Deltares, 2022. Scour and scour mitigation for Ten noorden van de Waddeneilanden Wind Farm Zone. Ref: WOZ2210243.

Deltares, 2023. Scour and scour mitigation for Ijmuiden Ver Wind Farm Zone. Ref: WOZ2220017.

DHI (2023a). IJmuiden Ver Wind Farm Zone: Part A, Metocean Modelling. Revision Final 1.0, dated 20 December 2023.

DHI (2023b). IJmuiden Ver Wind Farm Zone: Part B, Metocean Analysis. Revision Final 1.0, dated 20 December 2023.

DINOloket (2024). DINOloket: Data on Information on the Dutch Subsurface - Subsurface models: Seabed sediment. URL: https://www.dinoloket.nl/en/subsurface-models/map. Last accessed: 17/09/2024.

Dong, W., Moan, T., & Gao, Z. (2012). Fatigue reliability analysis of the jacket support structure for offshore wind turbine considering the effect of corrosion and inspection. Reliability Engineering & System Safety, 106, 11-27.

Fazeres-Ferradosa, T. (2012). Scour around marine foundations in mixed and layered sediments (Doctoral dissertation, MSc Dissertation, Faculdade de Engenharia, Universidade do Porto, Porto).

Fugro (2023). Geophysical Survey Results Report. Geophysical Survey at the Nederwiek zuid Investigation Area (NWZ IA) | Dutch Sector, The Netherlands. F217599_REP_001 | 05. 12 December 2023.

Fugro (2024a). Geophysical Survey Results Report. Geophysical Survey at the Nederwiek noord Investigation Area (NWN IA) | Dutch Sector, The Netherlands. F217599-REP-004| 03. 19 April 2024.

Fugro (2024b). Investigation Area Nederwiek Zuid. Investigation Results Geotechnics Seafloor Sampling Locations. F193460/NWZ/02 | 06 | 4 September 2024. Final (revised).

Fugro (2024c). Investigation Area Nederwiek (noord) Sites II & III. Investigation Results Geotechnics Seafloor Sampling Locations. F233104/NWN/02 | 01 | 14 June 2024. Preliminary.

Hoffmans, G. J.C.M. (2012). The influence of turbulence on soil erosion (Vol. 10).

Hoffmans, G.J.C.M., & Verheij, H.J. (2022). Scour Manual 2021. In Scour Manual 2021: Current-Related Erosion

JIP HASPRO (2023). Handbook of Scour and Cable Protection Methods.

Melling, G. J. (2015). Hydrodynamic and geotechnical controls of scour around offshore monopiles (Doctoral dissertation, University of Southampton).

Petersen, T. U., Sumer, B. M., Fredsøe, J., Raaijmakers, T. C., & Schouten, J. J. (2015). Edge scour at scour protections around piles in the marine environment—Laboratory and field investigation. Coastal Engineering, 106, 42-72.

Pilarczyk, K. (2000). Geosynthetics and geosystems in hydraulic and coastal engineering. CRC Press.

Raaijmakers, T. & Rudolph, D. (2006). Time-dependent scour development under combined current and wave conditions – laboratory experiments with online monitoring technique.

Raaijmakers, T. C. (2014). Dynamic scour prediction for offshore monopiles; validation against laboratory and field measurements.

Roulund, A., Sumer, B. M., Fredsoe, J., & Michelsen, J. (2002, November). 3-D numerical modeling of flow and scour around a pile. In Proc. First Intl Conf. on Scour of Foundations (pp. 17-20).

Rudolph, D., Raaijmakers, T., & Stam, C. J. (2008, November). Time-dependent scour development under combined current and wave conditions–hindcast of field measurements. In Proceedings Fourth International Conference on Scour and Erosion ICSE (Vol. 4, pp. 340-347).

Schiereck, G. J. (2017). Introduction to bed, bank and shore protection. CRC Press.

Sumer, B. M., Christiansen, N., & Fredsøe, J. (1997). The horseshoe vortex and vortex shedding around a vertical wall-mounted cylinder exposed to waves. Journal of Fluid Mechanics, 332, 41-70.

Sumer, B. M., Petersen, T. U., Locatelli, L., Fredsøe, J., Musumeci, R. E., & Foti, E. (2013). Backfilling of a scour hole around a pile in waves and current. Journal of Waterway, Port, Coastal, and Ocean Engineering, 139(1), 9-23.

Svasek Hydraulics (2024). Morphodynamics for Nederwiek Wind Farm Zone.

Welzel, M., Schendel, A., Hildebrandt, A., & Schlurmann, T. (2019). Scour development around a jacket structure in combined waves and current conditions compared to monopile foundations. Coastal engineering, 152, 103515.

A SCOUR PREDICTION SIMULATION TIMES NW-I AND NW-II/III.

This appendix analyses the required simulation times with the dynamic scour prediction tool.

The scour timescales refer to the time it takes for the scour hole to fully develop. These timescales differ between locations and are mostly dependent on the local hydrodynamic climate. The simulation time should be sufficiently long to ensure that the scour hole has fully developed by the end of the simulation. To investigate the required simulation time, simulations with a timespan of 30 years have been performed at 4 different locations. Two locations (A, B) are in site NW-I and two locations (C, D) are in site NW-II/III. The locations are picked to include one location with (relatively) high flow velocities and one location with (relatively) low flow velocities as the hydrodynamic climates are flow-dominated (Chapter 2). The results from these simulations are shown in Figure A-1 to Figure A-4.

In all four figures, the lines represent the asymptotic scour development towards the equilibrium scour hole depth as calculated with the Breusers formula. The superimposed fluctuations are caused by wave backfilling, creating a sawtooth-like pattern. It is evident that the waves are more impactful at shallower locations (Figure A-1 & Figure A-3) compared to the deeper locations (Figure A-2 & Figure A-4). The scour model will predict backfilling if the equilibrium scour hole depth is lower than the current scour depth. This often occurs when the hydrodynamic climate switches from current- to wave-dominated. Figure A-3 (best visible for the 5% non-exceedance line) visualizes this process with the steep decreases in scour hole depth at particular events. Due to the asymptotic nature of the scouring process towards the equilibrium scour hole depth, it often takes a long time for the scour depth to recover from these backfilling events. Multiple subsequent backfilling events can decrease the scour hole depth for extended periods. Therefore, the amount and the chronology of these backfilling events impact the maximum scour hole depths predicted by the model. A more thorough analysis of the time-dependent scour development is explained in Section 4.4.2.

Figure A-1 and Figure A-2 show that the scour development at NW-I can happen fast at either of the two locations. The primary scour hole develops up to approximately T = 10 years, though the bulk of the scour is expected to happen in the first 5 years after installation. It can generally be said that after T = 10 years, the fluctuations of the scour hole depth are determined by alternating backfilling and scouring events. A simulation time of T = 15 years is chosen to limit the computational time. It is possible that a longer simulation would lead to slightly deeper scour holes if a persistent period of low waves were to occur. However, this would only indicate a minor increase in the predicted scour depths and is expected to be covered in the model uncertainty.

Figure A-3 and Figure A-4 show that the scour development at the NW-II/III sites can differ. The (relatively) low flow velocities that occur further north yield a slower scour development. It is chosen to use a simulation time of T = 30 years for all simulations in NW-II/III to ensure that the main scour hole development is captured within the simulations.

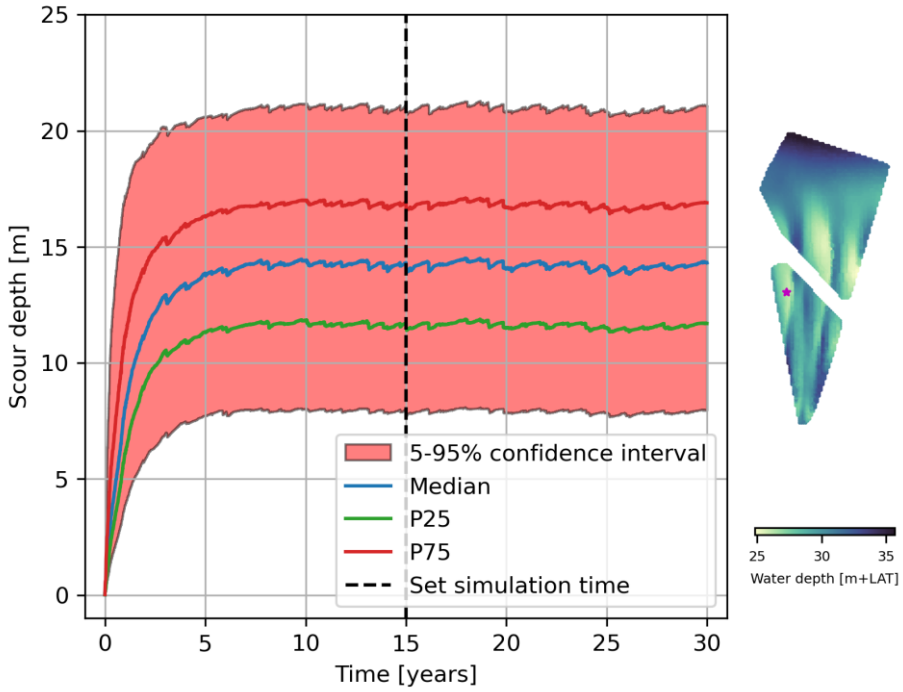

*Figure A-1: 30-year simulation results for a location in NW-I with (relatively) **high** flow velocities and a (relatively) **low** water depth. The location is visualized with the magenta star in the right image.*

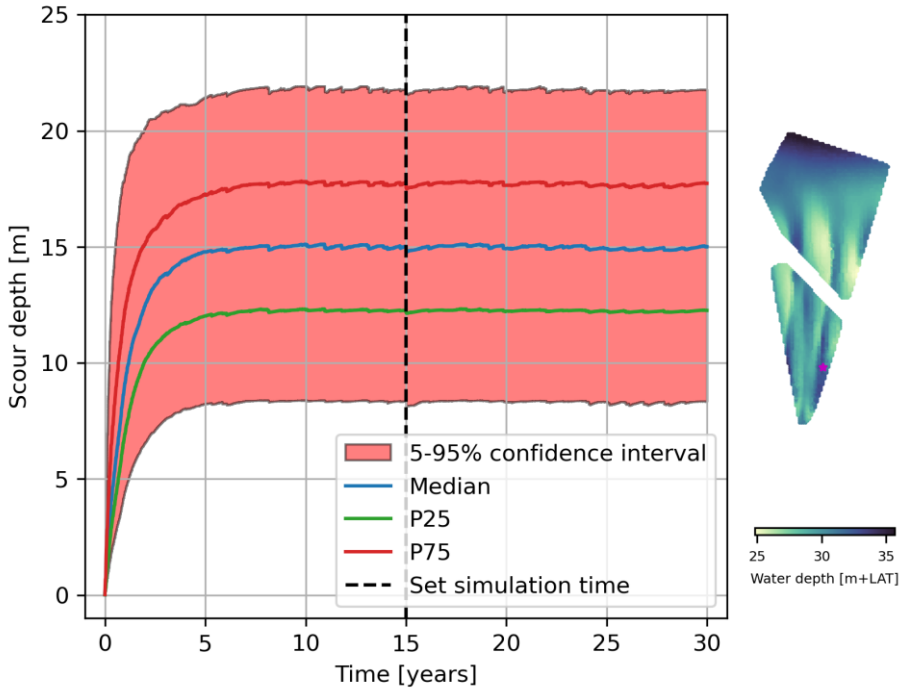

*Figure A-2: 30-year simulation results for a location in NW-I with (relatively) **low** flow velocities and a (relatively) **high** water depth. The location is visualized with the magenta star in the right image.*

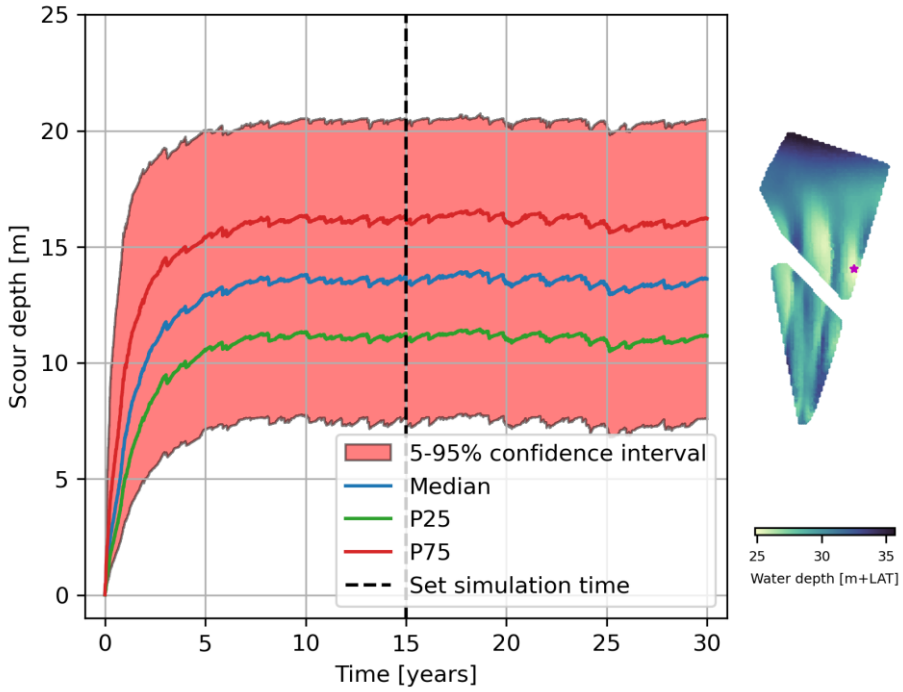

*Figure A-3: 30-year simulation results for a location in NW-II/NW-III with (relatively) **high** flow velocities and a (relatively) **low** water depth. The location is visualized with the magenta star in the right image.*

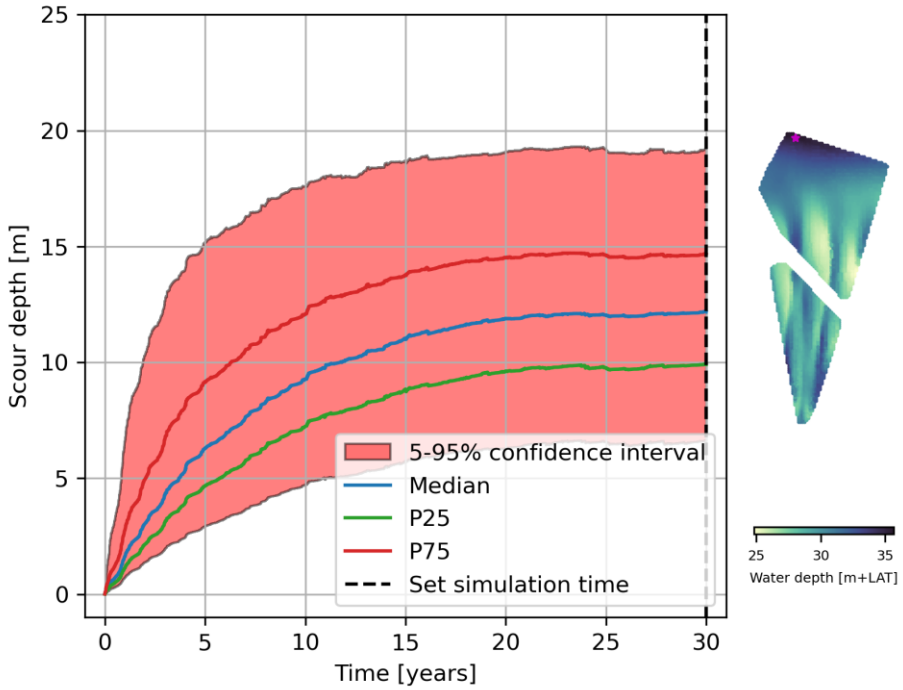

*Figure A-4: 30-year simulation results for a location in NW-II/NW-III with (relatively) **low** flow velocities and a (relatively) **high** water depth. The location is visualized with the magenta star in the right image.*

B APPENDIX: FEASIBILITY LEVEL DESIGN CONDITIONS FOR SCOUR MITIGATION

This appendix describes the extreme value analysis (EVA) methodology that has been applied to derive design conditions suited for a feasibility level scour protection design. Design conditions have been derived for return periods of 1,2, 5, 10, 20, and 50 years. Univariate extreme value conditions are derived by fitting an extreme value distribution (EVD) through historical extreme data points. From these EVDs, the current velocity magnitude as well as significant wave height are derived for different return periods. Subsequently, the wave peak periods corresponding to the extreme significant wave heights are defined.

B.1 General methodology

For each grid point, 43 years of data is considered (1980-2022, including 2022). To only consider statistically independent data points, a peak over threshold analysis is performed. This ensures that only a single data point per storm is included and that all data points are above a certain threshold. Subsequently a three-parameter Weibull distribution is fitted through all these historical extreme data points, resulting in an extreme value distribution for each grid point. The three-parameter Weibull distribution is chosen for two reasons. Firstly, because a visual inspection at a number of locations identified that the tail of the extreme value distribution can be reasonably well predicted by this distribution. Secondly, because it is known to be a robust fit, which is important because the EVA needs to be performed at all grid points. Even though Weibull fits are quite robust, it is known that the eventual distribution can be influenced by the threshold. If the threshold is too low, too many non-extreme data points are included, whereas if the threshold is too high, there are not enough data points for a reliable fit. To assess the influence of the threshold on the extreme values, fits are performed for different thresholds, corresponding to including 1-5 storms per year. After a sensitivity analysis, it is decided which of these fits are representative as design conditions.
It should be noted that in this study only a fit on omnidirectional data is performed. Given that it is to be used for feasibility level design, it is deemed that this methodology is sufficiently accurate. For detailed design, it is advisable to perform a thorough multi-variate extreme value analysis, including a convolution of different directional physical systems (e.g., separating northerly and south-westerly storms).

B.2 Waves

For the significant wave height, 9 thresholds are considered, such that 43, 65, 86, 108, 129, 151, 172, 194, 215 individual storms are included (corresponding to an average of 1, 1.5, …, 5 storms per year). The resulting 50-year return period significant wave height maps show physically explainable patterns and large coherence between spatial maps for different thresholds (see Figure B-2). The effect of the threshold on the resulting 50-year return period significant wave height is minor (between + and – 1%). As the choice for a three-parameter Weibull fit is already slightly conservative and because there is no basis that the highest EVA is the best EVA, it is chosen to average the nine EVA's with different thresholds. A spatial comparison between the highest wave height from the 43 years timeseries and the derived 50-year return period shows similar spatial patterns. Furthermore, the magnitude of the latter is similar or slightly higher than the former. This provides confidence in the reliability of the EVA. The resulting 50 year return period extreme wave height is visualized in Figure B-1 (left).

Design purposes require the peak wave period corresponding to the extreme significant wave height (e.g., Hs_RP50). To derive these peak periods, it is assumed that the wave steepness of the five most severe storms in the hindcast is representative for the wave steepness during future extreme storms. A check has been performed to verify that the steepness of extreme wave events is rather constant, which is the case. Using the hindcast-derived storm wave steepness and the extreme wave heights, the associated extreme peak wave periods are calculated. This is done by re-writing the definition of the wave steepness with the deep water wavelength to calculate the peak wave period. The resulting peak wave period for the 50-year return period is presented in Figure B-1 (middle).

B.3 Currents

To derive extreme current conditions a similar approach is followed as for the significant wave height. However, it is important to note that strictly speaking fitting an extreme value distribution through a tidal signal is not fully correct. This is because tidal signals are periodic and deterministic, whereas extreme value distributions are applicable to independent, rare events. Nevertheless, it is chosen to use this approach as this avoids the separation of velocity signals in a tidal and non-tidal part, which also introduces uncertainty.

The sensitivity of thresholds on the 50-year return period current magnitude is first investigated. This is done by visualizing results for thresholds corresponding to 1, 1.5, 2, … 5 storms per year (see Figure B-3). Here it can be observed that spatial patterns are again very identical, but that a higher threshold (i.e., less storms) results in slightly higher extreme current magnitudes. Keeping in mind the shortcoming of fitting an EVD through partially tidal data, it is chosen to use a high threshold. This is done to restrict the analysis as much as possible to extreme storm-driven events instead of fitting through many high tide conditions. Eventually, the resulting extreme values are based on averaging the three individual fits that included 43, 65 and 86 storms (i.e., top 3 panels of Figure B-3). The resulting 50-year return period current magnitude is visualized in Figure B-1 (right).

The combination of the RP50 wave height and RP50 current velocities is deemed too conservative to approximate the RP50 conditions. In reality, these parameters are combined with a joint probability assessment, which often results in lower wave heights and current velocities compared to their RP50 values. Such a joint probability was performed for three locations in the NWWFZ in DHI (2023a; 2023b). From this analysis, it was found that the RP50 wave conditions are combined with (approximately) the RP1 current velocities. It is decided to use the RP50 wave conditions as the waves are the governing force on the scour protection. The RP50 wave conditions is combined with the RP1 current conditions, which is shown in Figure B-4c.

B.4 Water levels

Lower water levels lead to higher loads on the scour protection. The water level should thus also be considered within the joint probability of the wave heights, current velocities, and water levels. Similar to the current velocities, this joint probability was performed for three locations in the NWWFZ (DHI, 2023a; 2023b). These joint probability water levels roughly coincide with the mean low water levels (MLW). It was thus decided to use the MLW as the design water level for the scour protection. The resulting water levels are visualized in Figure B-4d.

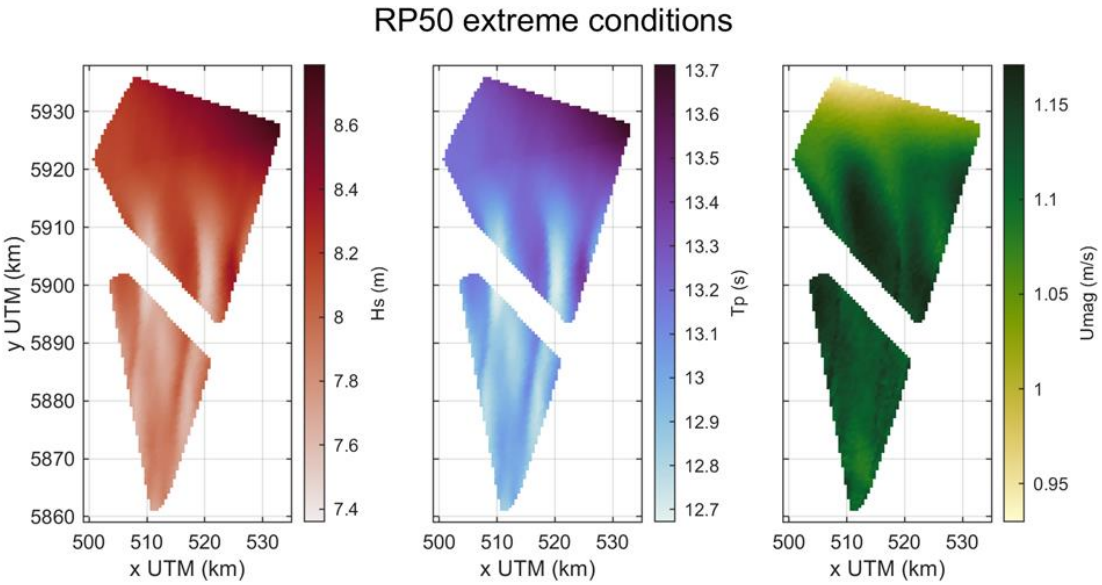

Figure B-1: RP50 wave height (A, left), peak wave period (B, middle), and current velocity (C, right).

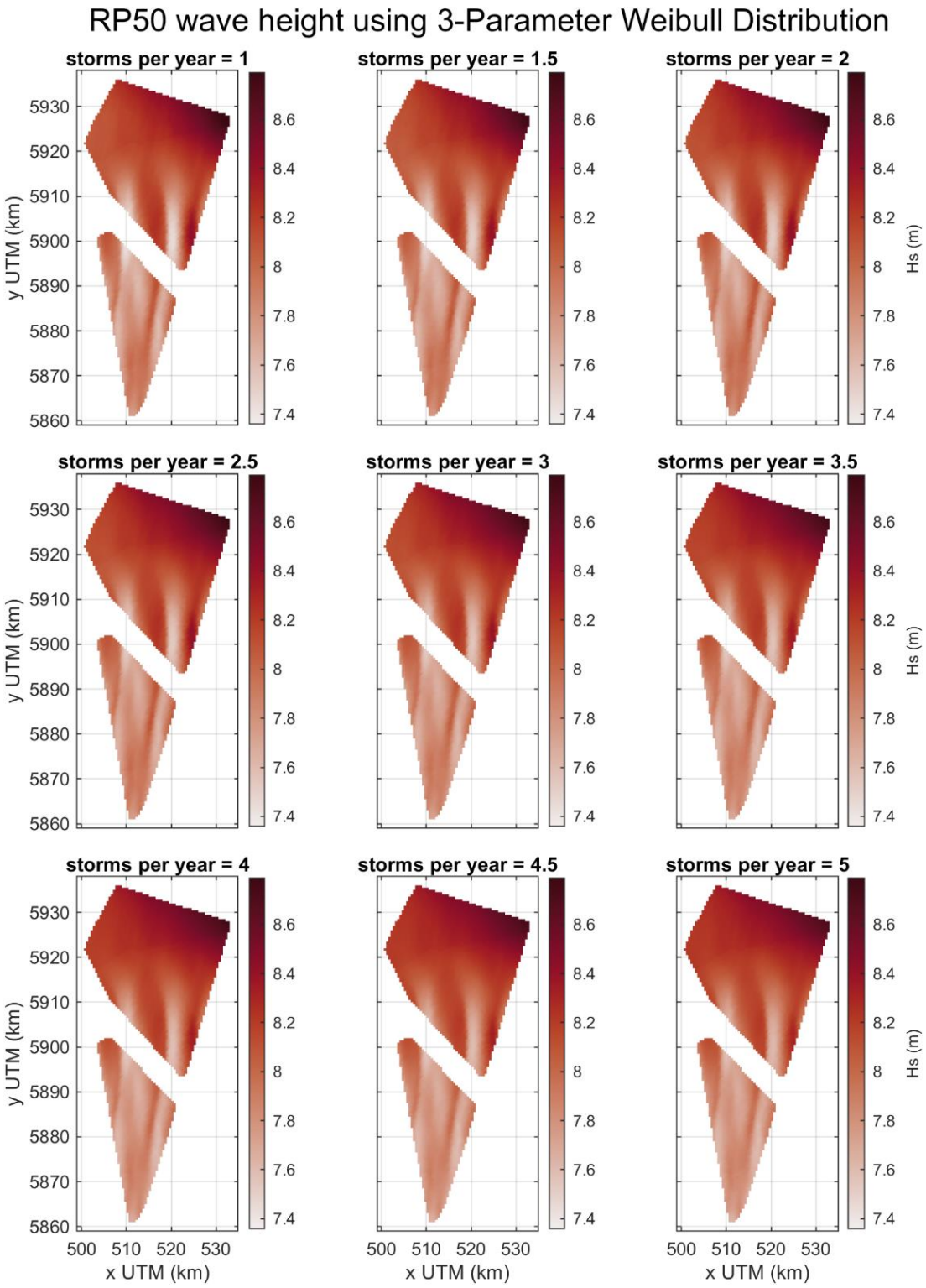

Figure B-2: Spatial variation of the RP50 wave height when extrapolated with a 3-parameter Weibull fit with a variable number of storms per year (1-5).

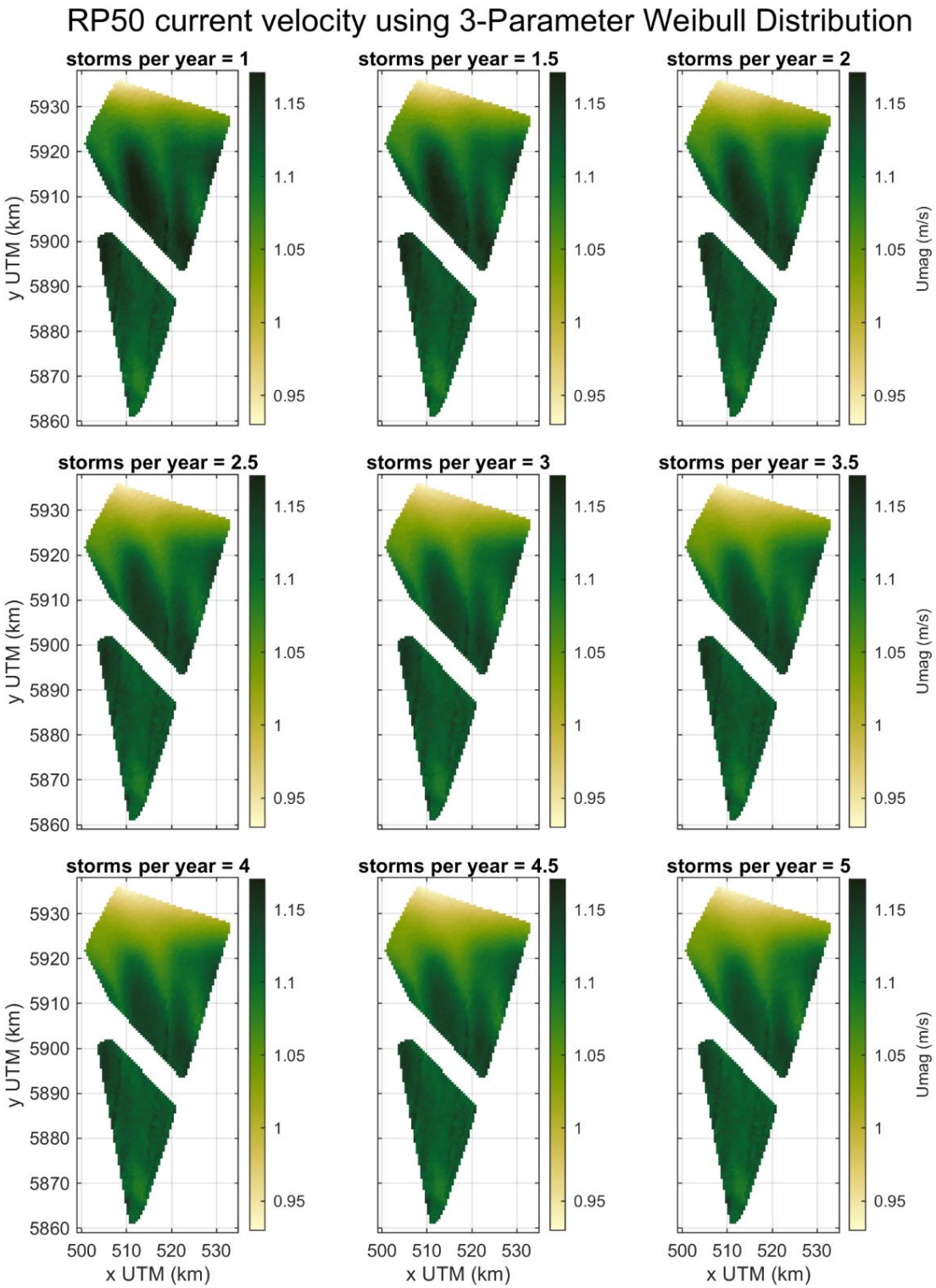

Figure B-3: Spatial variation of the RP50 current velocities when extrapolated with a 3-parameter Weibull fit with a variable number of storms per year (1-5).

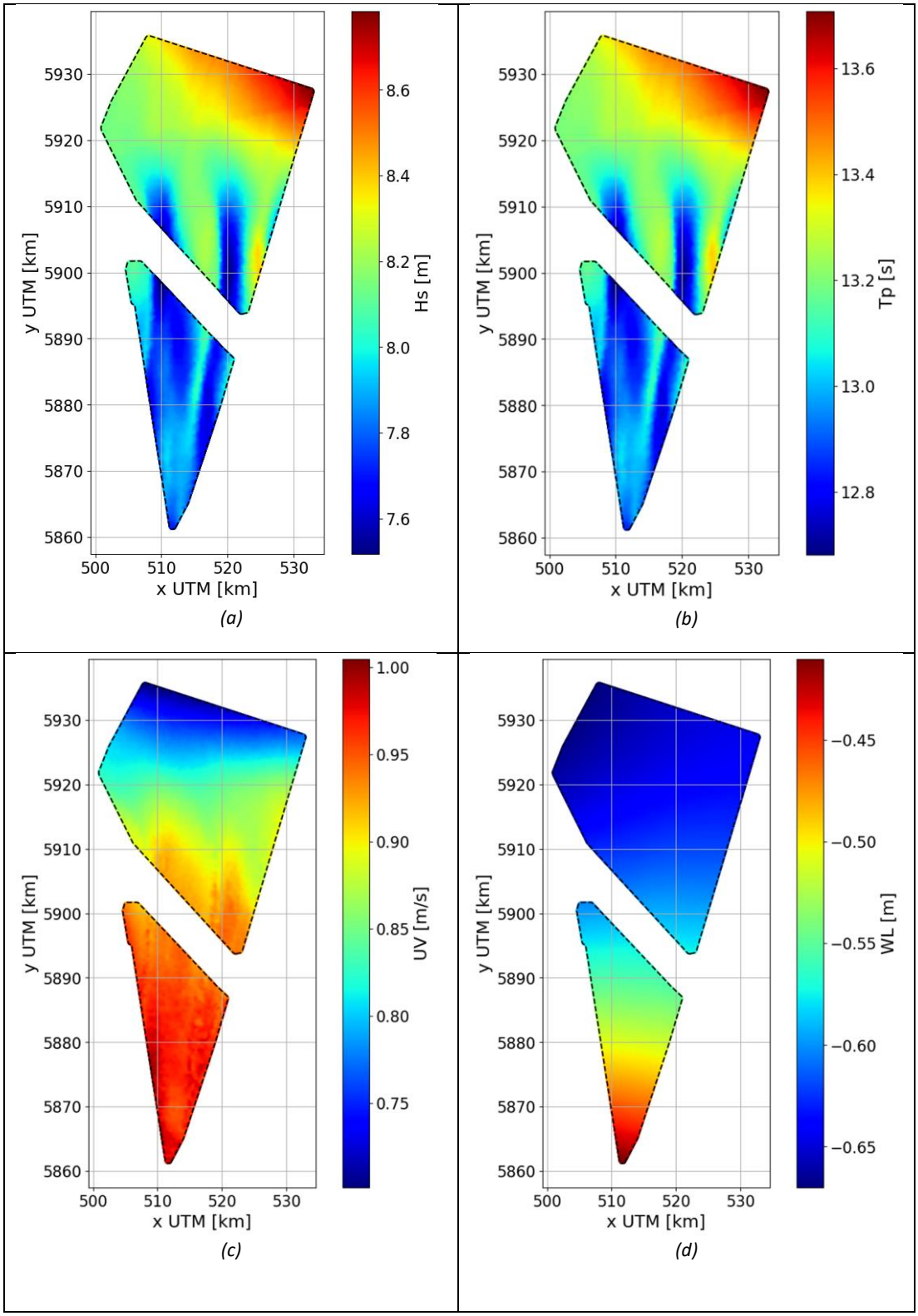

Figure B-4: Design significant wave height (RP50, a), design peak wave period (RP50, b), design current velocity (RP1, c), and design water level (mean low water, MLW, d). Parameters are used in the feasibility-level armour layer design.

B.5 References

DHI (2023a). IJmuiden Ver Wind Farm Zone: Part A, Metocean Modelling. Revision Final 1.0, dated 20 December 2023.

DHI (2023b). IJmuiden Ver Wind Farm Zone: Part B, Metocean Analysis. Revision Final 1.0, dated 20 December 2023.

SVAŠEK
HYDRAULICS
COASTAL, HARBOUR AND RIVER CONSULTANTS

The creative commons license terms 4.0 CC BY apply to this material.
Please take notice of the general terms “Creative Commons Attribution 4.0 International public License” before starting to use the license. These terms can be accessed by clicking on this link https://creativecommons.org/licenses/

This investigation was carried out by Svasek Hydraulics , commissioned by RVO, an agency of the Ministry Economic Affairs.

Whilst a great deal of care has been taken in compiling the contents of this investigation, RVO can not be held liable for any damages resulting from any inaccuracies and/or outdated information.

The information in this document is valid at the time of publishing (see month/year). Updates will be published on the website https://offshorewind.rvo.nl, at the relevant sitemap, General Information, submap Revision Log and Q&A. In the Revision Log is indicated which versions are the latest and what the changes are in relation to previous versions. The documents can be found at the relevant sites, indicated in the List of all reports and deliverables.

Contacts
Netherlands Enterprise Agency (RVO)
Graadt van Roggenweg 200 | 3531 AH | Utrecht
P.O. Box 8242 | 3503 RE | Utrecht
www.rvo.nl / https://english.rvo.nl

Netherlands Enterprise Agency (RVO) | November 2024